

# Synthetic, Structural, and Mechanistic Studies of Homogeneous Ziegler-Natta Catalysis

Thesis by  
Sharad Hajela

In Partial Fulfillment of the Requirements  
for the Degree of  
Doctor of Philosophy

California Institute of Technology  
Pasadena, California

1995

(Submitted May 25, 1995)

*For*  
*Mom and Dad*

**PLEASE NOTE**

Copyrighted materials in this document have not been filmed at the request of the author. They are available for consultation, however, in the author's university library.

iii,  
The poem by John Donne

**University Microfilms International**

*As virtuous men pass mildly away,  
And whisper their souls to go,  
Whilst some of their sad friends do say  
The breath goes now, and some say, No;*

*So let us melt, and make no noise,  
No tear-floods, nor sigh-tempests move,  
'Twere profanation of our joys  
To tell the laity our love.*

*Moving of th' earth brings harms and fears,  
Men reckon what it did and meant;  
But trepidation of the spheres,  
Though greater far, is innocent.*

*Dull sublunary lovers' love  
(Whose soul is sense) cannot admit  
Absence, because it doth remove  
Those things which elemented it.*

*But we, by a love so much refined  
That our selves know not what it is,  
Inter-assured of the mind,  
Care less, eyes, lips, and hands to miss.*

*Our two souls therefore, which are one,  
Though I must go, endure not yet  
A breach, but an expansion,  
Like gold to airy thinness beat.*

*If they be two, they are two so  
As stiff twin compasses are two;  
Thy soul, the fixed foot, makes no show  
To move, but doth, if th' other do.*

*And through it in the center sit,  
Yet when the other far doth roam,  
It leans and harkens after it,  
And grows erect, as that comes home.*

*Such wilt thou be to me, who must  
Like the other foot, obliquely run;  
Thy firmness makes my circle just,  
And makes me end where I begun.*

I am deeply grateful to Prof. John Bercaw for all his help, good advice, patience, and support. They all always say how great Bercaw is, and what a great experience it has been being in the Bercaw group. Its true. I can't imagine a better environment for learning how to do science.

The NMR studies of Chapter 1 could not have been done without the expert help of Prof. Les Field during his short visit with our group. Its amazing what you can learn by being a shadow for 4 weeks. The studies in Chapter 4 are the result of an intense collaborative effort with Jon Mitchell and Susan Brookhart. Get Jon in a synthetic groove and you have one of the most energetic chemists I have ever witnessed. Susan is one of the kindest people I know, and was unbelievably patient with me as I tried to explain the intricacies of "Bercaw Group Vacuum Techniques". Susan was the one of us who was finally able to get a decent "Binol" crystal (with the help of Bob's magical crystallizing tubes).

Bob (Calzone Fest) Blake, Tim (Turtle Pool) Herzog, Andy (Three and a Half Cases!) Kiely, Mike (King of the Blues) Abrams, Susan (Sleepy) Brookhart, Jon (Limus) Mitchell -- the best labmates (the spell checker didn't recognize the word and suggested lambastes instead!) anybody could wish for -- nothing I can say here can do justice to how important you all are to me. I hope somehow you know...

Chris (Lost in the Wonderland) Kenyon has been at various times my soulmate, my alter ego, and "The Antiparticle", but will always be my climbing partner and friend. Rock climbing trips with Chris, Peter (and Lorraine) Green, Mike and Susan have been the most enjoyable part of my extracurricular life at Caltech.

Other past and present group members have been extremely helpful to me. LeRoy Whinnery taught me about many of the group traditions. Warren (Warren) Piers was very helpful and encouraging when I started in the lab and

also introduced me to Stevie Ray Vaughn. Bryan Coughlin, in addition to initiating the "Bp project" has been an endless source of ideas, and an incredible resource in terms of keeping up with the literature. Jim (Where's Jim?) Gilchrist has been a great boon to the group for his expertise in NMR studies and his knowledge of organic synthesis-thanks for always being ready to listen to my crazy ideas.

Softball with the Hogs has been great fun. Thanks to Andy ("Hogs Forever, Second Place Never") and Bryan for coaching. Thanks especially to the Beer Coaches: Tim, Mike, Lin, and Cory.

Finally, I want to thank my friend and undergraduate advisor Ed Rosenberg for being so supportive over the years and for his inexhaustible contagious enthusiasm for chemistry. "Friday Night Madness" was a great run...

**Abstract** The reaction of  $\text{OpSc(H)(PMe}_3\text{)}$  ( $\text{Op} = \{(\eta^5\text{-C}_5\text{Me}_4)_2\text{SiMe}_2\}$ ) with isobutene produces  $\text{OpSc(CH}_3\text{)(PMe}_3\text{)}$  along with isobutane, 2-methylpentane, isobutene, 2-methyl-1-pentene, propane and *n*-pentane. These products arise from a series of reactions involving olefin insertion,  $\beta\text{-CH}_3$  and (faster)  $\beta\text{-H}$  elimination which proceeds until only the 2-methyl-1-alkenes ( $\text{C}_4\text{H}_8$ ,  $\text{C}_6\text{H}_{12}$ , *etc.*) and the predominant organoscandium product  $\text{OpSc(CH}_3\text{)(PMe}_3\text{)}$  remain. A transient observed in the reaction sequence has been characterized as  $\text{OpSc(CH}_2\text{CH}_2\text{CH}_3\text{)(PMe}_3\text{)}$ . Slower  $\sigma$  bond metathesis involving the methyl C-H bonds of  $\text{PMe}_3$  and the Sc-C bonds of the scandium alkyls accounts for the observation of saturated alkanes (2-methylalkanes ( $\text{C}_4\text{H}_{10}$ ,  $\text{C}_6\text{H}_{14}$ , *etc.*), normal alkanes ( $\text{C}_3\text{H}_8$ ,  $\text{C}_5\text{H}_{12}$ , *etc.*) as well as a minor organoscandium product  $\text{OpScCH}_2\text{PMe}_2$  in the product mixture.  $\beta$ -Ethyl migration is *not* observed for the closely related 2-ethyl-butyl derivative,  $\text{OpSc}\{\text{CH}_2\text{CH(C}_2\text{H}_5\text{)CH}_2\text{CH}_3\}\text{(PMe}_3\text{)}$ , obtained from reaction of 2-ethyl-1-butene with  $\text{OpSc(H)(PMe}_3\text{)}$ .

The cyclopentylmethyl derivative,  $\text{Cp}^*\text{ScCH}_2$  (*cyclo*- $\text{C}_5\text{H}_8$ ), slowly and cleanly decomposes in cyclohexane to give methylcyclopentane and a yellow crystalline precipitate. The  $^1\text{H}$  NMR spectrum of the yellow product is consistent with a compound containing one  $\text{Cp}^*$  and one  $(\eta^5, \eta^1)\text{-C}_5(\text{CH}_3)_4\text{CH}_2$ , the latter arising *via* metallation of a  $\text{Cp}^*$  ligand (*i.e.* a "tuck-in" complex). The structure of the complex which crystallizes as the dimer,  $[\text{Cp}^*\text{Sc}\{\mu\text{-(}\eta^5, \eta^1\text{)-C}_5(\text{CH}_3)_4\text{CH}_2\}]_2$ , when allowed to form slowly at room temperature is reported.

Reaction of the neutral ligand 1,4,7-trimethyl-1,4,7-triazacyclononane (*Cn*) with  $\text{MCl}_3(\text{THF})_3$  (*M* = Sc, Y) in acetonitrile affords the novel trihalide complexes  $\text{CnMCl}_3$ . Subsequent alkylation with  $\text{LiCH}_3$  in THF cleanly gives the corresponding trimethyl species  $\text{CnMMe}_3$ . Reactivity studies reveal that the metal carbon bonds of these  $12\text{ e}^-$ ,  $d^0$  complexes are remarkably unreactive toward insertion chemistry with typical unsaturated substrates such as olefins and acetylene. 2-butyne does, however, react with  $\text{CnYMe}_3$  by C-H activation to give a compound that is characterized as an equilibrium mixture of a major allenyl form with a minor propargyl component. In general,  $\text{CnScMe}_3$  is significantly more stable, but less reactive, than  $\text{CnYMe}_3$ . Activation of  $\text{CnScMe}_3$  with  $\text{B(C}_6\text{F}_5)_3$  or  $[\text{HMe}_2\text{NPh}][\text{B(C}_6\text{F}_5)_4]$  results in partially characterized complexes which exhibit olefin polymerization chemistry. The crystal structure of  $\text{CnScCl}_3$  has been determined.

We have recently described the highly iso-specific Ziegler-Natta polymerization of  $\alpha$ -olefins using the single component,  $\text{C}_2$  symmetric metallocene  $[\text{BpYH}]_2$ , ( $\text{Bp} = [\text{Me}_2\text{Si(C}_5\text{H}_2\text{-2-SiMe}_3\text{-4-CMe}_3)_2]$ ). The steric bias exerted by the cyclopentadienyl substitution pattern allows for formation of only the desired *racemic* product upon metallation, with no detectable amount of the undesired *meso* isomer. A natural extension is the further development of methods for obtaining enantiomerically pure catalysts based on the  $[\text{Bp}]$  ligand system. Such single-component systems, in addition to serving as powerful mechanistic probes of Ziegler-Natta catalysis, would also be promising candidates for use in a variety of other catalytic asymmetric transformations. The most desirable ligand design would produce *only one enantiomer* upon coordination to the metal. Thus, not only would the wasteful and tedious separation of the *meso* isomer be avoided, but the subsequent resolution of the racemate would also be obviated. We have found that employment of chiral silyl-linkers is an effective design strategy for the synthesis of such enantiomerically pure complexes. Described herein are our efforts which have led to the synthesis of the ligand  $[\text{BnBp}]^{2-}$ , designed to coordinate to give only one enantiomer, and  $\text{BnBpY-H}$ , the first example, as far as we are aware, of an enantiopure  $\text{C}_2$ -symmetric, group III metallocene which is competent for coordination polymerization of  $\alpha$ -olefins.

## Table of Contents

Acknowledgements		iv
Abstract		vi
Table of Contents		vii
List of Figures		viii
List of Tables		x
Chapter 1	Competitive Chain Transfer by $\beta$ -Hydrogen and $\beta$ -Methyl Elimination for a Model Ziegler-Natta Olefin Polymerization System [Me <sub>2</sub> Si( $\eta^5$ -C <sub>5</sub> Me <sub>4</sub> ) <sub>2</sub> ]Sc{CH <sub>2</sub> CH(CH <sub>3</sub> ) <sub>2</sub> }(PMe <sub>3</sub> ).	1
Chapter 2	Intramolecular $\sigma$ Bond Metathesis for Permethylscandocene-Alkyl Complexes Revisited: Structure of Permethylcyclopentadienyl- $\mu$ -tetramethylcyclopentadienylmethylene Scandium Dimer.	50
Chapter 3	A New Class of Highly Electron Deficient Group III Organometallic Complexes Based on 1,4,7-Trimethyl-1,4,7-triazacyclononane.	64
Chapter 4	Employment of Chiral Linkers for Directed Synthesis of Enantiopure, C <sub>2</sub> -Symmetric, <i>ansa</i> -Metallocenes: A Single Component, Isospecific, Ziegler-Natta Catalyst.	102



## List of Figures

### Chapter 1

Figure 1	Reaction of <b>1</b> with isobutene: white-wash stack plots (chemical shift vs time) of characteristic (Op ligand (CH <sub>3</sub> ) <sub>α</sub> ) resonances for the major organometallic species ( <b>2</b> , <b>3</b> , and <b>6</b> ) during the course of the reaction.	12
Figure 2	Integrated data for the major organometallic species reveals roughly a constant sum over the reaction course.	13
Figure 3	Reaction of <b>1</b> with isobutene: (top) white-wash stack plots (chemical shift vs time) highlighting the time dependent chemical shifts of characteristic (Op ligand (CH <sub>3</sub> ) <sub>β</sub> ) resonances for <b>2</b> , <b>3</b> , and <b>6</b> ) during the course of the reaction, and (bottom) contour plots of the same resonances (see text for details).	14
Figure 4	Reaction of <b>1</b> with isobutene: time course for the Sc-C $\alpha$ -hydrogen resonances for <b>2</b> and <b>6</b> . The upfield doublet is assigned to <b>2</b> and the downfield multiplet to <b>6</b> . The other three peaks (x) are due to constant, non-reactive impurities.	15
Figure 5	Reaction of <b>1</b> with isobutene: (a) time course for the Sc-CH <sub>3</sub> resonance of <b>2</b> and (b) the same resonance in the PMe <sub>3</sub> -depleted rearrangement (see text for details).	16
Figure 6	Integrated data for the major organometallic species reveals roughly a constant sum over the reaction course.	17

### Chapter 2

Figure 1	ORTEP drawing of the dimer with 50% probability ellipsoids showing the numbering system. H atoms omitted for clarity.	53
----------	---	----

### Chapter 3

Figure 1	Examples of isoelectronic group III and group IV complexes, with the target complex, <b>C</b> , highlighted in the box(see text for details).	67
Figure 2	Examples of recently reported late transition metal organometallic systems supported by neutral azamacrocycles.	68
Figure 3	ORTEP diagram for CnScCl <sub>3</sub> ( <b>2a</b> ). Selected bond distances: Sc-Cl (avg) 2.406 Å; Sc-N (avg) 2.337 Å. Selected bond angles: Cl-Sc-Cl (avg) 98.7°; N-Sc-N 75.4°; Cl-Sc-Cl 91.9°.	69
Figure 4	<sup>1</sup> H NMR spectrum of <b>3b</b> acquired in benzene- <i>d</i> <sub>6</sub> .	70

Figure 5	$^1\text{H}$ NMR spectra of <b>3a</b> acquired in THF- $d_8$ solvent (top) and benzene- $d_6$ (bottom) reveal large solvent dependent chemical shifts of the coordinated Cn ligand <i>endo</i> - and <i>exo</i> -methylene multiplets and Sc-CH <sub>3</sub> (see also Figure 4 for comparison).	71
Figure 6	NMR data for the 2-butyne reaction product, <b>5</b> , are most consistent with the $\eta^1$ -allenyl isomer shown.	74
Figure 7	VT- $^1\text{H}$ NMR studies of <b>5</b> reveal large temperature dependant shifts for the allenyl moiety.	76
Figure 8	Comparison of <b>5</b> with Casey's propargyl complex (see text for details).	77
Figure 9	Acetylene coordination might be required.	78
Figure 10	$^1\text{H}$ NMR spectrum of the product from reaction of <b>3a</b> as indicated (see text for details).	80
Figure 11	$^1\text{H}$ NMR spectrum of the product from reaction of <b>3a</b> as indicated (see text for details).	81
<b>Appendix 3</b>		
Figure 1	ORTEP diagram for CnScCl <sub>3</sub> ( <b>2a</b> ) with 50% probability ellipsoids showing the atomic numbering scheme.	96
<b>Chapter 4</b>		
Figure 1	Enantiomers of <i>rac</i> -BpY-R.	105
Figure 2	Simple retrosynthetic analysis for synthesis of desired ligands. [aux] = C <sub>2</sub> -symmetric with specific interactions with TMS groups of Cp's.	107
Figure 3	Synthesis of some other linked ligands (see text for details).	107
Figure 4	One of each of the enantiomeric pairs of diastereomers for <i>rac</i> - <b>1</b> .	108
Figure 5	One of each of the enantiomeric pairs of diastereomers for [BnBp]Y-R.	110
Figure 6	Selected spectra from the reaction of BpYCH(TMS) <sub>2</sub> with H <sub>2</sub> (see text for details).	114
Figure 7	Only the homochiral dimer is possible when the starting compound is enantiopure.	115
Figure 8	$^1\text{H}$ NMR (hydride region) for reaction of the three complexes with H <sub>2</sub> .	116
Figure 9	Cache depiction of the crystallographically determined asymmetric unit <i>rac</i> - <b>5</b> .	

## List of Tables

### Chapter 1

Table 1	$^1\text{H}$ NMR Data	23
---------	-----------------------	----

### Appendix 2

Table 1	Crystal Data for $[\text{Cp}^*\text{Sc}\{\mu-(\eta^5, \eta^1)\text{-C}_5(\text{CH}_3)_4\text{CH}_2\}]_2$	57
Table 2	Final Refined Parameters for $[\text{Cp}^*\text{Sc}\{\mu-(\eta^5, \eta^1)\text{-C}_5(\text{CH}_3)_4\text{CH}_2\}]_2$	58
Table 3	Anisotropic Thermal Parameters for $[\text{Cp}^*\text{Sc}\{\mu-(\eta^5, \eta^1)\text{-C}_5(\text{CH}_3)_4\text{CH}_2\}]_2$	59
Table 4	Complete Distances and Angles for $[\text{Cp}^*\text{Sc}\{\mu-(\eta^5, \eta^1)\text{-C}_5(\text{CH}_3)_4\text{CH}_2\}]_2$	60
Table 5	Non-refined Hydrogen Atom Parameters for $[\text{Cp}^*\text{Sc}\{\mu-(\eta^5, \eta^1)\text{-C}_5(\text{CH}_3)_4\text{CH}_2\}]_2$	63

### Appendix 3

Table 1	Crystal Data for $\text{CnScCl}_3$ (2a).	96
Table 2	Final Heavy Atom Parameters for $\text{CnScCl}_3$ (2a).	97
Table 3	Anisotropic Displacement Parameters for $\text{CnScCl}_3$ (2a).	98
Table 4	Complete Distances and Angles for $\text{CnScCl}_3$ (2a).	99
Table 5	Non-refined Hydrogen Atom Parameters for $\text{CnScCl}_3$ (2a).	101

### Chapter 4

Table 1	$^1\text{H}$ NMR Data	118
---------	-----------------------	-----

## Chapter 1

# Competitive Chain Transfer by $\beta$ -Hydrogen and $\beta$ -Methyl Elimination for a Model Ziegler-Natta Olefin Polymerization System $[\text{Me}_2\text{Si}(\eta^5\text{-C}_5\text{Me}_4)_2]\text{Sc}\{\text{CH}_2\text{CH}(\text{CH}_3)_2\}(\text{PMe}_3)$ .

Abstract	2
Introduction	3
Results and Discussion	7
Conclusions	20
Experimental	26
References and Notes	32
Appendix	35

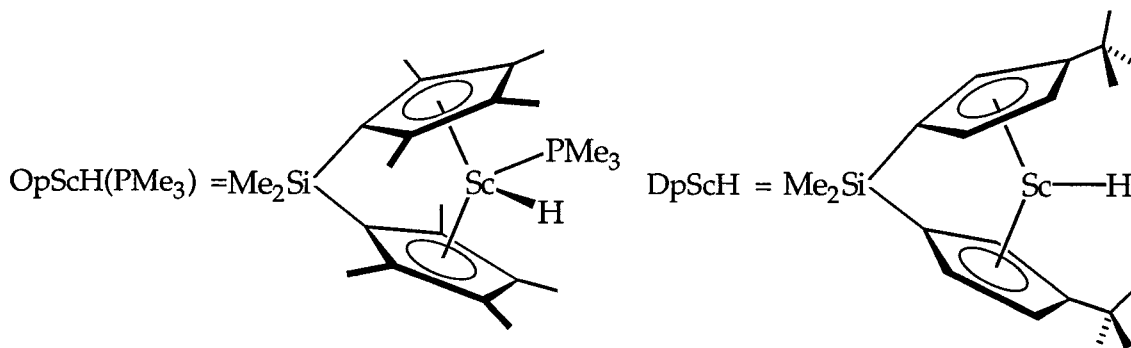
### Abstract

The reaction of  $\text{OpSc(H)(PMe}_3\text{)}$  ( $\text{Op} = \{(\eta^5\text{-C}_5\text{Me}_4)_2\text{SiMe}_2\}$ ) with isobutene produces  $\text{OpSc(CH}_3\text{)(PMe}_3\text{)}$  along with isobutane, 2-methylpentane, isobutene, 2-methyl-1-pentene, propane and *n*-pentane. These products arise from a series of reactions involving olefin insertion,  $\beta\text{-CH}_3$  and (faster)  $\beta\text{-H}$  elimination which proceeds until only the 2-methyl-1-alkenes ( $\text{C}_4\text{H}_8$ ,  $\text{C}_6\text{H}_{12}$ , *etc.*) and the predominant organoscandium product  $\text{OpSc(CH}_3\text{)(PMe}_3\text{)}$  remain. A transient observed in the reaction sequence has been characterized as  $\text{OpSc(CH}_2\text{CH}_2\text{CH}_3\text{)(PMe}_3\text{)}$ . Slower  $\sigma$  bond metathesis involving the methyl C-H bonds of  $\text{PMe}_3$  and the Sc-C bonds of the scandium alkyls accounts for the observation of saturated alkanes (2-methylalkanes ( $\text{C}_4\text{H}_{10}$ ,  $\text{C}_6\text{H}_{14}$ , *etc.*), normal alkanes ( $\text{C}_3\text{H}_8$ ,  $\text{C}_5\text{H}_{12}$ , *etc.*) as well as a minor organoscandium product  $\text{OpScCH}_2\text{PMe}_2$  in the product mixture.  $\beta$ -Ethyl migration is *not* observed for the closely related 2-ethyl-butyl derivative,  $\text{OpSc}\{\text{CH}_2\text{CH(C}_2\text{H}_5\text{)CH}_2\text{CH}_3\}\text{(PMe}_3\text{)}$ , obtained from reaction of 2-ethyl-1-butene with  $\text{OpSc(H)(PMe}_3\text{)}$ .

## Introduction

The scientific and industrial importance of Ziegler-Natta olefin polymerization has stimulated intensive research directed toward understanding the mechanistic aspects of this remarkable catalytic process.<sup>1</sup> Recently a number of research groups have developed soluble, relatively well defined Ziegler-Natta catalysts based on early transition metal metallocene derivatives.<sup>2</sup> These systems provide an unprecedented opportunity to understand the relationships between catalyst structure, activity and polymer microstructure.<sup>3</sup>

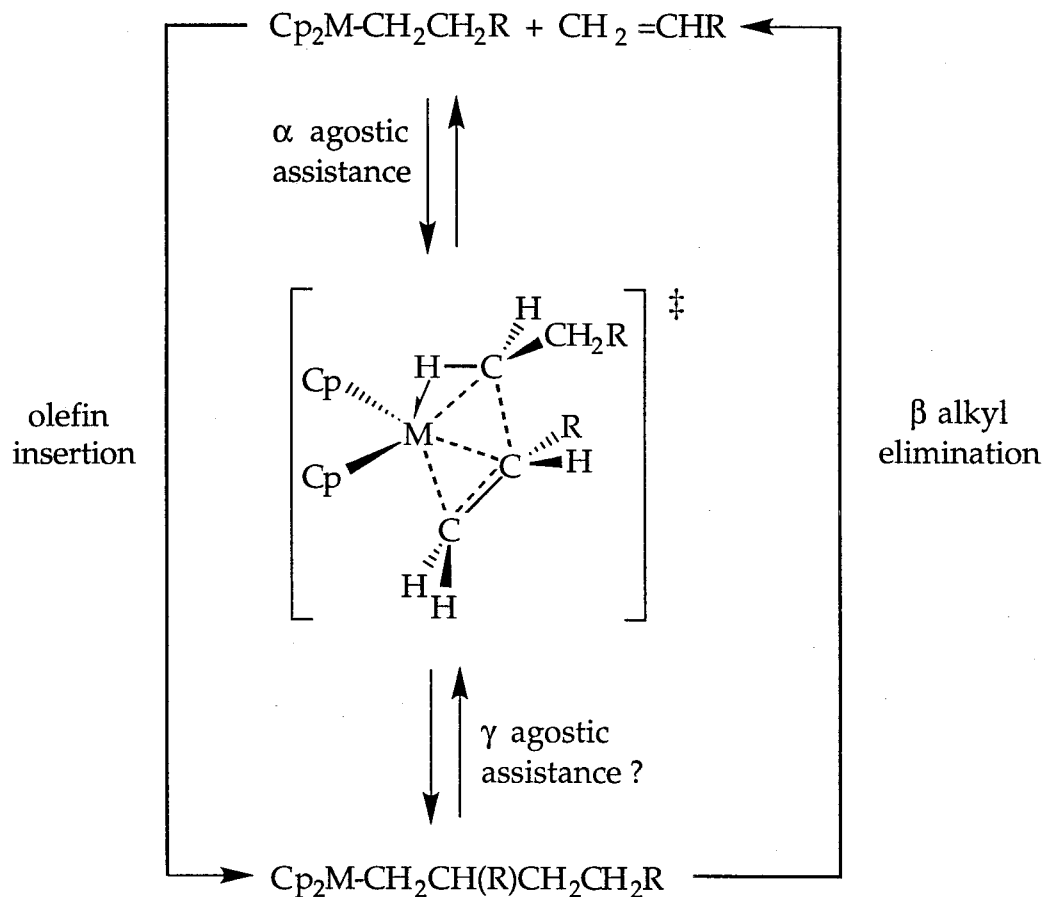
Development of Ziegler-Natta catalysts and catalyst model systems in this laboratory has concentrated largely on *bis*(cyclopentadienyl)scandium hydrides, alkyls and related compounds.<sup>4</sup> We have found that the linked scandocene derivatives  $\text{OpSc(H)(PMe}_3\text{)}$  (**1**) ( $\text{Op} = \{(\eta^5\text{-C}_5\text{Me}_4)_2\text{SiMe}_2\}$ ) and  $[\text{DpScH}]_2$  ( $\text{Dp} = \{(\eta^5\text{-C}_5\text{H}_3\text{CMe}_3)_2\text{SiMe}_2\}$ )<sup>5</sup> undergo a variety of reactions relevant to Ziegler-Natta catalysis (*e.g.* olefin insertion,  $\beta$ -H elimination,  $\beta$ -alkyl elimination).<sup>6</sup>



For example, both of these complexes are efficient catalysts for the dimerization and hydrodimerization of  $\alpha$ -olefins, as well as the cyclization and hydrocyclization of C6-C10  $\alpha,\omega$ -dienes to methylene cycloalkanes and methylcycloalkanes (*e.g.* eq 1-4).<sup>7</sup>

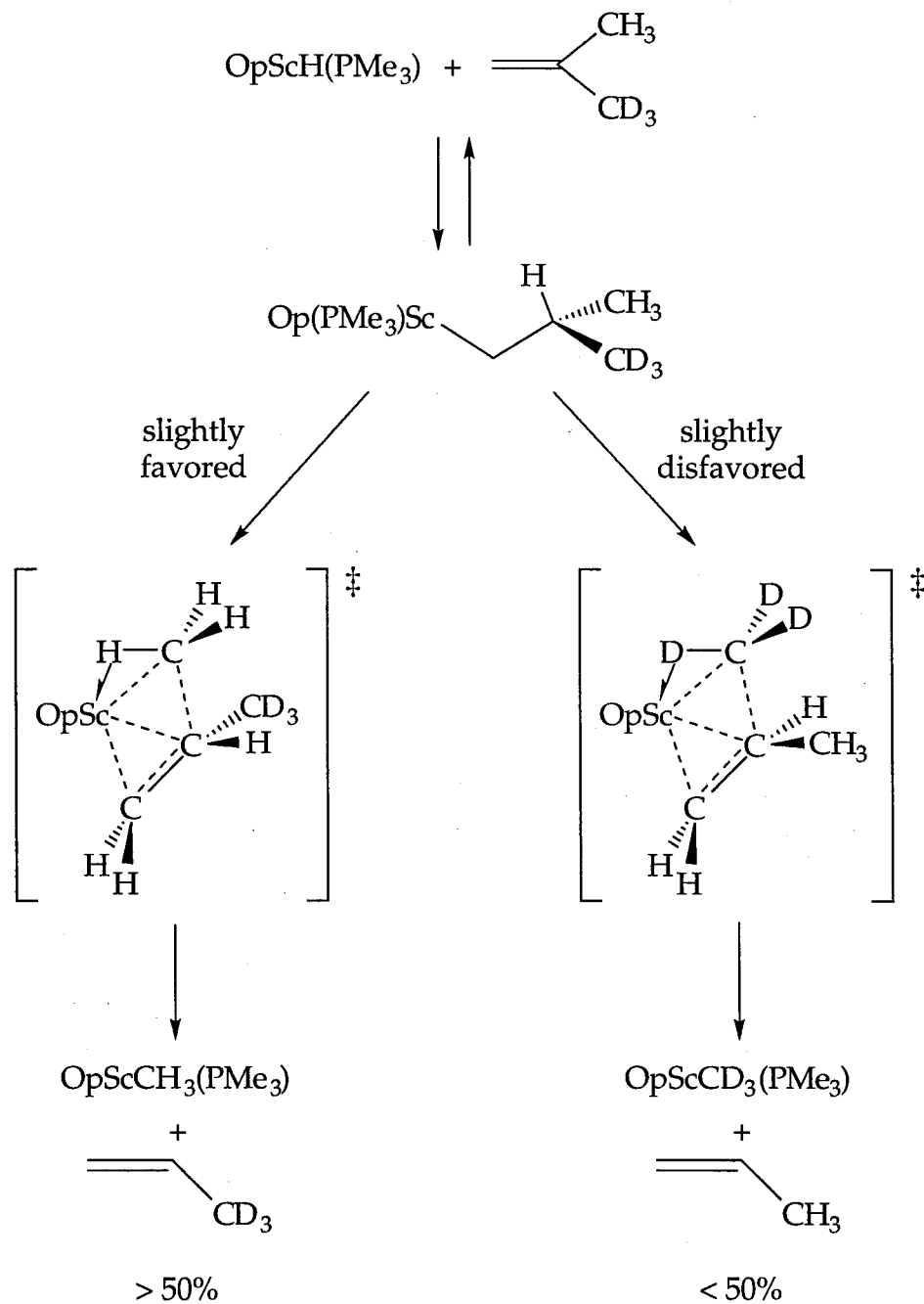


elimination. As shown below, the  $\beta$ -alkyl elimination reaction can be viewed as the microscopic reverse of the olefin insertion step for the chain propagation step in Ziegler-Natta polymerizations.



Given the recent results implicating an  $\alpha$ -agostic assisted pathway for olefin insertion in these<sup>11</sup> and related systems,<sup>12</sup> we expected that the reverse reaction should also proceed through an agostic transition state (*i.e.* a  $\gamma$ -agostic assisted alkyl migration). We reasoned that if a  $\gamma$ -agostic transition state were indeed operative in the  $\beta$ -Me elimination step, it would manifest itself in a measureably perturbed isotopic distribution<sup>13</sup> in the products resulting from the appropriately deuterium labeled reactants, as shown below.





Indeed, when the reaction is carried out as outlined above, formation of the organoscandium reaction product,  $\text{OpScCX}_3\text{(PMe}_3\text{)}$  ( $\text{X} = \text{H, D}$ ), proceeds with an observed isotope effect of  $k_{\text{CH}_3}/k_{\text{CD}_3} = 1.3$ , which is in the range expected from the previous studies. However, attempts to measure the complimentary isotope effect in the expected propene coproduct revealed that it had been taken

on to other products during the course of the reaction. These results both implicate a more complicated reaction pathway than that assumed above, and also preclude interpretation of the observed isotope effect in terms of a  $\gamma$ -agostic transition state. In the hopes of clarifying the mechanistic course of this reaction, we have carefully examined the reactivity of  $\text{OpSc(H)(PMe}_3\text{)}$  with isobutene and other *gem*-disubstituted olefins. These studies reveal that chain transfer by  $\beta$ -CH<sub>3</sub> elimination is complicated by competitive  $\beta$ -H elimination in this system and that  $\beta$ -elimination of higher alkyls does not occur.

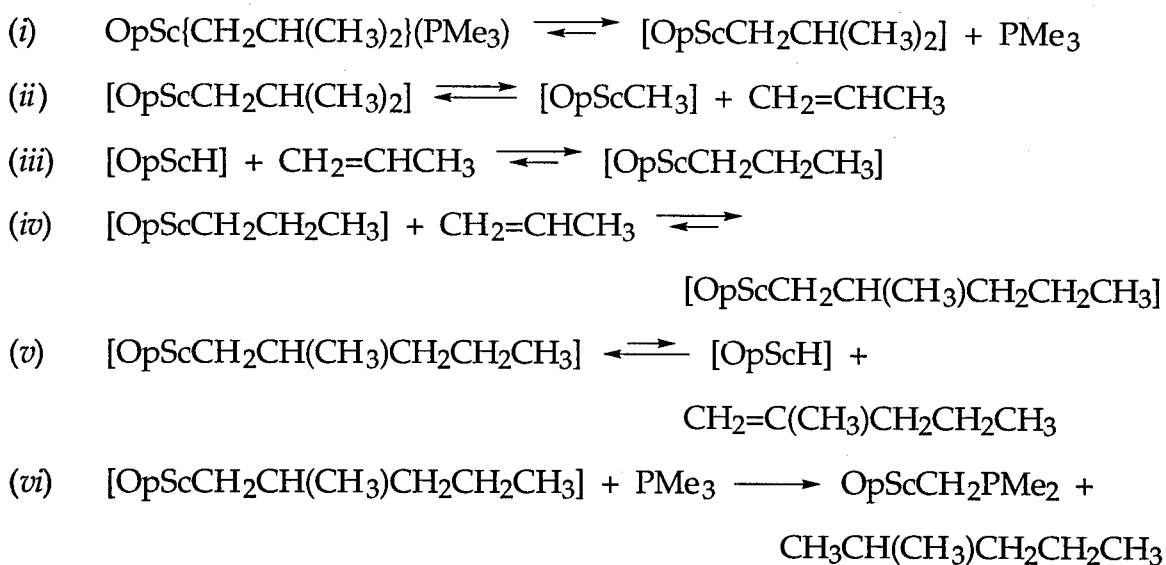
## Results and Discussion

**Reaction of  $\text{OpSc(H)(PMe}_3\text{)}$  with Isobutene: Identification of Products and Proposed Reaction Scheme.** Isobutene adds quickly and cleanly to  $\text{OpSc(H)(PMe}_3\text{)}$  (1) affording  $\text{OpSc}\{\text{CH}_2\text{CH}(\text{CH}_3)_2\}(\text{PMe}_3)$  (2). The isobutyl complex 2 then slowly rearranges to afford the previously reported methyl derivative  $\text{OpSc}(\text{CH}_3)(\text{PMe}_3)$ , implicating  $\beta$ -CH<sub>3</sub> elimination of propene. Free propene, however, is not detected by monitoring the process by <sup>1</sup>H NMR spectroscopy. Rather, careful examination of spectra and gas chromatographic analysis reveals the diverse set of products shown in Scheme 1.<sup>14</sup> The processes proposed to account for the formation of both the major organoscandium product  $\text{OpSc}(\text{CH}_3)(\text{PMe}_3)$  (3), the minor one  $\text{OpScCH}_2\text{PMe}_2$  (4) as well as the hydrocarbons are outlined in Scheme 2. Five separate processes are invoked: (1) reversible loss of trimethylphosphine from the hydride and alkyl derivatives, (2) reversible insertions of both *gem*-disubstituted and  $\alpha$ -olefins into the Sc-H bond of  $[\text{OpScH}]$  affording 2-methylalkyl and *n*-alkyl derivatives, respectively, (3)  $\beta$ -CH<sub>3</sub> elimination for the 2-methylalkyl derivatives, yielding  $\alpha$ -olefin and



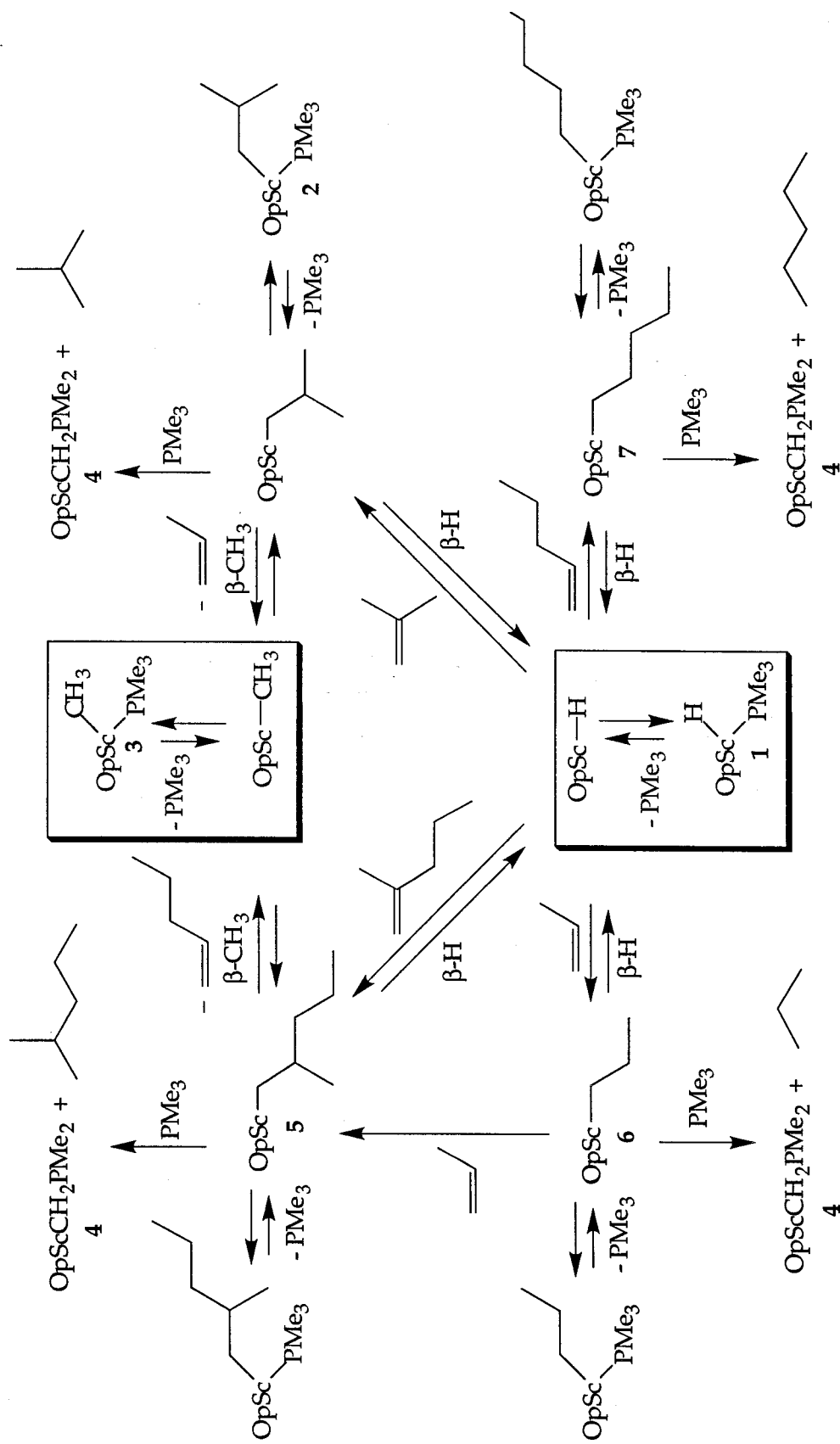
[OpScCH<sub>3</sub>], (4) insertion of  $\alpha$ -olefin into Sc-C bonds of the *n*-alkyl derivatives, and (5)  $\sigma$  bond metathesis<sup>15</sup> of a scandium-carbon bond of the scandium alkyls with a methyl C-H bond of trimethylphosphine affording alkane and OpScCH<sub>2</sub>PMe<sub>2</sub> (4).<sup>16</sup>

The two C<sub>6</sub> products, 2-methylpentane and 2-methyl-1-pentene, are formed from OpSc{CH<sub>2</sub>CH(CH<sub>3</sub>)<sub>2</sub>}(PMe<sub>3</sub>) by (i) loss of PMe<sub>3</sub>, (ii)  $\beta$ -CH<sub>3</sub> elimination from [OpScCH<sub>2</sub>CH(CH<sub>3</sub>)<sub>2</sub>] releasing propene, (iii) addition of propene to [OpSc-H], which is in equilibrium with all alkyl derivatives except OpSc(CH<sub>3</sub>)(PMe<sub>3</sub>), (iv) a second insertion of propene to yield [OpScCH<sub>2</sub>CH(CH<sub>3</sub>)CH<sub>2</sub>CH<sub>2</sub>CH<sub>3</sub>], which can then undergo (v)  $\beta$ -H elimination to [OpSc-H] and 2-methyl-1-pentene, or (vi)  $\sigma$  bond metathesis with PMe<sub>3</sub> yielding 2-methylpentane and OpScCH<sub>2</sub>PMe<sub>2</sub> (4).

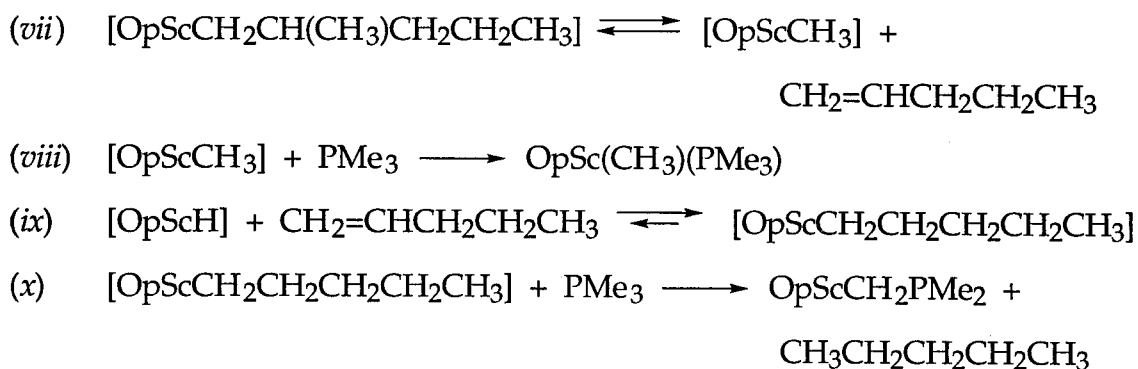


Perhaps most surprising is the observation of *n*-pentane in the product mixture. According to the proposed scheme, it is formed by the same beginning steps (i) - (iv), followed by (vii)  $\beta$ -CH<sub>3</sub> elimination of 1-pentene from [OpScCH<sub>2</sub>CH(CH<sub>3</sub>)CH<sub>2</sub>CH<sub>2</sub>CH<sub>3</sub>], which after trapping with PMe<sub>3</sub> (viii) leads to

Scheme 2



the major organoscandium product  $\text{OpSc}(\text{CH}_3)(\text{PMe}_3)$ , (ix) reaction of 1-pentene with  $[\text{OpScH}]$  to yield  $[\text{OpScCH}_2\text{CH}_2\text{CH}_2\text{CH}_2\text{CH}_3]$ , and finally (x)  $\sigma$  bond metathesis with  $\text{PMe}_3$  yielding *n*-pentane and  $\text{OpScCH}_2\text{PMe}_2$ .



Interestingly, the only olefins present at the end of this complex reaction sequence are *gem*-disubstituted 2-methyl-1-alkenes; the  $\alpha$ -olefins (propene, 1-pentene) re-enter the sequence by addition to  $[\text{OpScH}]$  or  $[\text{OpScCH}_3]$ , ultimately resulting in the normal  $\text{C}_{\text{odd}}$  alkane or a  $\text{C}_{\text{even}}$  2-methyl-1-alkene or 2-methylalkane.

**$^1\text{H}$ -NMR Observation of Reaction Intermediates and Relative Affinities for Trimethylphosphine.** Although the reaction of  $\text{OpSc}(\text{H})(\text{PMe}_3)$  with isobutene is far too complex for meaningful kinetic analysis, we did follow the course of the reaction by  $^1\text{H}$  NMR spectroscopy in an attempt to identify any intermediates predicted by the working mechanistic hypothesis shown in Scheme 2. Thus, **1** and isobutene were allowed to react in an NMR tube in cyclohexane- $d_{12}$ .  $^1\text{H}$  spectra were automatically acquired regularly over a period of about 12 hours, spectra were analyzed in conventional 1-D form, and white-wash stacked plots of the spectra were generated. This form of presentation of the data makes following the appearance and disappearance of reactants, products, and intermediates much easier than analysis of the same

data as a series of conventional 1-dimensional spectra.

An example of the utility of these plots is shown in Figure 1, which highlights a set of resonances characteristic of the one of the two equivalent<sup>17</sup> Op-ligand methyl groups (likely the  $\alpha$  methyl groups)<sup>18</sup> of the OpSc-alkyl complexes. As can be seen the  $^1\text{H}$  NMR resonance attributed to the isobutyl complex **2** decreases with time while that for the product methyl **3** increases. An additional resonance is clearly observed to grow in and eventually disappear. This intermediate has been identified as  $\text{OpSc}(\text{CH}_2\text{CH}_2\text{CH}_3)(\text{PMe}_3)$  (**6**) by independent synthesis from  $\text{OpSc}(\text{H})(\text{PMe}_3)$  and propene (*vide infra*).

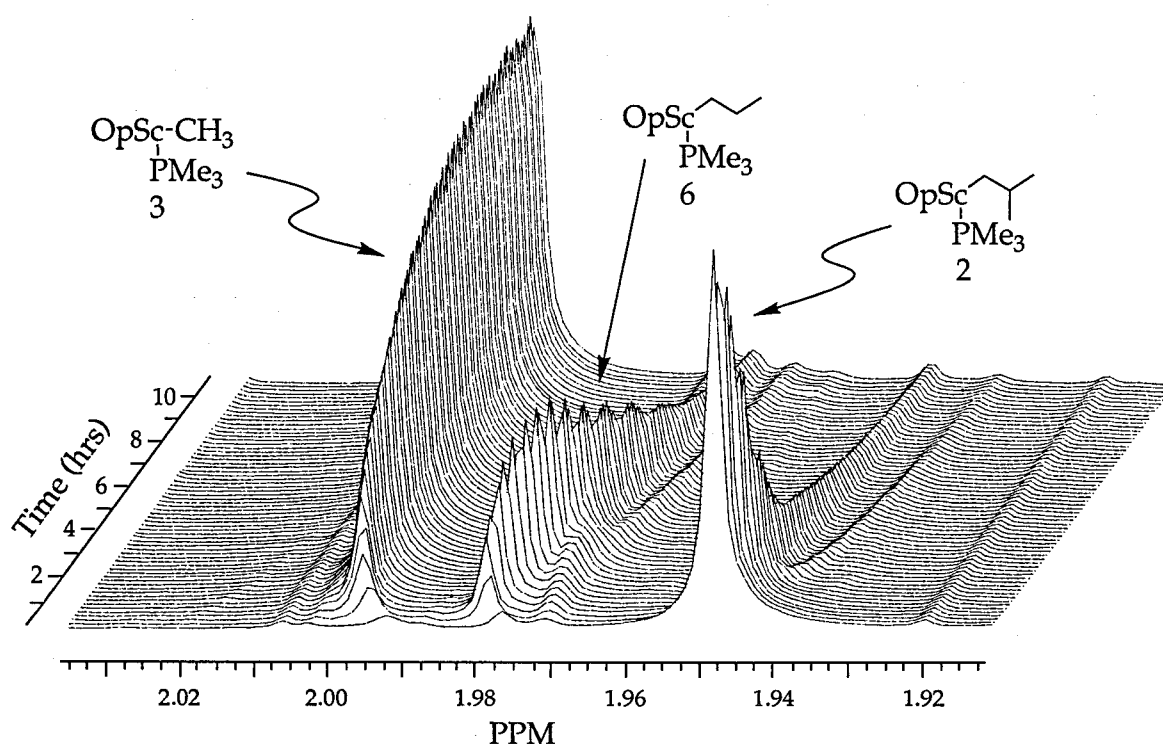


**Figure 1.** Reaction of **1** with isobutene: white-wash stack plots (chemical shift vs time) of characteristic (Op ligand  $(\text{CH}_3)_\alpha$ ) resonances for the major organometallic species (**2**, **3**, and **6**) during the course of the reaction.

As illustrated in Figure 2, integrations reveal roughly a constant sum for these three resonances over the course of the reaction. Thus, no other organoscandium intermediates grow in to detectable levels of concentration.

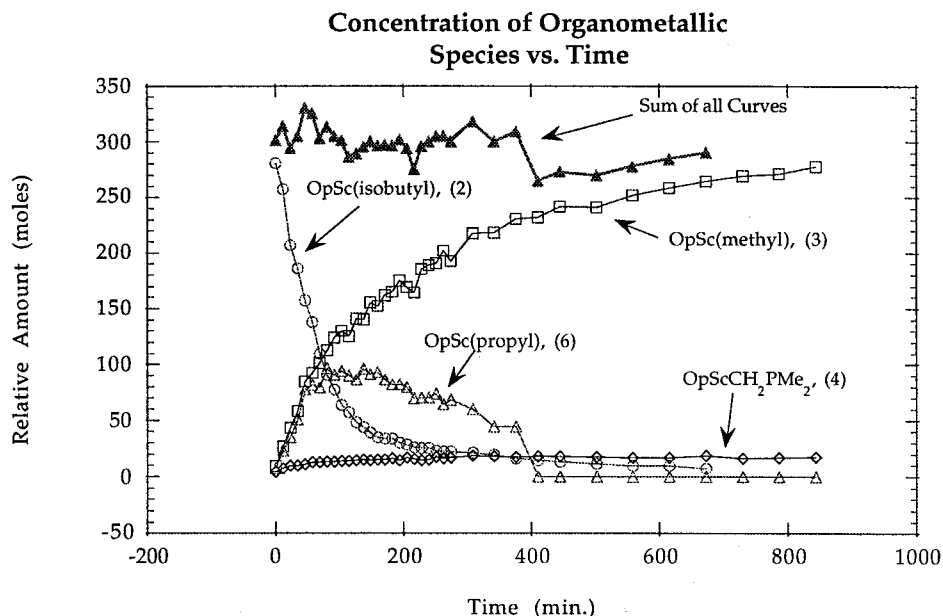
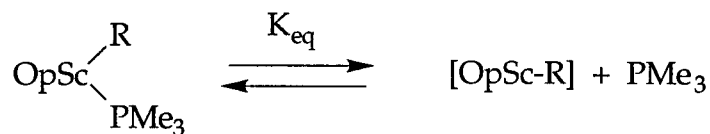


**Figure 2.** Integrated data for the major organometallic species reveals roughly a constant sum over the reaction course.

Close examination of the time course of the chemical shifts reveals a smooth change, and it is particularly obvious in Figure 3, where the contour plots (bottom) illustrate the dramatic chemical shift changes for the  $(\text{CH}_3)_\beta$  for **2** and the transient **6**. We attribute this chemical shift variation with time to a gradual decrease in the concentration of free trimethylphosphine as **2** converts to **3**. Since the observed  $^1\text{H}$  chemical shift represents a weighted average of that for the trimethylphosphine-bound and trimethylphosphine-free alkyl species, the average shift varies with  $[\text{PMe}_3]_{\text{free}}$ . Whereas we have not attempted to quantify the trimethylphosphine binding constants, simple steric arguments predict the following order:





$$(K_{\text{eq}})^{\text{R}=\text{H}} < (K_{\text{eq}})^{\text{R}=\text{CH}_3} < (K_{\text{eq}})^{\text{R}=\text{CH}_2\text{CH}_2\text{CH}_3} < (K_{\text{eq}})^{\text{R}=\text{CH}_2\text{CHMe}_2} < (K_{\text{eq}})^{\text{R}=\text{CH}_2\text{CHMeR}'}$$

Thus, as the isobutyl derivative, **2** (which binds trimethylphosphine relatively weakly), proceeds to the methyl derivative, **3** (which tightly binds trimethylphosphine), the  $[\text{PMe}_3]_{\text{free}}$  gradually decreases.

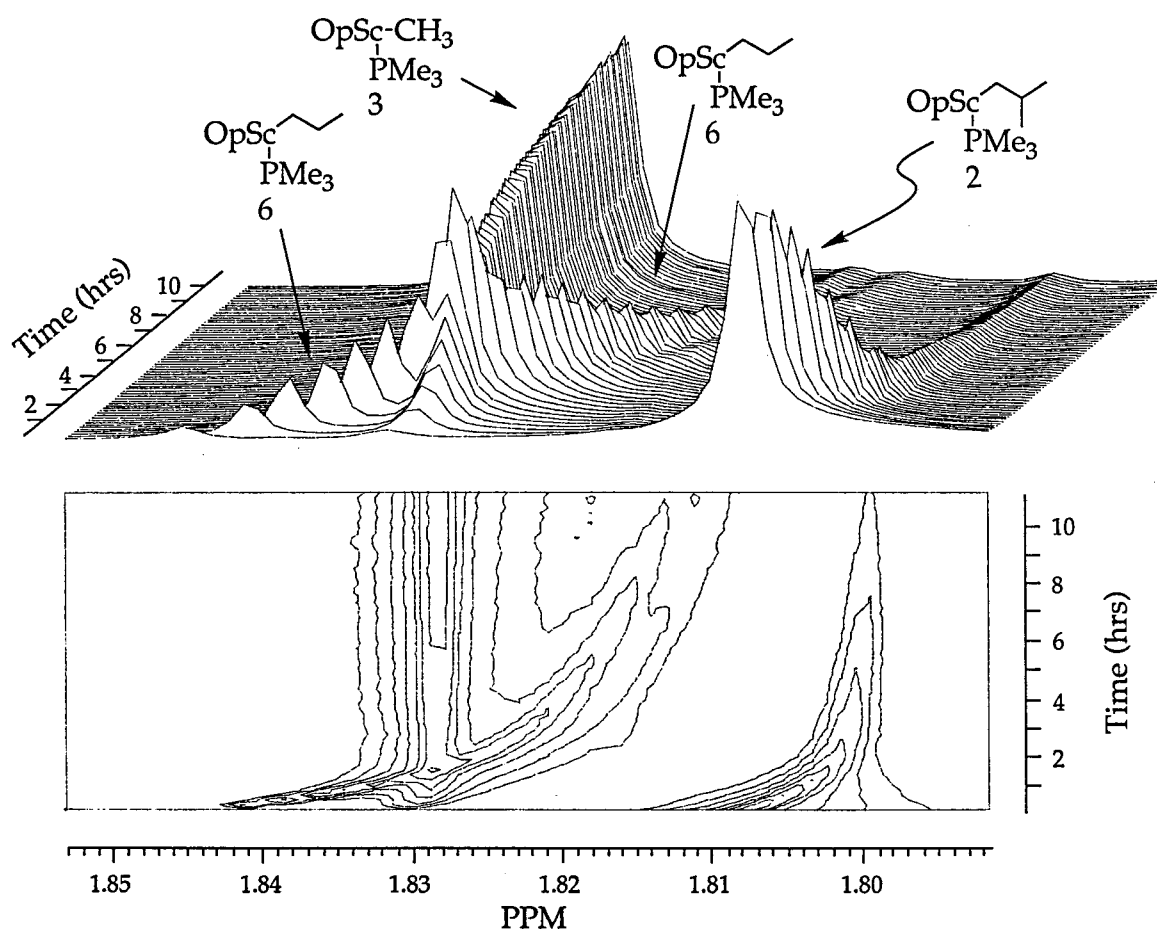


**Figure 3.** Reaction of **1** with isobutene: (top) white-wash stack plots (chemical shift vs time) highlighting the time dependent chemical shifts of characteristic (Op ligand  $(\text{CH}_3)_\beta$ ) resonances for **2**, **3**, and **6**) during the course of the reaction, and (bottom) contour plots of the same resonances (see text for details).

The propyl derivative **6**, with its intermediate affinity for trimethylphosphine, exhibits the greatest variation in relative concentrations for **6** and the trimethylphosphine-free species  $[\text{OpScCH}_2\text{CH}_2\text{CH}_3]$  as can be seen in Figure 4, which highlights Sc- $\alpha$ -CH<sub>2</sub> region of the <sup>1</sup>H NMR spectra during the course of the reaction.

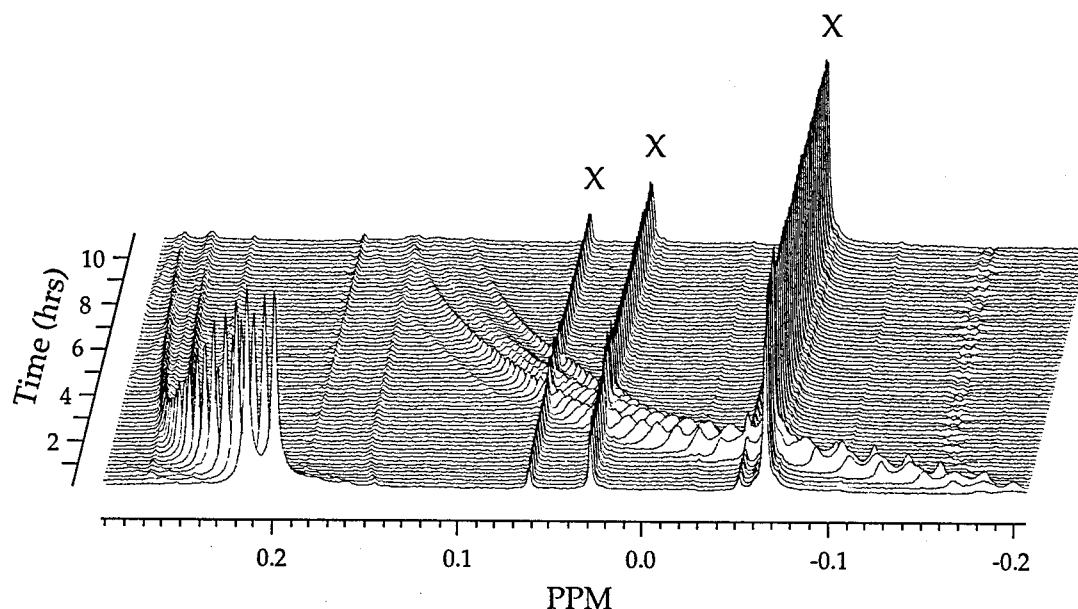


**Figure 4.** Reaction of **1** with isobutene: time course for the Sc- $\alpha$ -hydrogen resonances for **2** and **6**. The upfield doublet is assigned to **2** and the downfield multiplet to **6**. The other three peaks (x) are due to constant, non-reactive impurities.

Also in support of a much larger trimethylphosphine affinity for the methyl derivative **3** *vs.* the isobutyl derivative **2** is the observation that *ca.* 80% of the trimethylphosphine can be removed with solvent cyclohexane *in vacuo* when a solution of  $\text{OpSc}[\text{CH}_2\text{CH}(\text{CH}_3)_2](\text{PMe}_3)$  (**2**) is taken to dryness. By contrast, trimethylphosphine is nearly entirely retained when solutions of the methyl derivative **3** are treated similarly. Interestingly, when the (80%) phosphine-free isobutyl derivative so obtained rearranges to the methyl derivative upon redissolving in cyclohexane, large chemical shift changes (Figure 5) accompany the Sc-CH<sub>3</sub> resonance for this phosphine "starved" system; the signals for the

isobutyl show relatively little change in chemical shift over the course of the reaction. These observations are consistent with the relative ordering of trimethylphosphine affinity listed.

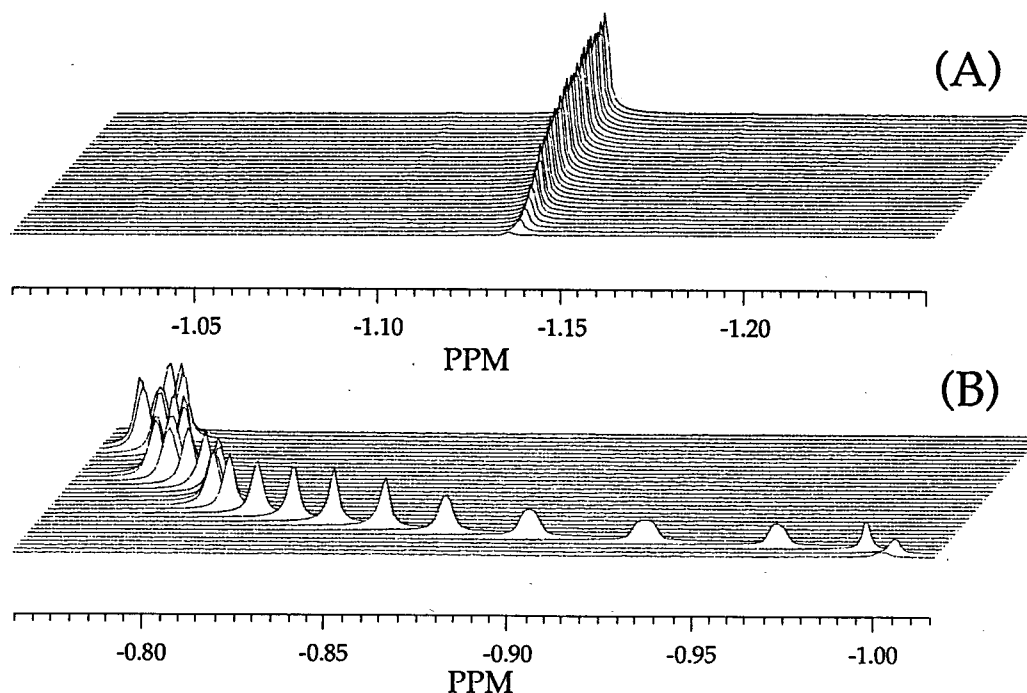


**Figure 5.** Reaction of 1 with isobutene: (a) time course for the Sc-CH<sub>3</sub> resonance of 2 and (b) the same resonance in the PMe<sub>3</sub>-depleted rearrangement (see text for details).

As shown in Figure 6, addition of an eleven-fold excess of PMe<sub>3</sub> to solutions of 2 slows the rate of conversion to 3, but only increases the half-time for reaction by about a factor of three, again supporting the implication that under the conditions of the NMR experiments trimethylphosphine is substantially dissociated from 2. Addition of 1 and 2 equivalents of PMe<sub>3</sub> slows the reaction almost imperceptibly. Addition of a six-fold excess of isobutene slows the conversion half time by less than a factor of 1.5; the cause of this effect is not obvious.

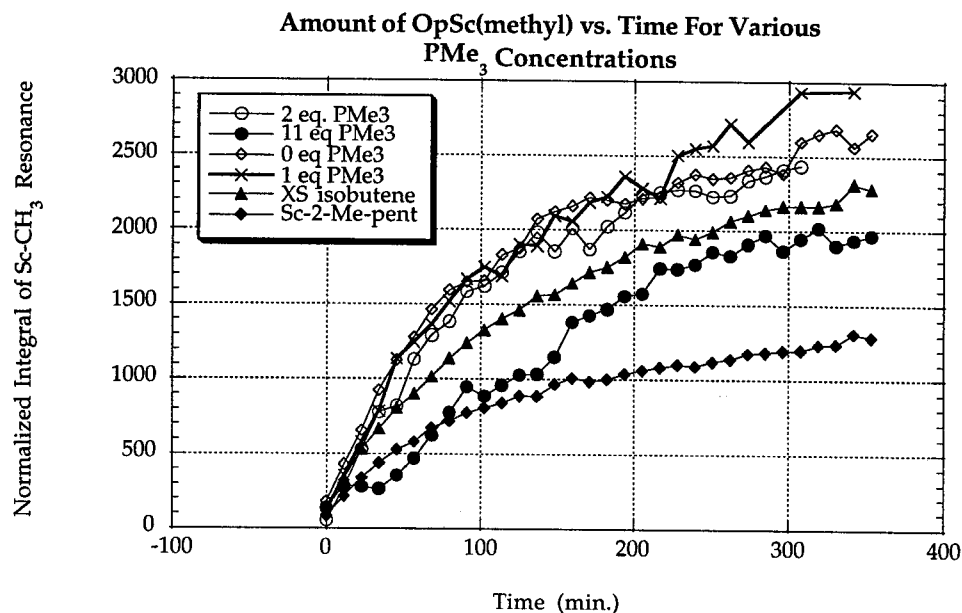
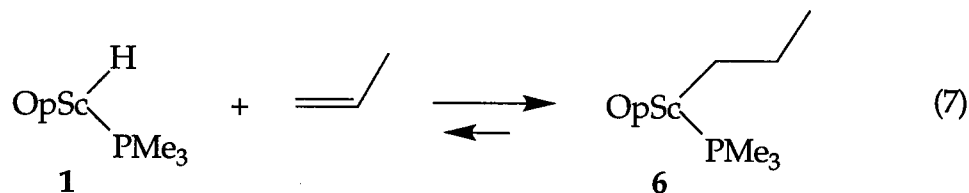


**Figure 6.** Integrated data for the major organometallic species reveals roughly a constant sum over the reaction course.

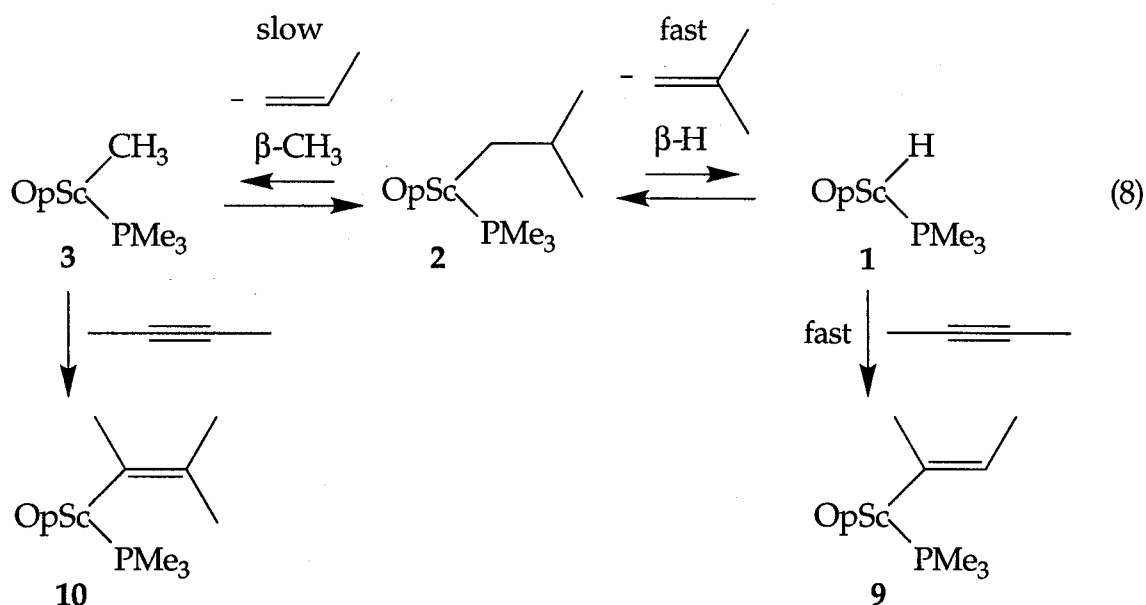
**Model Reactions of Suspected Reaction Intermediates.** The identity of the propyl intermediate,  $\text{OpSc}(\text{CH}_2\text{CH}_2\text{CH}_3)(\text{PMe}_3)$  (**6**) has been confirmed by its independent synthesis (eq 7).



This reaction is readily reversed, and a number of the other reactions proposed in Scheme 2 ensue, as is apparent by monitoring the course of the reaction of **1** with two equivalents of propene. Thus, whereas the first product is indeed **6**, it ultimately rearranges to the now familiar methyl derivative **3** and a lesser amount of  $\text{OpScCH}_2\text{PMe}_2$  (**4**), along with the hydrocarbons, 2-methylpentene

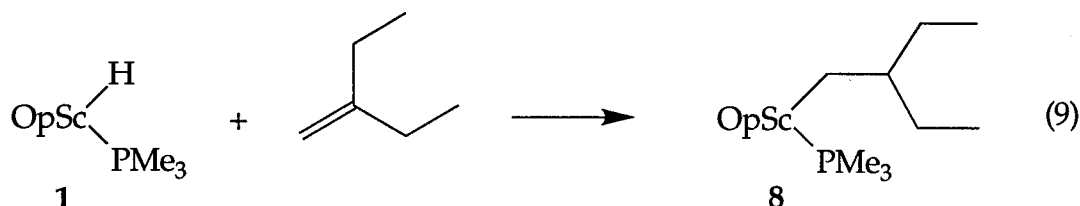
and a small amount of pentane.<sup>19</sup> These same products are also obtained by treating  $\text{OpSc(H)(PMe}_3\text{)}$  with 2-methylpentene, again in accord with Scheme 2.

The facility of  $\beta$ -H elimination for the isobutyl derivative is illustrated by its rapid reaction with 2-butyne, wherein an immediate conversion to isobutene and  $\text{OpSc}\{\text{C(CH}_3\text{)=CH(CH}_3\text{)}\}(\text{PMe}_3)$  (**9**) is observed (eq 8). Moreover, addition of a 1:1 mixture of 2-butyne and propene to **3** affords primarily  $\text{OpSc}\{\text{C(CH}_3\text{)=C(CH}_3\text{)}_2\}(\text{PMe}_3)$  (**10**). Since <5% of **10** is generated in the reaction of **2** with 2-butyne, we may conclude that in the reaction of  $\text{OpSc}\{\text{CH}_2\text{CH(CH}_3\text{)}_2\}(\text{PMe}_3)$  (**2**) with  $\text{CH}_3\text{C}\equiv\text{CCH}_3$ ,  $\beta$ - $\text{CH}_3$  elimination and propene insertion for **3** are slow, compared to  $\beta$ -H elimination for **2** and trapping of **1** by 2-butyne.

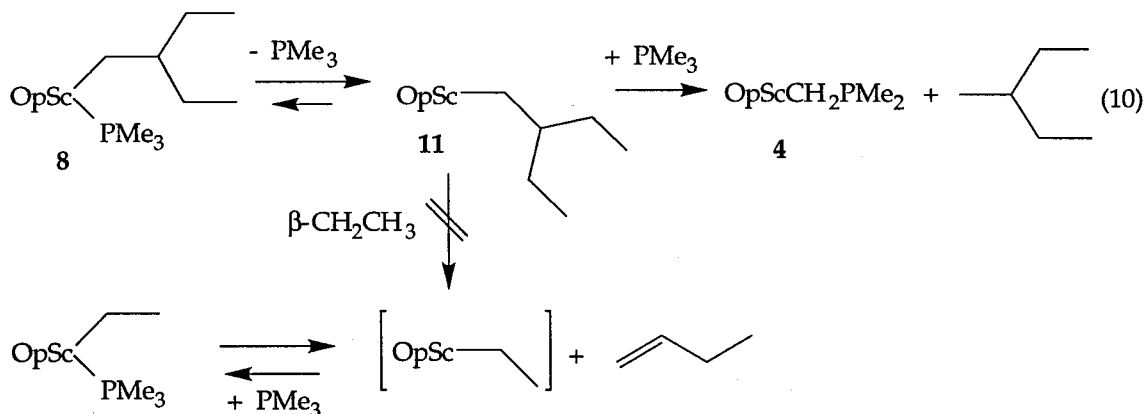


An important implication is that  $\beta$ -H elimination is faster than  $\beta$ -methyl elimination. Moreover, alkyls such as **2** may effectively act as reservoirs of the very reactive hydride,  $[\text{OpScH}]$ , capable of promoting the dimerization of  $\alpha$  olefins, even when both are at relatively low concentrations.

**OpSc{CH<sub>2</sub>CH(CH<sub>2</sub>CH<sub>3</sub>)<sub>2</sub>}(PMe<sub>3</sub>): β-Ethyl Elimination?** Given the facility of β-methyl elimination for OpSc{CH<sub>2</sub>CH(CH<sub>3</sub>)<sub>2</sub>}(PMe<sub>3</sub>) and the 2-methyl-1-pentyl derivative, we wondered whether β elimination of higher alkyls could also proceed. Treatment of **1** with 2-ethyl-1-butene cleanly affords OpSc{CH<sub>2</sub>CH(CH<sub>2</sub>CH<sub>3</sub>)<sub>2</sub>}(PMe<sub>3</sub>) (**8**) (eq 9).



Unlike the isobutyl derivative for which β-CH<sub>3</sub> begins immediately upon formation, there is no evidence for β-CH<sub>2</sub>CH<sub>3</sub> elimination for **8**. There is no indication (<sup>1</sup>H NMR) for a new alkyl OpSc(CH<sub>2</sub>CH<sub>3</sub>)(PMe<sub>3</sub>), nor do any products arise from dimerization, *etc.* of 1-butene by **1**. Rather, **8** only undergoes a slow decomposition to **4** and 3-methylpentane over the period of several days.



The very low affinity of the 2-ethylbutyl derivative **8** for trimethylphosphine allows the isolation of OpScCH<sub>2</sub>CH(CH<sub>2</sub>CH<sub>3</sub>)<sub>2</sub> (**11**) by slow removal of PMe<sub>3</sub> along with solvent cyclohexane when solutions of **8** are taken to dryness. When dissolved in cyclohexane-*d*<sub>12</sub> **11** is stable for days at 25°C, with

no evidence of reactions (*i.e.* generation of 1-butene dimer) that would be expected should  $\beta$ -CH<sub>2</sub>CH<sub>3</sub> elimination occur.

## Conclusions

The organoscandium derivatives  $\text{OpScCH}_2\text{CH}(\text{CH}_3)\text{R}$  offered an opportunity to examine competitive  $\beta$ -H,  $\beta$ -CH<sub>3</sub> and  $\beta$ -R elimination. The decomposition of the isobutyl derivative,  $\text{OpSc}[\text{CH}_2\text{CH}(\text{CH}_3)_2](\text{PMe}_3)$ , proved to be rather complex, but nonetheless revealing. Whereas a facile and reversible  $\beta$ -H elimination of isobutene is maintained (Scheme 3), decomposition begins with the slower  $\beta$ -CH<sub>3</sub> elimination to propene and the stable methyl derivative. The further reactions of propene (dimerization, *etc.*) immediately catalyzed by  $[\text{OpScH}]$ , provides the thermodynamic driving force for the undoubtedly endothermic  $\beta$ -CH<sub>3</sub> elimination from  $\text{OpSc}[\text{CH}_2\text{CH}(\text{CH}_3)_2](\text{PMe}_3)$ . Free propene is not in evidence; rather it is immediately converted to the reactive propyl derivative by reaction with  $[\text{OpScH}]$ , and a commensurate amount of free isobutene is released. As additional propene is released, further reaction with  $\text{OpSc}(\text{CH}_2\text{CH}_2\text{CH}_3)(\text{PMe}_3)$  ensues (Scheme 3). This propensity for alkyls capable of  $\beta$ -H eliminating to provide catalytically very reactive  $[\text{OpScH}]$  is perhaps best illustrated by the observation that treatment  $\text{OpSc}(\text{CH}_3)(\text{PMe}_3)$  (**3**) with propene does not, in fact, result in buildup of the isobutyl derivative **2**. When a small amount of **2** is formed, it immediately undergoes  $\beta$ -H elimination to isobutene, and the  $[\text{OpScH}]$  so generated rapidly catalyzes the dimerization, *etc.* of the remaining propene according to Scheme 2.

Formation of  $\text{OpScCH}_2\text{PMe}_2$  (**4**) via  $\sigma$  bond metathesis between  $\text{PMe}_3$  and the alkyl derivatives is especially clean for the 2-ethyl-butyl derivative, since no

other reaction pathways are available, apart from reversible (and non-productive)  $\beta$ -H elimination. Alkane formation thus results by this previously unrecognized catalyst deactivation pathway<sup>20</sup> leading to very stable **4**.<sup>21</sup>

Competitive  $\beta$ -H and  $\beta$ -CH<sub>3</sub> elimination have been noted previously in propylene polymerization;  $\beta$ -CH<sub>3</sub> elimination is now recognized as an important, and in some cases dominant chain transfer step.<sup>22</sup> Both Teuben and Resconi have noted that for the sterically crowded *bis*(pentamethylcyclopentadienyl)zirconium and -hafnium systems, chain transfer by  $\beta$ -CH<sub>3</sub> elimination dominates. Furthermore, Resconi was able to quantify the ratio of rate constants for the two processes by NMR analysis of end groups.  $\beta$ -CH<sub>3</sub> was found to be *ca.* 10 times faster for zirconium and as much as 50 times preferred for the hafnium system. Interestingly, for the less crowded  $[(\eta^5\text{-C}_5\text{H}_5)_2\text{M}]$  (M = Zr, Hf) systems,  $\beta$ -H elimination is preferred over  $\beta$ -CH<sub>3</sub> elimination by at least a factor of 100. These findings have been rationalized on the basis that for the  $\beta,\beta$ -disubstituted alkyl intermediates,  $[\text{Cp}^*_2\text{M-CH}_2\text{CH}(\text{CH}_3)\text{R}]^+\text{X}^-$ , unfavorable steric interactions between the Cp\* ligands and the two  $\beta$  alkyl substituents destabilize the transition state for  $\beta$ -H elimination. Our findings that  $\beta$ -H elimination dominates for the more open, linked *bis*(cyclopentadienyl) system,  $\text{OpScCH}_2\text{CH}(\text{CH}_3)\text{R}$ , may be accommodated by these same arguments.<sup>23</sup> Even though  $\beta$ -H elimination is dominant,  $\beta$ -CH<sub>3</sub> elimination is clearly in evidence, most convincingly demonstrated by the eventual generation of >95%  $\text{OpSc}(\text{CH}_3)(\text{PMe}_3)$  from  $\text{OpSc}\{\text{CH}_2\text{CH}(\text{CH}_3)_2\}(\text{PMe}_3)$ . The reluctance of  $\text{OpSc}\{\text{CH}_2\text{CH}(\text{CH}_2\text{CH}_3)_2\}(\text{PMe}_3)$  (**8**) and coordinatively even less saturated  $\text{OpScCH}_2\text{CH}(\text{CH}_2\text{CH}_3)_2$  (**11**) to undergo  $\beta$ -ethyl elimination is also in accord with the findings of Resconi, who reported that for 1-butene polymerizations, chain transfer by  $\beta$ -C<sub>2</sub>H<sub>5</sub> does not



occur, even for the *bis*(pentamethycyclopentadienyl)zirconium and -hafium catalysts.

We are resigned to conclude that, on the one hand, this system is not amenable to the desired interpretation of the observed isotope effect ( $k_{\text{CH}_3}/k_{\text{CD}_3} = 1.3$ , *vide supra*) in terms of a competitive  $\gamma$ -agostic transition state for  $\beta$ -methyl elimination. On the other hand,  $\beta$ -CX<sub>3</sub> (X = H,D) elimination is apparently, on average, slightly favored for X = H over X = D. This intriguing result implicates involvement of the methyl C-X bonds in the rate determining step for the reaction; however, the precise mechanistic nature of this involvement remains to be elucidated.

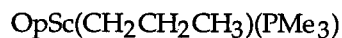
Table 1.  $^1\text{H}$  NMR Data<sup>a</sup>.

Compound	Assignment	$\delta(\text{ppm})$
<hr/>		
OpSc[CH <sub>2</sub> CH(CH <sub>3</sub> ) <sub>2</sub> ](PMe <sub>3</sub> )		
(2)	(CH <sub>3</sub> ) <sub>2</sub> Si	0.948 (s)
	( $\eta^5$ -C <sub>5</sub> (CH <sub>3</sub> ) <sub>4</sub> ) <sub>2</sub>	1.951 (s,12H) ; 1.819 (s,12H)
	ScCH <sub>2</sub> CH(CH <sub>3</sub> ) <sub>2</sub>	0.207 (d), $^3J_{\text{H-H}}=7.55$ Hz
	ScCH <sub>2</sub> CH(CH <sub>3</sub> ) <sub>2</sub>	2.22 (m)
	ScCH <sub>2</sub> CH(CH <sub>3</sub> ) <sub>2</sub>	0.715 (d), $^3J_{\text{H-H}}=6.42$ Hz
	P(CH <sub>3</sub> ) <sub>3</sub>	0.977 (br)
OpSc(CH <sub>3</sub> )(PMe <sub>3</sub> ) <sup>b</sup>		
(3)	(CH <sub>3</sub> ) <sub>2</sub> Si	0.826 (s)
	( $\eta^5$ -C <sub>5</sub> (CH <sub>3</sub> ) <sub>4</sub> ) <sub>2</sub>	1.987 (s,12H) ; 1.835 (s,12H)
	ScCH <sub>3</sub>	-1.033 (s)
	P(CH <sub>3</sub> ) <sub>3</sub>	1.040 (d), $^2J_{\text{P-H}}=4.14$ Hz
OpScCH <sub>2</sub> CH(CH <sub>3</sub> ) <sub>2</sub>		
(2-PMe <sub>3</sub> -free)	(CH <sub>3</sub> ) <sub>2</sub> Si	0.948 (s)
	( $\eta^5$ -C <sub>5</sub> (CH <sub>3</sub> ) <sub>4</sub> ) <sub>2</sub>	1.946 (s,12H) ; 1.808 (s,12H)
	ScCH <sub>2</sub> CH(CH <sub>3</sub> ) <sub>2</sub>	0.300 (d), $^3J_{\text{H-H}}=7.81$ Hz
	ScCH <sub>2</sub> CH(CH <sub>3</sub> ) <sub>2</sub>	2.243 (m)
	ScCH <sub>2</sub> CH(CH <sub>3</sub> ) <sub>2</sub>	0.705 (d), $^3J_{\text{H-H}}=6.35$ Hz
OpScCH <sub>3</sub>		
(3-PMe <sub>3</sub> -free)	(CH <sub>3</sub> ) <sub>2</sub> Si	0.899 (s)
	( $\eta^5$ -C <sub>5</sub> (CH <sub>3</sub> ) <sub>4</sub> ) <sub>2</sub>	1.935 (s,12H) ; 1.841 (s,12H)
	ScCH <sub>3</sub>	-0.833(s)



(PMe<sub>3</sub>)

(5)	(CH <sub>3</sub> ) <sub>2</sub> Si	0.950 (s)
	(η <sup>5</sup> -C <sub>5</sub> (CH <sub>3</sub> ) <sub>4</sub> ) <sub>2</sub>	1.940 (s,12H) ; 1.814 (s,6H) ; 1.807 (s,6H)
	ScCH <sub>2</sub> CH(CH <sub>3</sub> )(CH <sub>2</sub> ) <sub>2</sub> CH <sub>3</sub>	0.147 (m)
	ScCH <sub>2</sub> CH(CH <sub>3</sub> )(CH <sub>2</sub> ) <sub>2</sub> CH <sub>3</sub>	0.605 (d), <sup>3</sup> J <sub>H-H</sub> =6.35 Hz
	ScCH <sub>2</sub> CH(CH <sub>3</sub> )(CH <sub>2</sub> ) <sub>2</sub> CH <sub>3</sub>	0.887(t), <sup>3</sup> J <sub>H-H</sub> =7.08 Hz
	P(CH <sub>3</sub> ) <sub>3</sub>	0.966 (br)



(6)	(CH <sub>3</sub> ) <sub>2</sub> Si	0.948 (s)
	(η <sup>5</sup> -C <sub>5</sub> (CH <sub>3</sub> ) <sub>4</sub> ) <sub>2</sub>	1.951 (s,12H) ; 1.819 (s,12H)
	ScCH <sub>2</sub> CH <sub>2</sub> CH <sub>3</sub>	0.207 (m)
	ScCH <sub>2</sub> CH <sub>2</sub> CH <sub>3</sub>	0.88 (m, overlapping)
	P(CH <sub>3</sub> ) <sub>3</sub>	1.018(sl. br. d)



(8)	(CH <sub>3</sub> ) <sub>2</sub> Si	0.942 (s)
	(η <sup>5</sup> -C <sub>5</sub> (CH <sub>3</sub> ) <sub>4</sub> ) <sub>2</sub>	1.948 (s,12H) ; 1.797 (s,12H)
	ScCH <sub>2</sub> CH(CH <sub>2</sub> CH <sub>3</sub> ) <sub>2</sub>	0.012 (d), <sup>3</sup> J <sub>H-H</sub> =7.62 Hz
	ScCH <sub>2</sub> CH(CH <sub>2</sub> CH <sub>3</sub> ) <sub>2</sub>	0.672 (t), <sup>3</sup> J <sub>H-H</sub> =7.18 Hz
	P(CH <sub>3</sub> ) <sub>3</sub>	0.942 (br)



(11)	(CH <sub>3</sub> ) <sub>2</sub> Si	0.948 (s)
	(η <sup>5</sup> -C <sub>5</sub> (CH <sub>3</sub> ) <sub>4</sub> ) <sub>2</sub>	1.945 (s,12H) ; 1.794 (s,12H)
	ScCH <sub>2</sub> CH(CH <sub>2</sub> CH <sub>3</sub> ) <sub>2</sub>	0.034 (d), <sup>3</sup> J <sub>H-H</sub> =7.63 Hz
	ScCH <sub>2</sub> CH(CH <sub>2</sub> CH <sub>3</sub> ) <sub>2</sub>	0.671 (t), <sup>3</sup> J <sub>H-H</sub> =7.15 Hz

OpScCH <sub>2</sub> PMe <sub>2</sub>		
(4)	(CH <sub>3</sub> ) <sub>2</sub> Si	0.948 (s)
	(η <sup>5</sup> -C <sub>5</sub> (CH <sub>3</sub> ) <sub>4</sub> ) <sub>2</sub>	1.946 (s,12H) ; 1.808 (s12H)
	ScCH <sub>2</sub> P(CH <sub>3</sub> ) <sub>2</sub>	0.324 (d), <sup>2</sup> J <sub>P-H</sub> =9.09 Hz
	ScCH <sub>2</sub> P(CH <sub>3</sub> ) <sub>2</sub>	1.277 (d), <sup>2</sup> J <sub>P-H</sub> =5.96 Hz
OpSc[C(CH <sub>3</sub> )=CH(CH <sub>3</sub> )](PMe <sub>3</sub> )		
(9)	(CH <sub>3</sub> ) <sub>2</sub> Si	0.934 (s)
	(η <sup>5</sup> -C <sub>5</sub> (CH <sub>3</sub> ) <sub>4</sub> ) <sub>2</sub>	1.888 (s,12H) ; 1.755 (s12H)
	ScC(CH <sub>3</sub> )C(H)(CH <sub>3</sub> )	3.690 (m), <sup>3</sup> J <sub>H-H</sub> =5.35 Hz , 4J <sub>H-H</sub> =1.71 Hz
	ScC(CH <sub>3</sub> )C(H)(CH <sub>3</sub> )	1.724 (m), 4J <sub>H-H</sub> =0.76 Hz
	ScC(CH <sub>3</sub> )C(H)(CH <sub>3</sub> )	1.920 (br)
	P(CH <sub>3</sub> ) <sub>3</sub>	0.923 (d), <sup>2</sup> J <sub>P-H</sub> =2.73 Hz
OpScC(CH <sub>3</sub> )=C(CH <sub>3</sub> ) <sub>2</sub>		
(10-PMe <sub>3</sub> -free)	(CH <sub>3</sub> ) <sub>2</sub> Si	0.987 (s, 3H) ; 0.968 (s, 3H)
	(η <sup>5</sup> -C <sub>5</sub> (CH <sub>3</sub> ) <sub>4</sub> ) <sub>2</sub>	1.880 (s, 6H) ; 1.840 (s, 6H)
		1.830 (s, 6H) ; 1.789 (s, 6H)
	ScC(CH <sub>3</sub> )C(CH <sub>3</sub> ) <sub>2</sub>	1.625 (m)
	ScC(CH <sub>3</sub> )C(CH <sub>3</sub> ) <sub>2</sub>	1.245 (m), 1.180 (m)

<sup>a</sup> All spectra were recorded at 500 MHz in cyclohexane-*d*<sub>12</sub> at ambient temperature.

<sup>b</sup> NMR data for this compound in C<sub>6</sub>D<sub>6</sub> has been previously reported (ref. 6).

## Experimental Section

**General Considerations.** All air and/or moisture sensitive compounds were manipulated using standard high vacuum line, Schlenk, or cannula techniques, or in a dry box under a nitrogen atmosphere, as described previously.<sup>24</sup> Argon and nitrogen gases were purified and dried by passage over columns of MnO on vermiculite and activated molecular sieves. Solvents were stored under vacuum over titanocene<sup>25</sup> or sodium benzophenone ketyl. <sup>1</sup>H and <sup>13</sup>C NMR spectra were recorded on a Bruker AM500 (500.13 MHz for <sup>1</sup>H) spectrometer in cyclohexane-*d*<sub>12</sub> at room temperature unless otherwise specified. Synthesis of CH<sub>2</sub>CH(CH<sub>3</sub>)(CD<sub>3</sub>) was accomplished using the procedure described by Foote and coworkers.<sup>26</sup> The preparations of OpScCl·LiCl·2(Et<sub>2</sub>O), OpScCH(SiMe<sub>3</sub>)<sub>2</sub>, and OpSc(H)PMe<sub>3</sub> were carried out as previously described.<sup>27</sup>

**NMR Tube Reactions.** Most of the reactions were carried out in sealed NMR tubes. The tubes were fitted with a 180°, concentric, Teflon needle valve which was blown directly onto the tube (the tubes employed were purchased from J. Young<sup>28</sup>), which could be attached to the high vacuum line by a simple adapter tube. These assemblies allow convenient loading of solids in the glove-box as well as a reversible vacuum tight seal which allows facile manipulations of volatiles into and out of the tube assembly. In a typical experiment, the NMR tube was loaded with OpSc(H)(PMe<sub>3</sub>) (*ca.* 10 mg) in the glove-box. On the vacuum line, cyclohexane-*d*<sub>12</sub> (*ca.* 1 mL) was condensed into the evacuated tube assembly at -78°C, to produce a solution of approximate concentration of 0.024 M, followed by the desired olefin at -196°C. The tube was then removed from the vacuum line and warmed to room temperature with shaking. The insoluble white OpSc(H)(PMe<sub>3</sub>) was allowed to react (about 3-5 min) with the olefin to give the soluble (typically yellow-orange) alkyl derivative, and the tube was then

stored at  $-78^{\circ}\text{C}$  until just prior to insertion into the NMR probe. In the cases in which the phosphine was pumped off of the reactions, this was accomplished by carefully evacuating the NMR tube after formation of the alkyl complex, and then redissolving in fresh cyclohexane- $d_{12}$ .

**Reaction of  $\text{OpSc(H)(PMe}_3\text{)}$  with isobutene: Analysis of Volatiles by Gas Chromatography.** In the dry box a small volume, moderate pressure reaction vessel equipped with a Teflon needle valve was charged with  $\text{OpSc(H)(PMe}_3\text{)}$ , (22 mg, 0.0528 mmol).  $\text{C}_6\text{D}_{12}$  (ca. 1.5 mL) was vacuum transferred onto the solid at  $-78^{\circ}\text{C}$ . Isobutene (293 Torr in 3.3 mL at  $25^{\circ}\text{C}$ , 0.0528 mmol) was condensed into the reaction vessel. The solution was allowed to warm to room temperature and the initially cloudy, white solution slowly (ca. 20 min) changed to a clear orange. The reaction was allowed to stir overnight, during which time a significant amount of finely divided orange/yellow precipitate was deposited. The volatiles were condensed into an NMR tube, first analyzed by  $^1\text{H}$  NMR, and then by gc. Gas chromatographic analyses were carried out on a Perkin-Elmer 8410 Gas Chromatograph equipped with a flame ionization detector and 12 ft Chromasorb W column treated with 13% DBT (dibutyl tetrachlorophthalate). Satisfactory separation of a mixture of propane, isobutane, isobutene, n-pentane, 1-pentene, 2-methylpentane, 2-methylpentene, and cyclohexane was accomplished using detector and injector temperatures of  $200^{\circ}\text{C}$ , column temperature of  $31^{\circ}\text{C}$ , and a helium flow rate of 20 mL/min. The reaction vessel containing the residual solid (mostly  $\text{OpSc(CH}_3\text{)(PMe}_3\text{)}$ ) was taken back into the dry box and used for the following procedure.

**Addition of Propene to the Generated  $\text{OpSc(CH}_3\text{)(PMe}_3\text{)}$ .** In the glove-box the residual solid from the previous procedure was redissolved into ca. 2 mL of cyclohexane- $d_{12}$ , and the resulting solution was divided into two NMR tubes.

$^1\text{H}$ -NMR spectra of the first tube indicated clean conversion of  $\text{OpSc}(\text{H})(\text{PMe}_3)$  to  $\text{OpSc}(\text{CH}_3)(\text{PMe}_3)$ . The second tube was taken onto the vacuum line, and to the cooled ( $-196^\circ\text{C}$ ), evacuated tube, was condensed in approximately 1 eq of propene. The tube was warmed to ambient temperature and  $^1\text{H}$ -NMR spectra were recorded after 30 min and 90 min.

**Reaction of  $\text{OpSc}(\text{H})(\text{PMe}_3)$  with isobutene- $d_3$ :** In the dry box, a small volume, moderate pressure reaction vessel equipped with a Teflon needle valve was charged with  $\text{OpSc}(\text{H})(\text{PMe}_3)$ , (22 mg, 0.0528 mmol).  $\text{C}_6\text{D}_{12}$  (*ca.* 1.5 mL) was vacuum transferred onto the solid at  $-78^\circ\text{C}$ . Isobutene- $d_3$  (293 Torr in 3.3 mL at  $25^\circ\text{C}$ , 0.0528 mmol) was condensed into the reaction vessel. The solution was allowed to warm to room temperature and the initially cloudy, white solution slowly (*ca.* 20 min) changed to a clear orange. The reaction was allowed to stir overnight, during which time a significant amount of finely divided orange/yellow precipitate was deposited. The volatiles were condensed away from the residual solid and the solid redissolved in  $\text{C}_6\text{D}_{12}$  for subsequent NMR analysis. The isotope effect was calculated by integration of the residual  $\text{Sc-CH}_3$  resonance against that for the other resonances for the product  $\text{OpSc}(\text{CX}_3)(\text{PMe}_3)$ ,  $\text{X} = \text{H}, \text{D}$ .

**Preparation of  $\text{OpSc}(\text{CH}_3)(\text{PMe}_3)$ .** In the dry box a 25 ml round bottom flask attached to a  $180^\circ$  Teflon needle valve was charged with  $\text{OpSc}(\text{H})(\text{PMe}_3)$ , (100 mg, 0.238 mmol). Petroleum ether (*ca.* 8 ml) was vacuum transferred onto the solid at  $-78^\circ\text{C}$ . Isobutene (1.2 eq) was condensed into the reaction vessel from a calibrated gas volume. The assembly was allowed to warm to room temperature and the initially cloudy, white solution slowly (*ca.* 30 min) turned orange and had a small amount of solid which remained undissolved. The solution was allowed to stir overnight after which time it was filtered and dried *in-vacuo*

leaving  $\text{OpSc}(\text{CH}_3)(\text{PMe}_3)$  as a slightly waxy orange-yellow solid in *ca.* 85% yield. Elemental analysis; calculated for  $\text{C}_{24}\text{H}_{42}\text{PScSi}$ : C 66.31%, H 9.76% ; found (average of two runs): C 66.76% , H 9.87%.

**Reaction of  $\text{OpSc}(\text{CH}_3)(\text{PMe}_3)$  with 2-Butyne.**  $\text{OpSc}(\text{CH}_3)(\text{PMe}_3)$  (10 mg, 0.023 mmol), prepared as described above, was loaded into a sealable NMR tube. On the vacuum line, cyclohexane- $d_{12}$  (*ca.* 1 mL) was condensed into the evacuated tube assembly at  $-78^\circ\text{C}$ . 2-Butyne (2 eq) was then condensed in, at  $-196^\circ\text{C}$ , from a calibrated gas volume. The tube was warmed to ambient temperature and an NMR spectrum taken after approximately 10 min was consistent with clean conversion to  $\text{OpSc}\{\text{C}(\text{CH}_3)=\text{C}(\text{CH}_3)_2\}(\text{PMe}_3)$  (**10**). Removal of all volatiles followed by redissolution in fresh cyclohexane- $d_{12}$  afforded the  $\text{PMe}_3$ -free complex  $\text{OpScC}(\text{CH}_3)=\text{C}(\text{CH}_3)_2$  as indicated by its  $^1\text{H}$  NMR spectrum.

**Reaction of  $\text{OpSc}(\text{H})(\text{PMe}_3)$  with isobutene: Addition of 2-Butyne to the Generated  $\text{OpSc}\{\text{CH}_2\text{CH}(\text{CH}_3)_2\}(\text{PMe}_3)$ .**  $\text{OpSc}\{\text{CH}_2\text{CH}(\text{CH}_3)_2\}(\text{PMe}_3)$  was prepared in an NMR tube as described above. 2-Butyne (4 eq) was then condensed in, at  $-196^\circ\text{C}$ , from a calibrated gas volume. The tube was warmed to ambient temperature and an NMR spectrum was taken after approximately 10 min. A spectrum taken the next day showed no change.

**Competitive Reaction of  $\text{OpSc}(\text{CH}_3)(\text{PMe}_3)$  with 2-Butyne and Propene.**

$\text{OpSc}(\text{CH}_3)(\text{PMe}_3)$  (10 mg, 0.023 mmol), prepared as described above, was loaded into a sealable NMR tube. On the vacuum line, cyclohexane- $d_{12}$  (*ca.* 1 mL) was condensed into the evacuated tube assembly at  $-78^\circ\text{C}$ . 2-Butyne (1.5 eq) and propene (1.5 eq) were then condensed in, at  $-196^\circ\text{C}$ , from a calibrated gas volume. The tube was warmed to ambient temperature and an NMR spectrum taken after approximately 30 min was consistent with >95% conversion to



OpSc{C(CH<sub>3</sub>)=C(CH<sub>3</sub>)<sub>2</sub>}(PMe<sub>3</sub>) (**10**) as the organometallic product. A spectrum taken the next day showed no change.

**<sup>1</sup>H NMR Monitoring of the Decomposition of OpSc{CH<sub>2</sub>CH(CH<sub>3</sub>)<sub>2</sub>}(PMe<sub>3</sub>).**

The decomposition of OpSc{CH<sub>2</sub>CH(CH<sub>3</sub>)<sub>2</sub>}(PMe<sub>3</sub>), prepared as described above, to OpSc(CH<sub>3</sub>)(PMe<sub>3</sub>) was followed by <sup>1</sup>H-NMR spectroscopy using automatic accumulation programs.<sup>29</sup> Spectra were recorded every 11.4 min over a period of about 12 hr.

**Preparation of OpScCH<sub>2</sub>CH(CH<sub>2</sub>CH<sub>3</sub>)<sub>2</sub>.** In the dry box a 25 ml round bottom flask attached to a 180° Teflon needle valve was charged with OpSc(H)(PMe<sub>3</sub>), (100 mg, 0.238 mmol). Petroleum ether (*ca.* 8 ml) was vacuum transferred onto the solid at -78 °C. 2-ethyl-1-butene (1.2 eq) was condensed into the reaction vessel from a calibrated gas volume. The solution was allowed to warm to room temperature and the initially cloudy, white solution slowly (*ca.* 30 min) turned orange and had some solid which remained undissolved. The solution was filtered and dried *in-vacuo* leaving a orange-yellow solid. Elemental analysis; calculated for C<sub>25</sub>H<sub>41</sub>ScSi: C 72.40%, H 9.99% ; found (average of three runs): C 68.55% , H 9.71%. Yield: 70%.

**Preparation of OpScI(PMe<sub>3</sub>).** A medium sized, medium porosity swivel frit equipped with two 250 ml flasks and a 90° needle valve was taken into the glovebox and charged with OpScH(PMe<sub>3</sub>) (720 mg, 1.71 mmol, 1 eq). On the vacuum line, petroleum ether (80 ml) was condensed onto the solid. The OpScH(PMe<sub>3</sub>) remained largely undissolved (white solid) but the solution took on an orange hue (possibly indicating some decomposition had occurred to the sample). MeI (279.6 mg, 1.97 mmol, 1.15 eq) was condensed into the reaction flask from a calibrated volume (348.8 torr in 104.5 ml) and the stirred solution

was allowed to warm to room temperature. The color of the solution remained unchanged but the color of the precipitate changed from white to yellow. The solution was concentrated to *ca.* 40 ml, cooled to -78°C, filtered, washed once with fresh solvent and dried *in vacuo* to afford OpScI(PMe<sub>3</sub>) as a fine yellow powder. <sup>1</sup>H NMR (C<sub>6</sub>D<sub>6</sub>): δ 2.08 (singlet, broad, 12H), δ 1.91 (singlet, 12H), δ 0.92 (singlet, 6H), δ 0.82 (doublet, 9H, <sup>2</sup>J<sub>PH</sub> 4.6 Hz). Analysis calculated for C<sub>23</sub>H<sub>39</sub>IPScSi: C 50.54%, H 7.21%; found: C 51.28%, H 7.29%.

**Preparation of OpScBr.** In a typical reaction, a small, medium porosity swivel frit equipped with two 25 ml flasks and a 90° needle valve was taken into the glovebox and charged with OpScH(PMe<sub>3</sub>) (200 mg, 0.475 mmol, 1 eq). On the vacuum line, methylcyclohexane (20 ml) was condensed onto the solid, followed by 2-ethyl-1-butene (60.0 mg, 0.087 ml, 0.713 mmol, 1.5 eq). The reaction was warmed to room temperature and after about 10 min the insoluble hydride had reacted to give a clear yellow-orange solution of OpScCH<sub>2</sub>C(C<sub>2</sub>H<sub>5</sub>)<sub>2</sub>(PMe<sub>3</sub>). Solvent and trimethylphosphine were removed *in vacuo* leaving phosphine-free OpScCH<sub>2</sub>C(C<sub>2</sub>H<sub>5</sub>)<sub>2</sub> as a yellow-orange powder. The solid was redissolved in methylcyclohexane (15 ml). Isopropyl bromide (0.07 ml) was condensed into the reaction, which was warmed to RT and allowed to stir overnight. The ensuing yellow precipitate was collected by filtration. Yields range from 15-50%. <sup>1</sup>H NMR (C<sub>6</sub>D<sub>6</sub>): δ 2.02 (singlet, broad, 12H), δ 1.77 (singlet, broad, 12H), δ 0.96 (singlet, 6H).

## References and Notes

1. For reviews on Ziegler-Natta chemistry see:
  - (a) Boor, J. *Ziegler-Natta Catalysts and Polymerizations*; Academic Press: New York, 1979.
  - (b) Pino, P.; Mulhaupt, R. *Angew. Chem., Int. Ed. Engl.* **1980**, *19*, 857.
  - (c) Tait, P.J.T. in *Comprehensive Polymer Science*; Allen, G., Bevington, J.C., Eds.; Pergamon Press: Oxford, **1989**, Chapters 1 and 2.
  - (d) Sinn, H.; Kaminsky, W. *Adv. Organomet. Chem.* **1980**, *18*, 99.
2. For examples with leading references see:
  - (a) Jordan, R.F. *Adv. Organomet. Chem.* **1991**, *32*, 325.
  - (b) Hlatky, G.C.; Turner, H.W.; Eckman, R.R. *J. Am. Chem. Soc.* **1989**, *111*, 2728.
  - (c) Kaminsky, W.; Külper, K.; Brintzinger, H.H.; Wild, F.W.P. *Angew. Chem., Int. Ed. Engl.* **1985**, *27*, 507.
  - (d) Watson, P.L. *J. Am. Chem. Soc.* **1990**, *112*, 9406.
  - (e) Eshuis, J.J.W.; Tan, Y.Y.; Teuben, J.H.; Renkema, J. *J. Mol. Catal.* **1990**, *62*, 277.
  - (f) Jeske, G.; Lauke, H.; Mauermann, H.; Sweptson, P.N.; Schumann, H.; Marks, T.J. *J. Am. Chem. Soc.* **1990**, *112*, 8091.
  - (g) Watson, P.L. *J. Am. Chem. Soc.* **1982**, *104*, 6471.
3. Kaminsky, W.; Sinn, H. *Transition Metals and Organometallics as Catalysts for Olefin Polymerization*, Springer-Verlag: Berlin, 1988.
4.
  - (a) Thompson, M.E.; Bercaw, J.E. *Pure Appl. Chem.* **1984**, *56*, 1
  - (b) Thompson, M.E.; Baxter, S.M.; Bulls, A.R.; Burger, B.J.; Nolan, M.C.; Santarsiero, B.D.; Schaefer, W.P.; Bercaw, J.E. *J. Am. Chem. Soc.* **1987**, *109*, 203.
  - (c) Bercaw, J.E. *Pure Appl. Chem.* **1990**, *62*, 1151 and references therein.
  - (d) Piers, W. E.; Shapiro, P. J.; Bunel, E. E.; Bercaw, J. E. *Synlett* **1990**, *2*, 74, and references therein.
5. Although molecular weights measurements indicate DpScH is predominantly dimeric, we assume that the reactive form is monomeric.
6. Bunel, E. E. Ph.D. Thesis California Institute of Technology, 1989.
7. Piers, W. E.; Shapiro, P. J.; Bunel, E. E.; Bercaw, J. E. *Synlett* **1990**, 74-84.
8. Bunel, E.; Burger, B.J.; Bercaw, J.E. *J. Am. Chem. Soc.* **1988**, *110*, 976.
9.
  - (a) Piers, W.E.; Bercaw, J.E. *J. Am. Chem. Soc.* **1990**, *112*, 9406.
  - (b) Krauledat, H.; Brintzinger, H.H. *Angew. Chem., Int. Ed. Engl.* **1990**, *29*,

- 
1412.  
(c) Cotter, W.D.; Bercaw, J.E. *J. Organomet. Chem.* **1991**, 417, C1.
10. Bunel, E. E. Ph.D. Thesis California Institute of Technology, 1989.
  11. Piers, W. E.; Bercaw, J. E. *J. Am. Chem. Soc.* **1990**, 112, 9406.
  12. (a) Krauledat, H.; Brintzinger, H. H. *Angew. Chem., Int. Ed. Engl.* **1990**, 29, 1412.  
(b) Leclerc, M. K.; Brintzinger, H. H. *J. Am. Chem. Soc.* **1995**, 117, 1651.
  13. This experiment is essentially a modification of the "isotopic perturbation of stereochemistry" experiment originally conceived by Grubbs and coworkers: Clawson, L.; Soto, J.; Buchwald, S. L.; Steigerwald, M. L.; Grubbs, R. H. *J. Am. Chem. Soc.* **1985**, 107, 3377.
  14. On reflection, the  $\beta$ -CH<sub>3</sub> elimination of propene is almost certainly endothermic, so that conversion of  $\text{OpSc}(\text{CH}_2\text{CHMe}_2)(\text{PMe}_3)$  to  $\text{OpSc}(\text{CH}_3)(\text{PMe}_3)$  demands concurrent exothermic reaction(s) of propene to other reaction products (as observed).
  15. Thompson, M.E.; Baxter, S.M.; Bulls, A.R.; Burger, B.J.; Nolan, M.C.; Santarsiero, B.D.; Schaefer, W.P.; Bercaw, J.E. *J. Am. Chem. Soc.* **1987**, 109, 203.
  16. Whereas there is no definitive evidence that would rule out an intramolecular extrusion of alkane from the trimethylphosphine adducts,  $\text{OpScR}(\text{PMe}_3)$ , the relative rates for formation of **4** correlate roughly inversely with trimethylphosphine affinity (*vide infra*), suggesting a bimolecular reaction between  $\text{OpScR}$  and free trimethylphosphine. The resistance of  $\text{OpSc}(\text{CH}_3)(\text{PMe}_3)$  to decompose to  $\text{CH}_4$  and **4** is in further support of this proposal. Since the methyl derivative has the highest affinity for  $\text{PMe}_3$  and hence the alkyl with the lowest concentration of  $[\text{OpScR}]$ , it would be expected to undergo the bimolecular reaction  $([\text{OpScR}] + \text{PMe}_3 \rightarrow \text{4} + \text{RH})$  most slowly.
  17. Whereas the four methyl groups of the  $\{(\eta^5\text{-C}_5(\text{CH}_3)_4)_2\text{SiMe}_2\}$  ligands for the trimethylphosphine adducts of the alkyl derivatives, *viz.*  $\text{OpSc}(\text{R})(\text{PMe}_3)$ , are inequivalent, rapid trimethylphosphine dissociation/association results in pairwise inequivalency.
  18. The tentative assignments of  $(\text{CH}_3)_\alpha$  and  $(\text{CH}_3)_\beta$  are based on the observation that only the (upfield) resonance for  $(\text{CH}_3)_\beta$  splits for the 2-methyl-1-pentyl derivative,



19. Although definitive evidence for the formation of 1-pentene is lacking, there are two uncharacterized multiplets of low signal-to-noise observed at  $\delta$  4.3 and 4.7 tentatively assigned to the geminal hydrogens of the dimer that would result from [OpScH]-catalyzed dimerization of 1-pentene.
20. This  $\sigma$  bond metathesis reaction with trimethylphosphine appears to be the first observation of a non-redox reaction with  $\text{PMe}_3$ , although oxidative addition of  $\text{PMe}_3$  to electron-rich middle- and late-transition metal complexes has been previously observed:
  - (a) Rabinovich, D.; Zelman, R.; Parkin, G. *J. Am. Chem. Soc.* **1990**, *112*, 9632.
  - (b) Shinomoto, R.S.; Desrosiers, P.J.; Harper, T.G.P.; Flood, T.C. *J. Am. Chem. Soc.* **1990**, *112*, 704.
  - (c) Wenzel, T.T.; Bergman, R.G. *J. Am. Chem. Soc.* **1989**, *108*, 4856.
21. H/D exchange between  $\text{C}_6\text{D}_6$  and  $\text{P}(\text{CH}_3)_3$  catalyzed by  $[\text{Cp}^*_2\text{ScH}]_x$  has been reported. Although this exchange is almost certainly mediated by  $[\text{Cp}^*_2\text{ScCH}_2\text{PMe}_2]$ , it does not buildup to detectable levels. Thompson, M.E.; Bercaw, J.E. *Pure Appl. Chem.* **1984**, *56*, 1.
22.
  - (a) Roe, D.C.; Watson, P.L. *J. Am. Chem. Soc.* **1982**, *104*, 6471.
  - (b) Eshuis, J.J.W.; Tan, Y.Y.; Teuben, J.H.; Renkema, J. *J. Mol. Catal.* **1990**, *62*, 277.
  - (c) Resconi, L.; Piemontesi, F.; Francisocono, G.; Abis, L.; Fiorani, T. *J. Am. Chem. Soc.* **1992**, *114*, 1025.
23. Piers, W. E.; Shapiro, P. J.; Bunel, E. E.; Bercaw, J. E. *Synlett* **1990**, 74.
24. Burger, B.J.; Bercaw, J.E. *Experimental Organometallic Chemistry*; Wayda, A.L., Darensbourg, M.Y., Eds.; ACS Symposium Series 357; American Chemical Society: Washington, DC, 1987.
25. Marvich, R.H.; Brintzinger, H.H. *J. Am. Chem. Soc.* **1971**, *93*, 2046.
26. Foote, C. Personal communication.
27.
  - (a) Bunel, E.E. Ph.D. Thesis California Institute of Technology, 1989.
  - (b) Piers, W.E.; Shapiro, P.J.; Bunel, E.E.; Bercaw, J.E. *Synlett* **1990**, *2*, 74, and references therein.
28. Purchased from Brunfelt Co. cat. no. 1300-060-528PP-7

- 
29. The automation program (for Bruker Aspect systems) is given in Appendix 1.

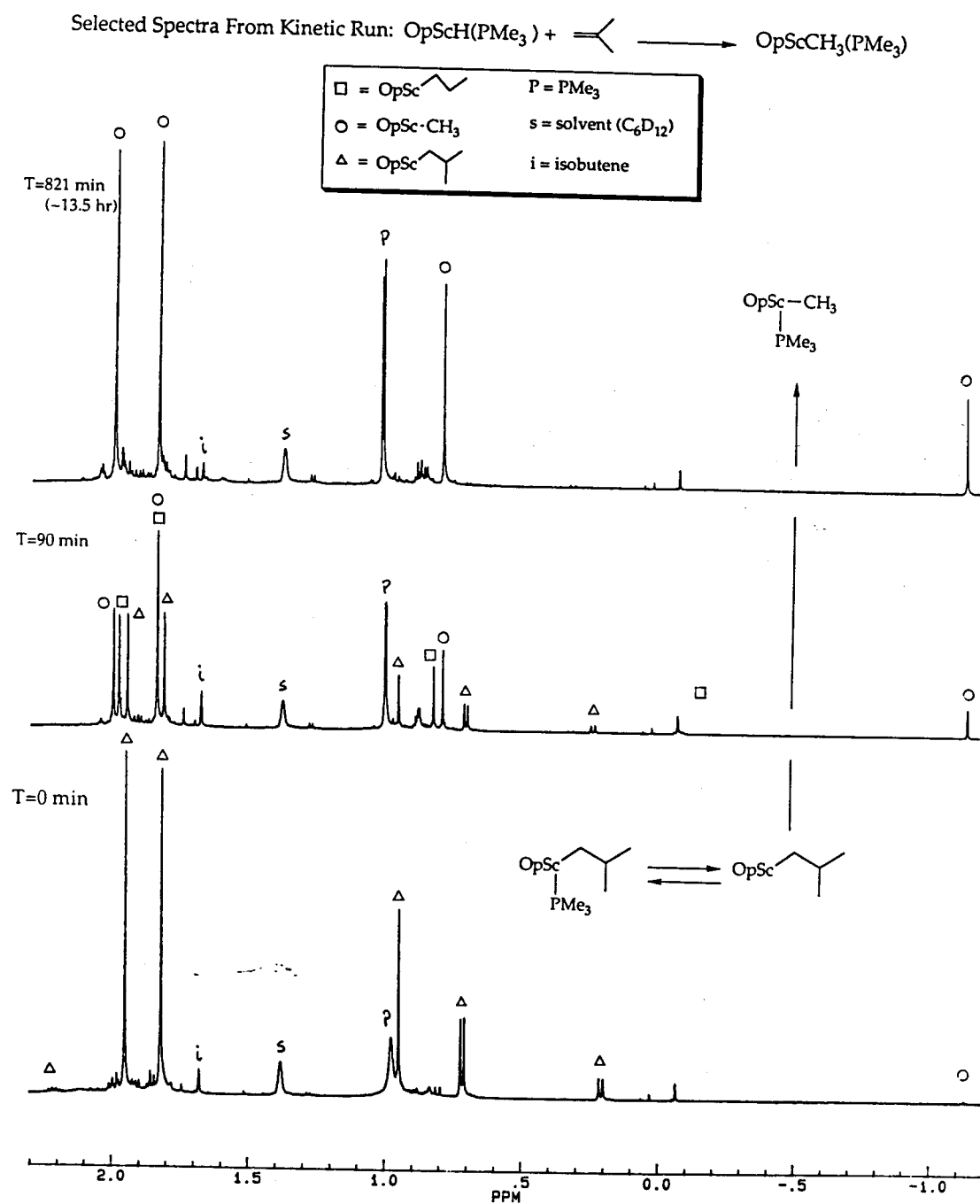
## **Appendix 1**

### **Selected Spectra of Products and Reactions**

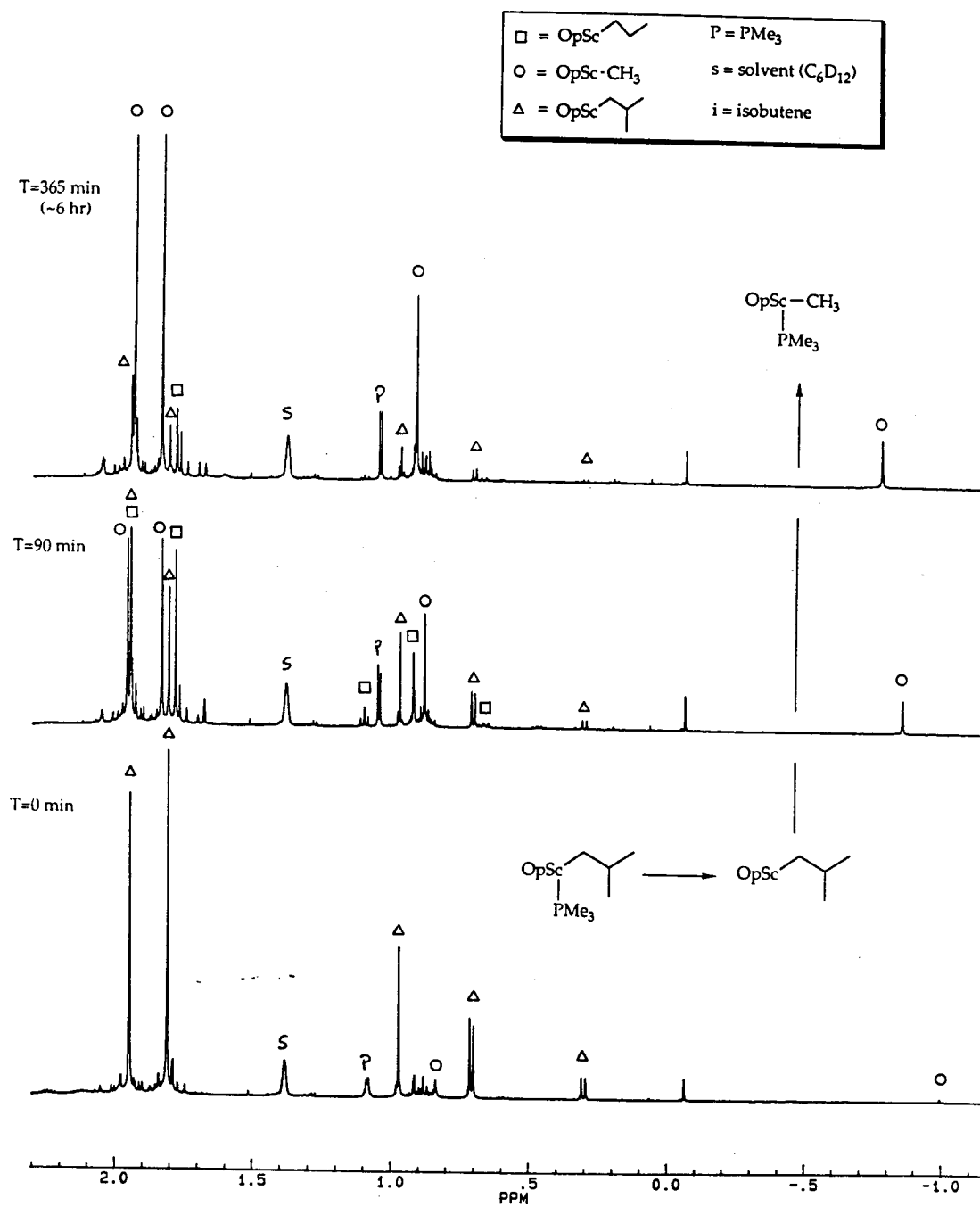
#### **For Chapter 1.**

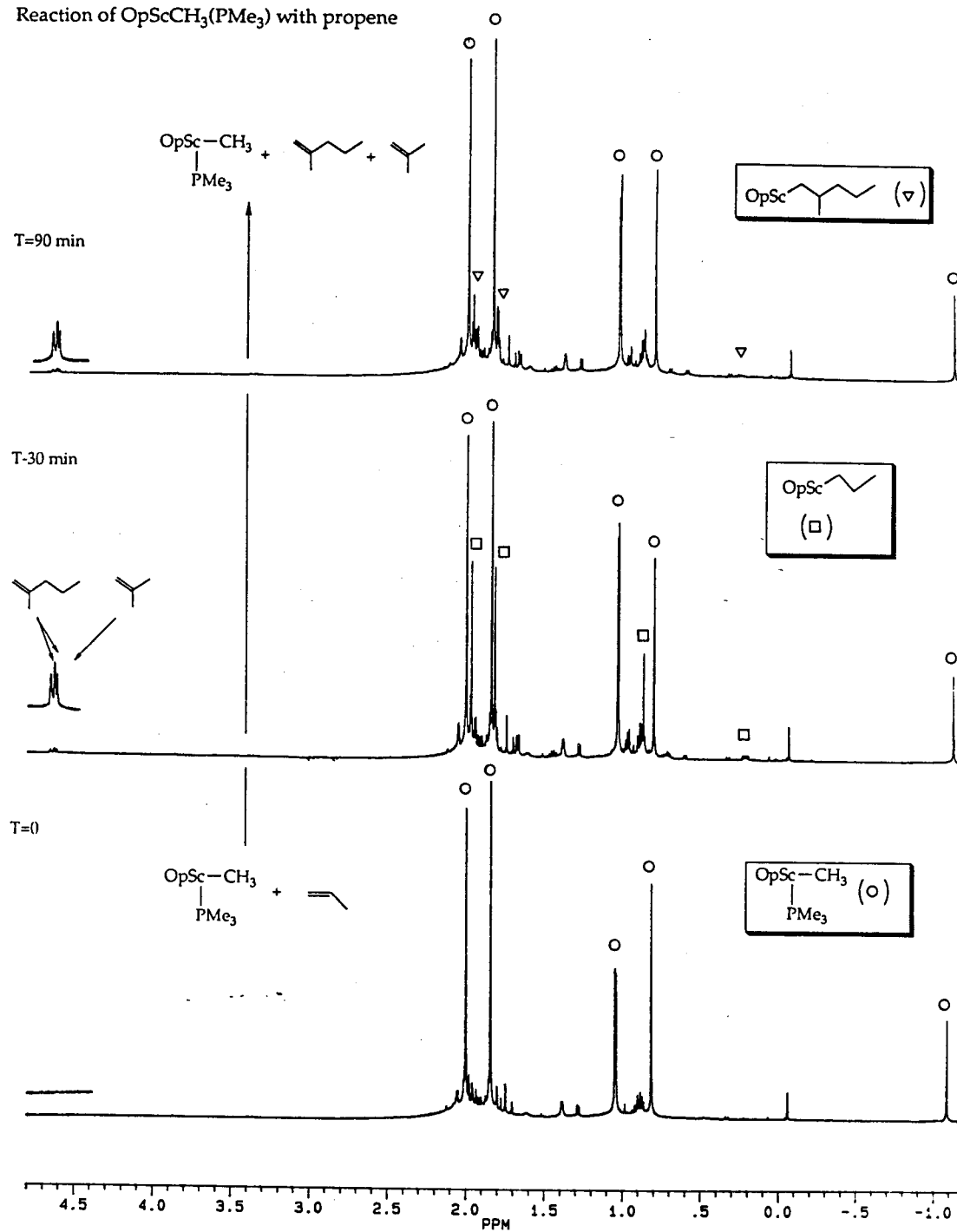


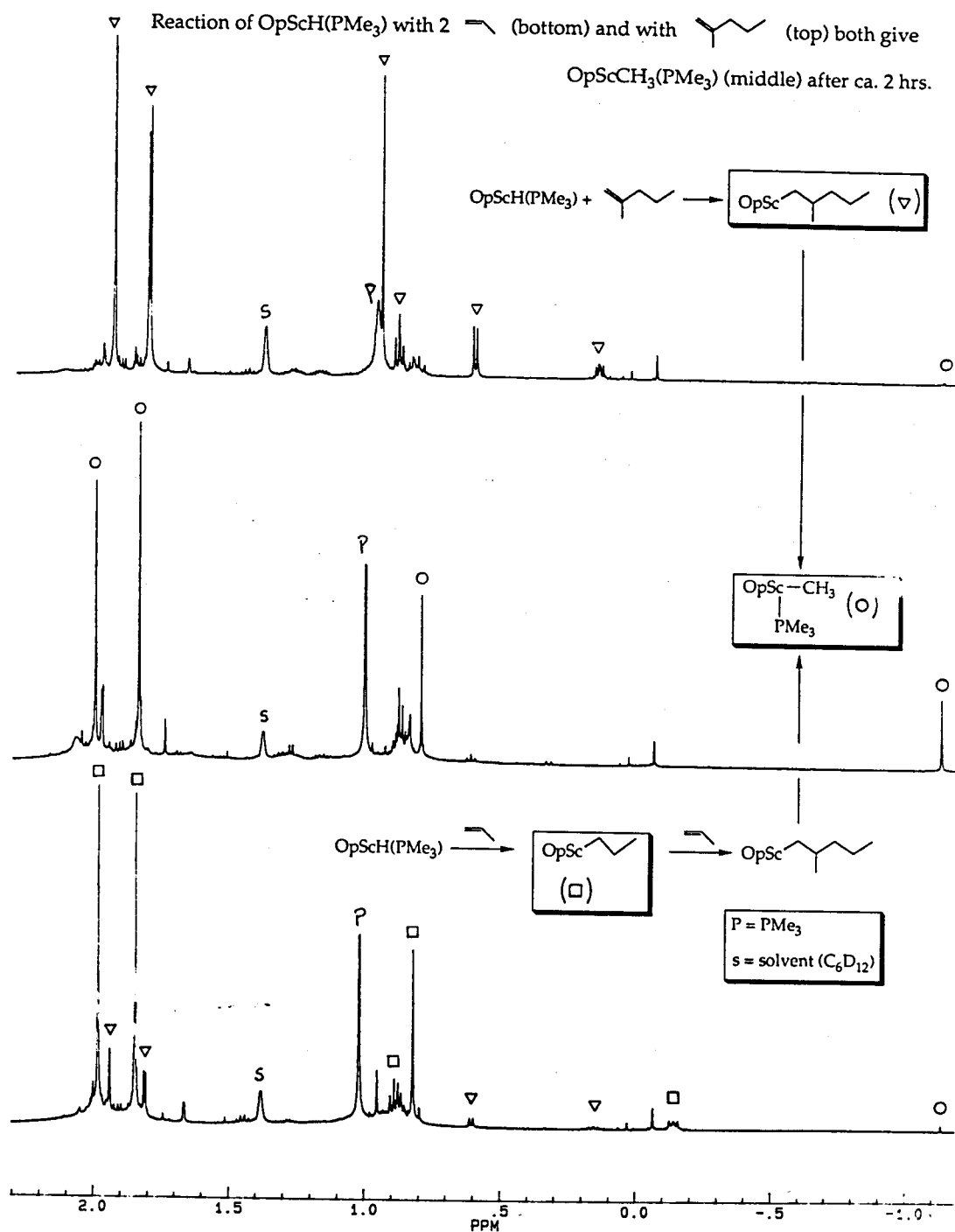




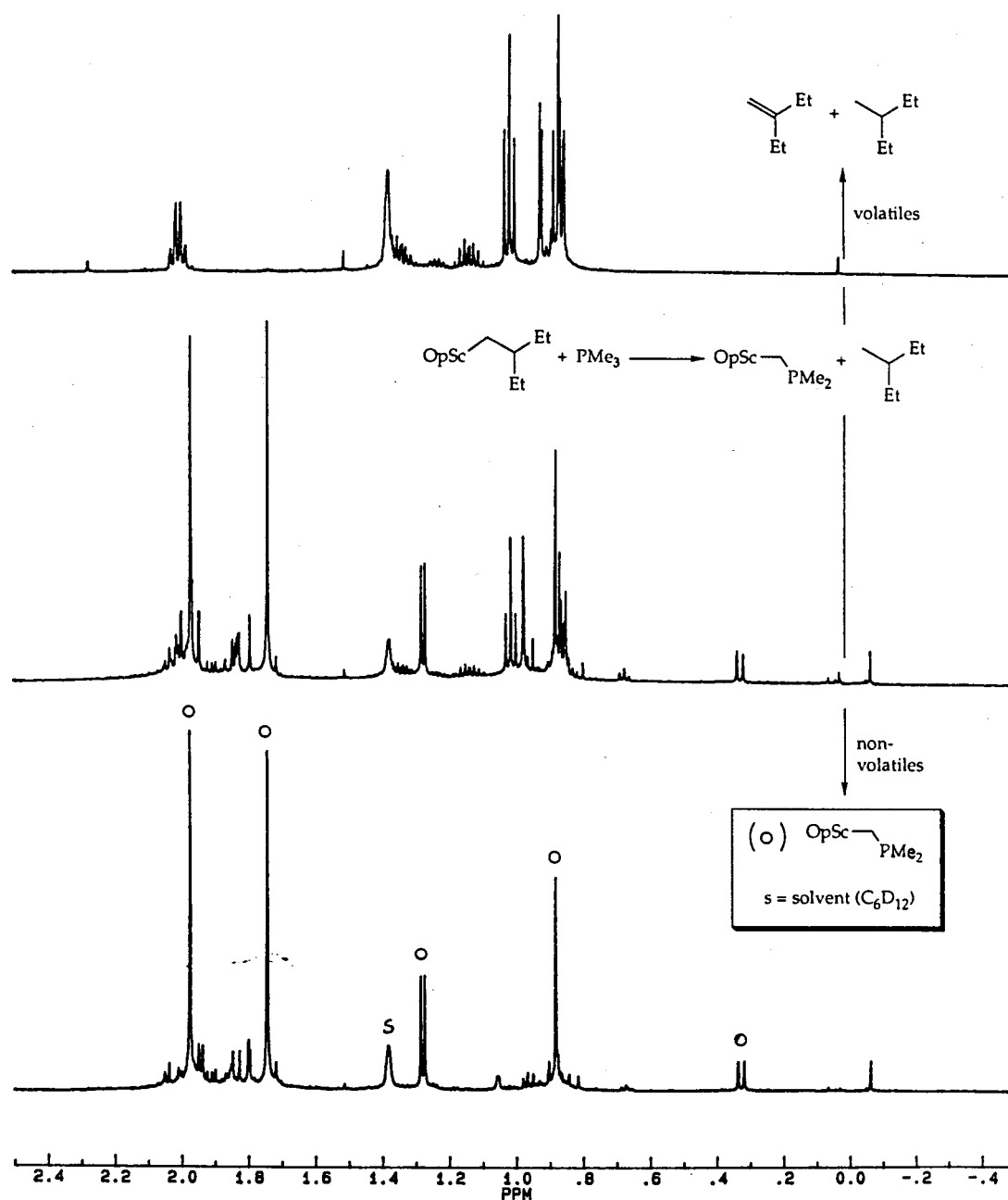
# Rearrangement of OpSc(isobutyl) After Pumping Off $\text{PMe}_3$

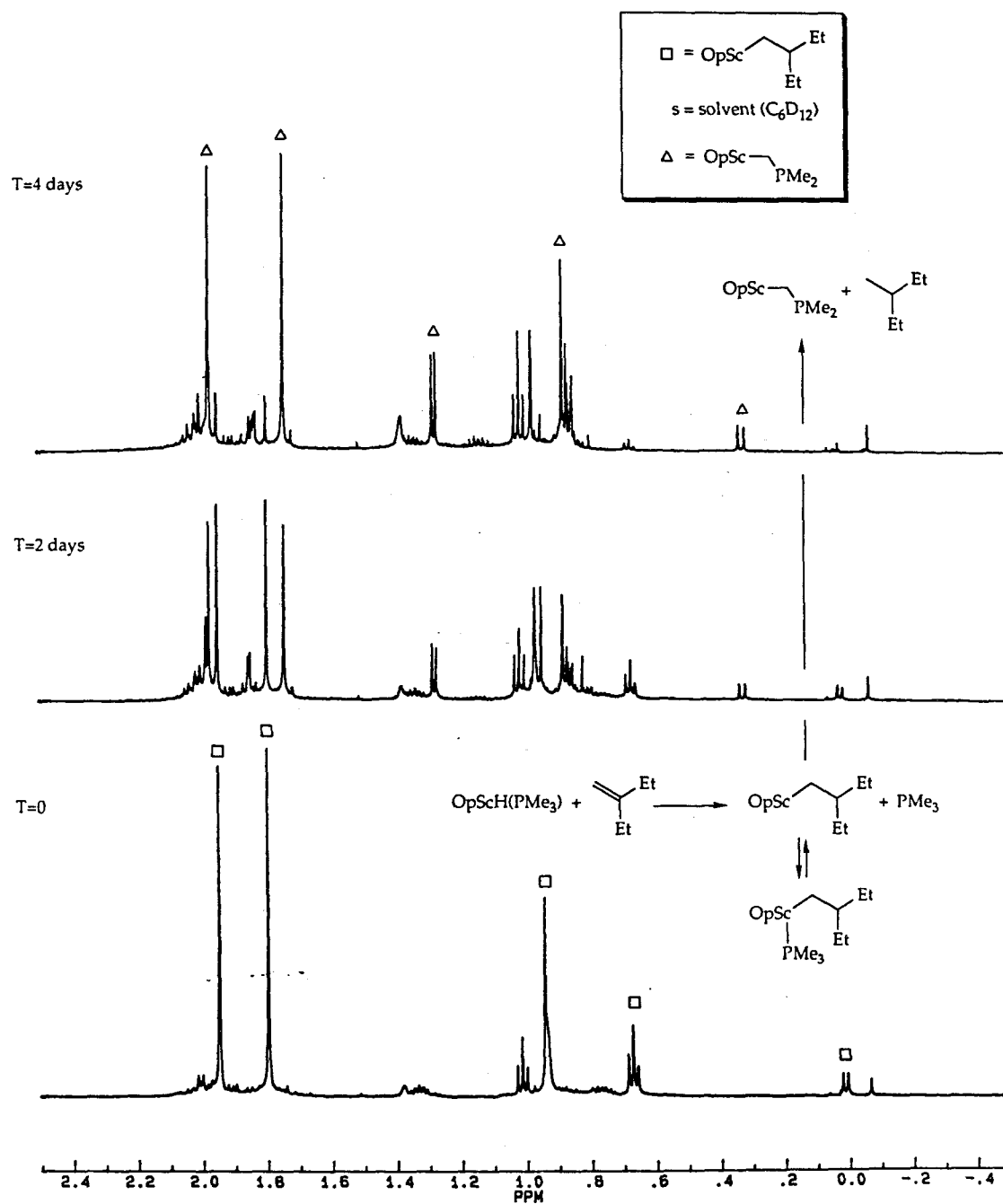


Reaction of  $\text{OpScCH}_3(\text{PMe}_3)$  with propene

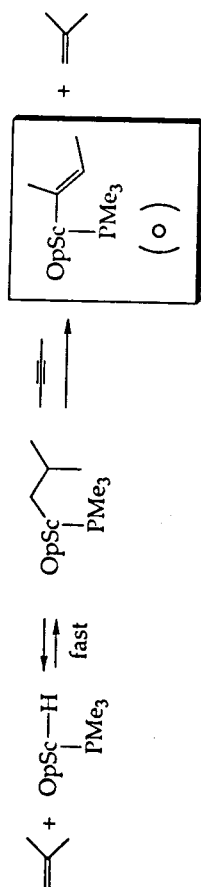


Characterization  $\text{OpScCH}_2\text{PMe}_2$  by Pumping off Volatiles



Rearrangement of  $\text{OpSc}(\text{2-ethylbutyl})$  to  $\text{OpScCH}_2\text{PMe}_2$ 

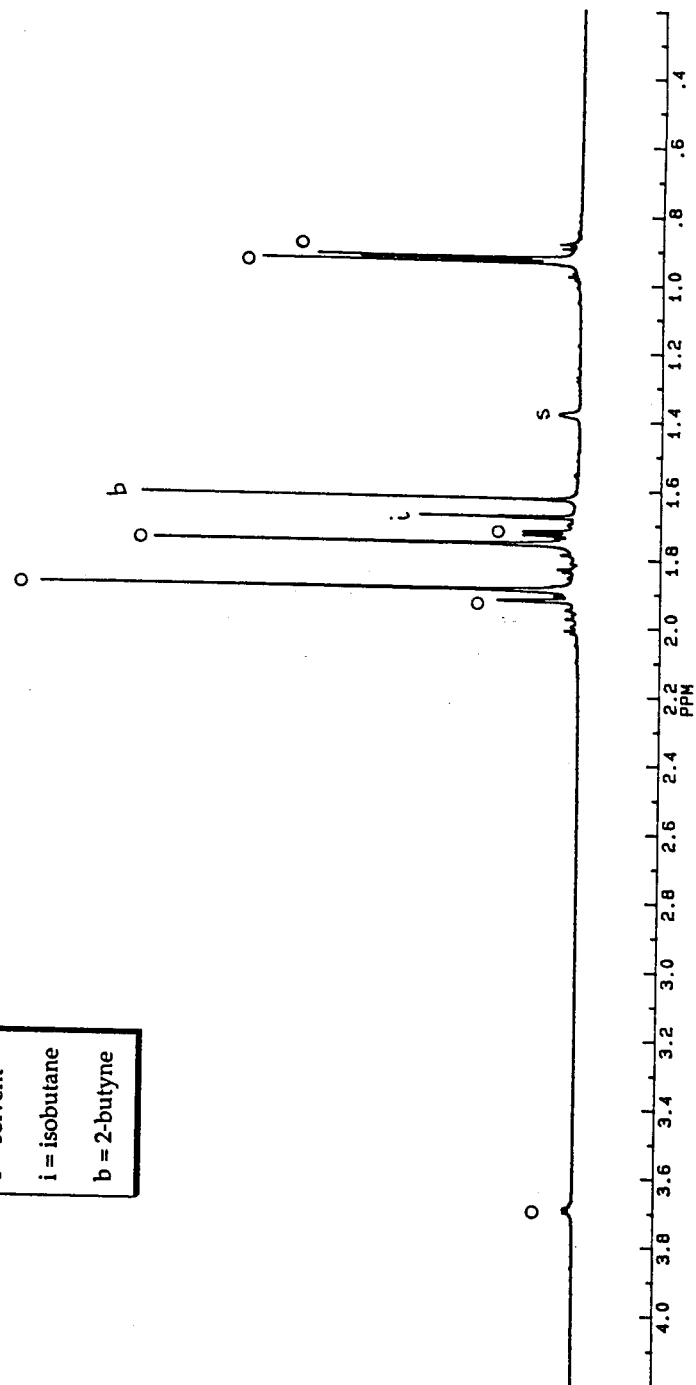
REACTION OF OPSC (ISOBUTYL) WITH EXCESS 2-BUTYNE

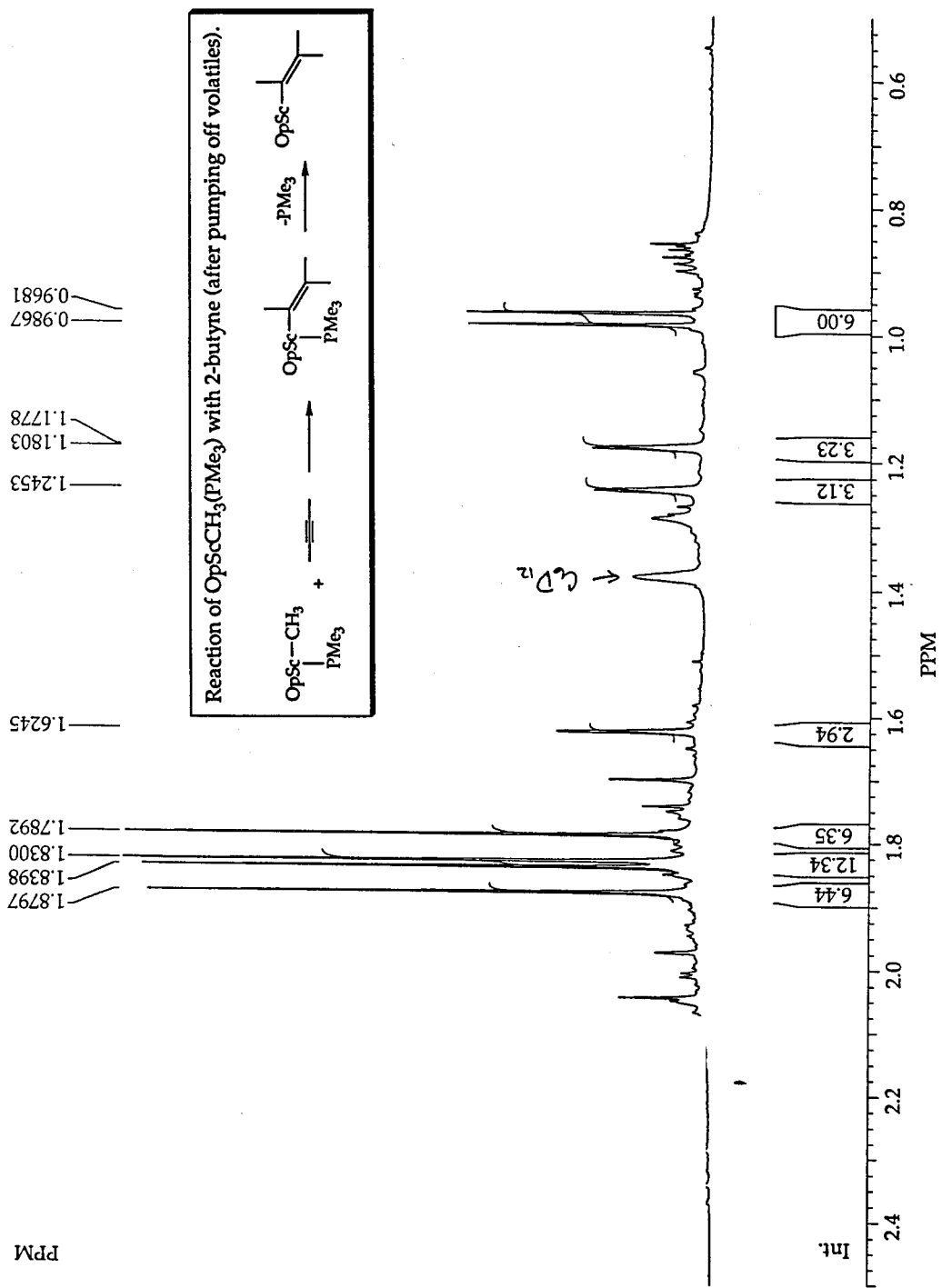


s = solvent

i = isobutane

b = 2-butyne

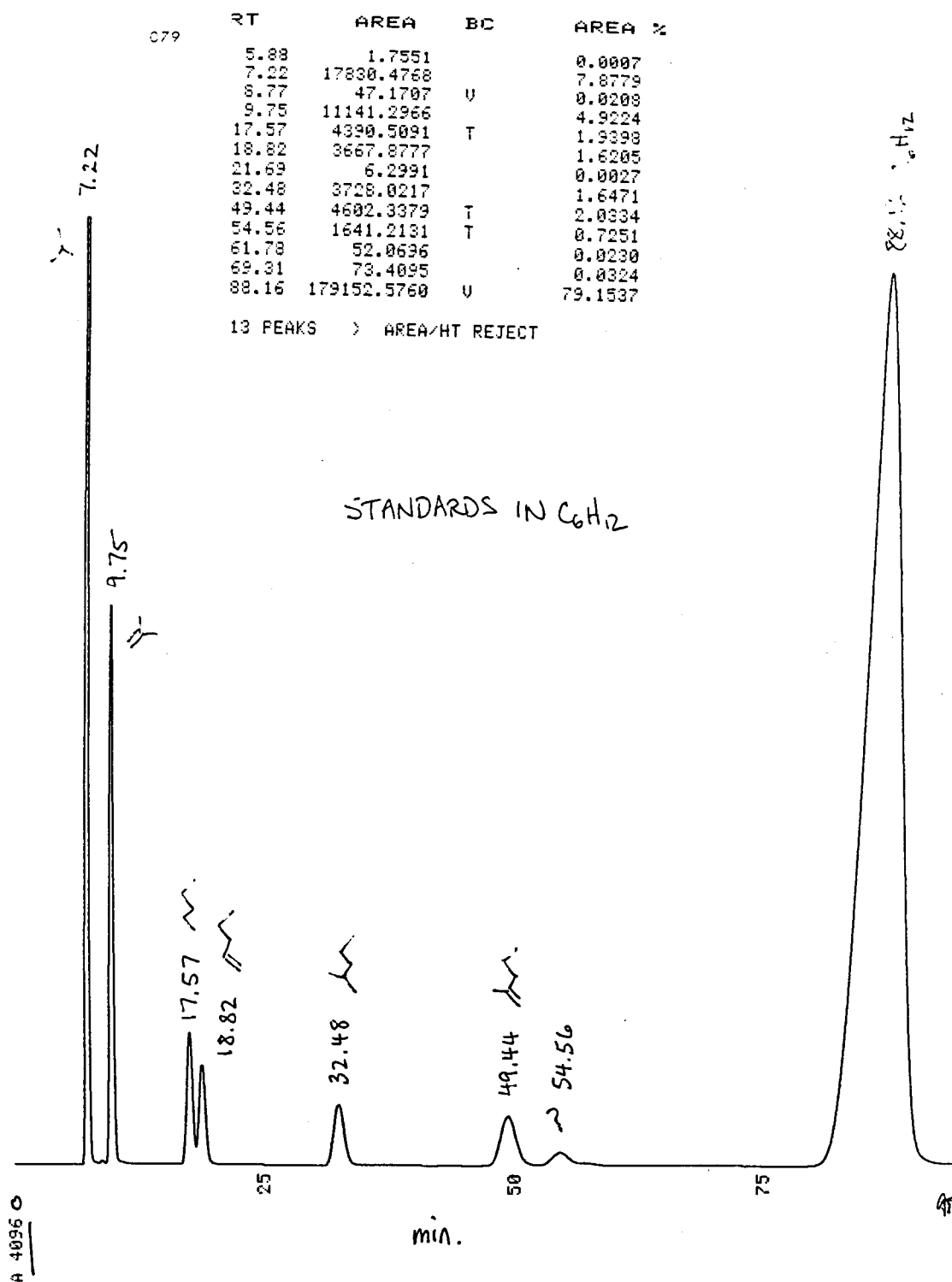




PPM

Int.





RUN 4 14:54 91/06/87

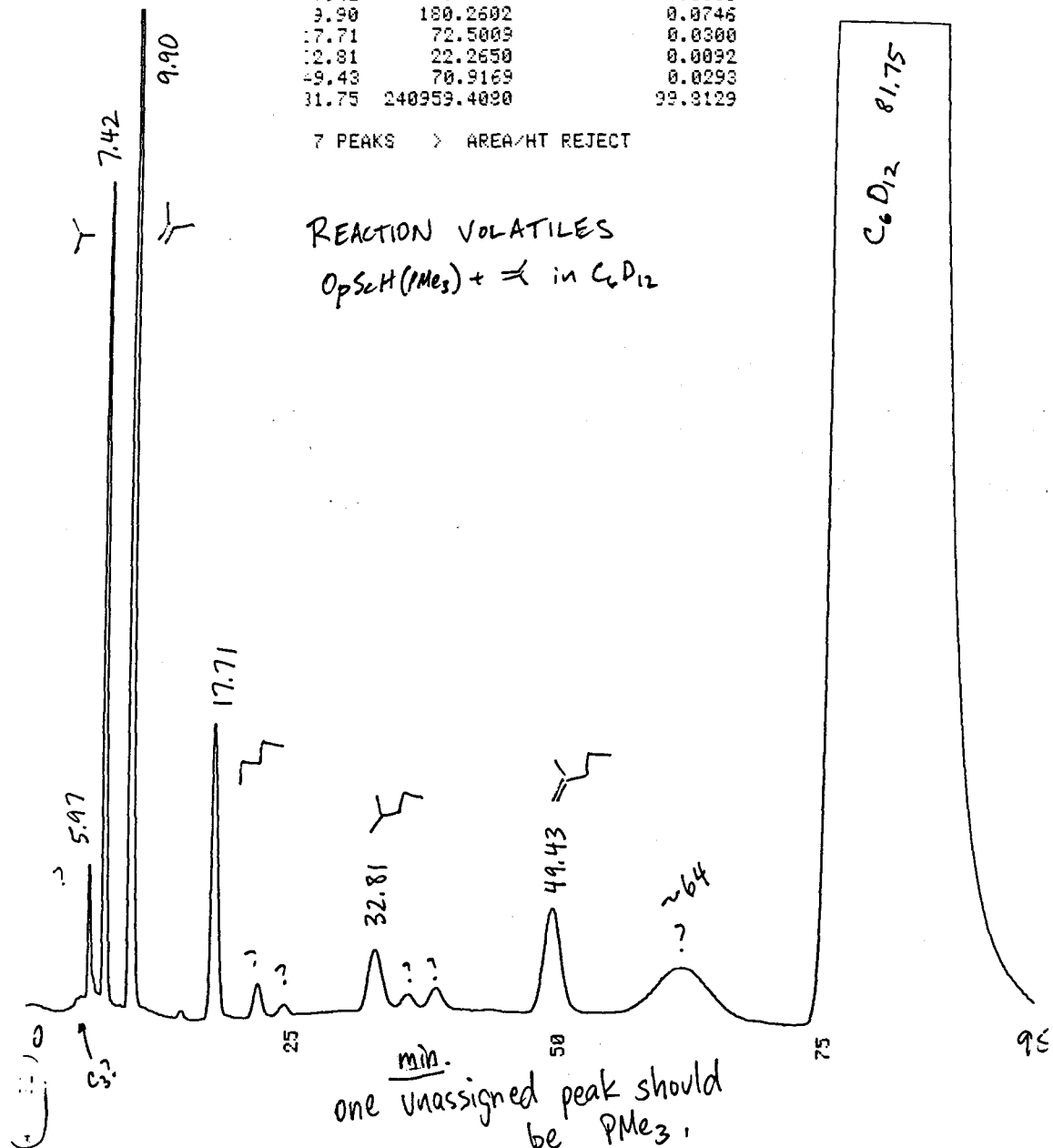
METHOD 1 MODIFIED CALCUL

RT	AREA	BC	AREA %
5.97	13.6453		0.0056
7.42	91.9962		0.0381
9.90	180.2602		0.0746
17.71	72.5009		0.0300
32.81	22.2650		0.0092
49.43	70.9169		0.0293
81.75	240959.4020		99.9129

7 PEAKS > AREA/HT REJECT

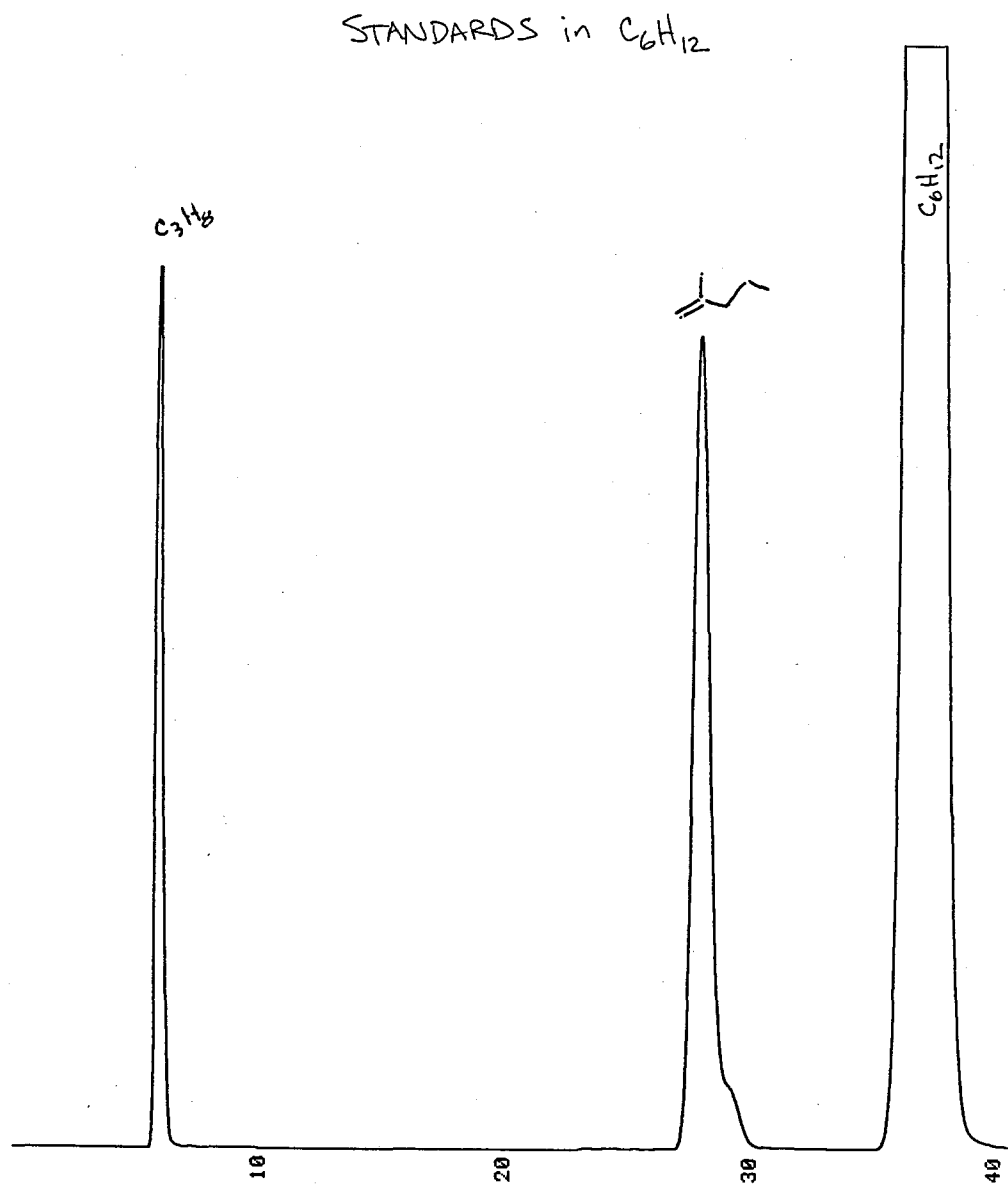
REACTION VOLATILES

$\text{OpSeH(PMe}_3\text{)} + \text{X in C}_6\text{D}_{12}$

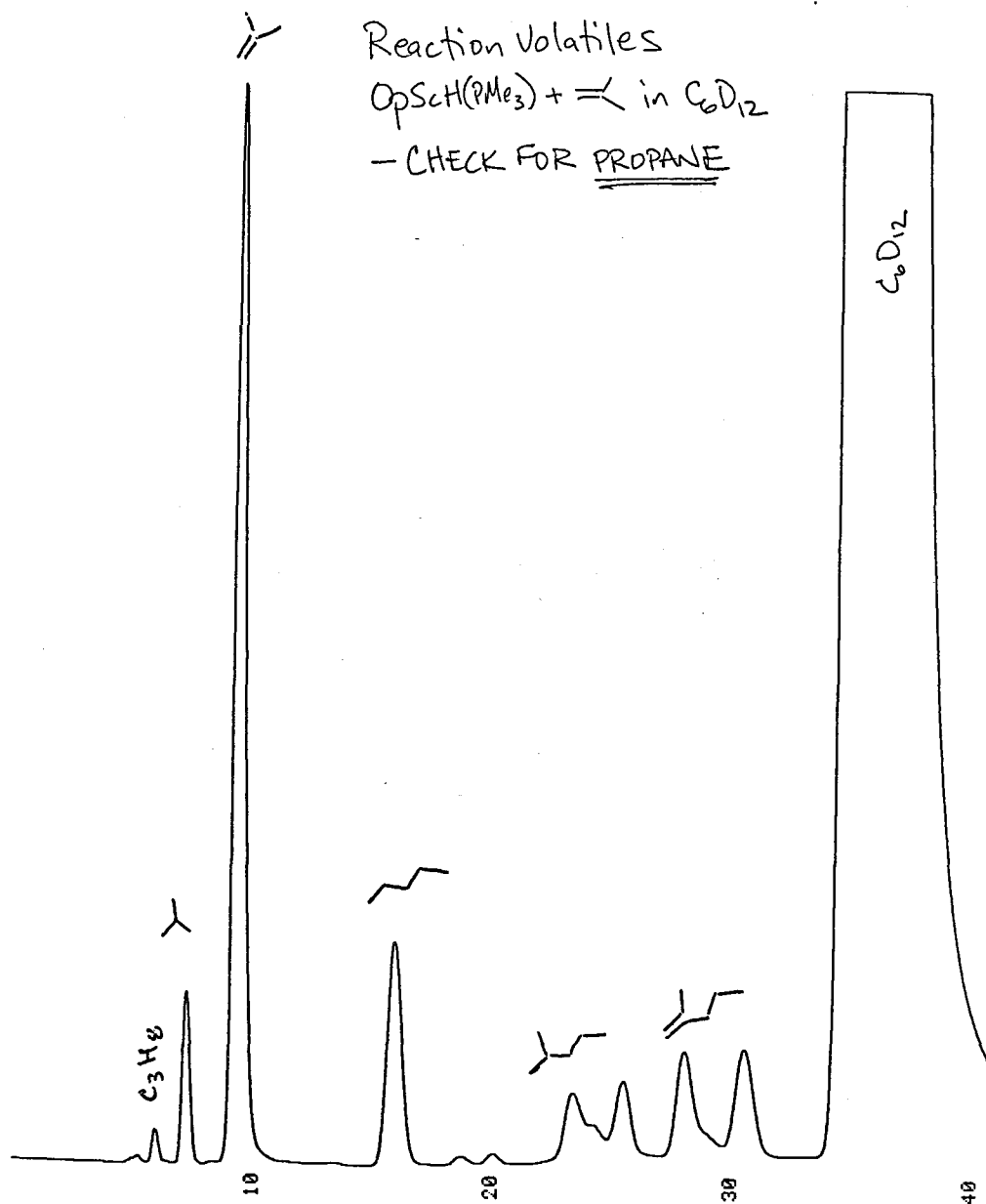


METHOD 3 MODIFIED

A 1024



RUN 11 4:53 93/04/20  
METHOD 3 MODIFIED  
A 32



```
*LIST KINETIC.AU
```

```
----- FILE: KINETIC .AU
```

```
; ** KINETIC **
```

```
; PROGRAM TO ACQUIRE A SERIES OF EXPERIMENTS  
; AT INTERVALS AND SAVE ON THE HARD DISK
```

```
; LDF/SPH 10TH MAY 1991
```

```
1  ZE                      ; ZERO THE MEMORY  
2  D1                      ; RELAXATION DELAY  
3  GO=2  
4  WR #1                  ; WRITE THIS EXPNT. TO DISK  
5  IF #1                  ; INCREMENT THE FILE EXTENSION  
6  D2                      ; DELAY BETWEEN EXPERIMENTS (SECONDS)  
7  IN=1                   ; LOOP BACK AND START THE NEXT EXPERIMENT  
8  EXIT  
  
; PW = PULSE WIDTH CA. 50 DEG. 4 US  
; D1 = DELAY BETWEEN SCANS CA 2 SECS  
; D2 = DELAY BETWEEN EXPERIMENTS (SECONDS)  
; NS = NUMBER OF SCANS PER EXPERIMENT  
; NE = NUMBER OF EXPERIMENTS  
; RD = 0
```

## Chapter 2

### **Intramolecular $\sigma$ Bond Metathesis for Permethylscandocene-Alkyl Complexes Revisited: Structure of Permethylcyclopentadienyl- $\mu$ -tetramethylcyclopentadienylmethylene Scandium Dimer.**

<b>Abstract</b>	<b>51</b>
<b>Introduction</b>	<b>52</b>
<b>Results and Discussion</b>	<b>52</b>
<b>Experimental</b>	<b>54</b>
<b>References and Notes</b>	<b>55</b>
<b>Appendix</b>	<b>56</b>

### Abstract

The cyclopentylmethyl derivative,  $\text{Cp}^*_2\text{ScCH}_2(\text{cyclo-C}_5\text{H}_8)$ , slowly and cleanly decomposes in cyclohexane to give methylcyclopentane and a yellow crystalline precipitate. The  $^1\text{H}$  NMR spectrum of the yellow product is consistent with a compound containing one  $\text{Cp}^*$  and one  $(\eta^5, \eta^1)\text{-C}_5(\text{CH}_3)_4\text{CH}_2$ , the latter arising *via* metallation of a  $\text{Cp}^*$  ligand (*i.e.* a "tuck-in" complex). The structure of the complex which crystallizes as the dimer,  $[\text{Cp}^*\text{Sc}\{\mu\text{-(}\eta^5, \eta^1\text{)-C}_5(\text{CH}_3)_4\text{CH}_2\}]_2$ , when allowed to form slowly at room temperature is reported.

## Introduction

Alkyl and hydride derivatives of permethylscandocene are of interest both for their C-H bond activation chemistry<sup>1</sup> and as model systems for homogeneous Ziegler-Natta catalysis.<sup>2</sup> A notable feature of these complexes is their ability to activate the primary C-H bonds of molecules such as CH<sub>4</sub>, CH<sub>3</sub>CH<sub>2</sub>CH<sub>3</sub>, Si(CH<sub>3</sub>)<sub>4</sub>, and P(CH<sub>3</sub>)<sub>3</sub>.<sup>1</sup> During the course of some recent mechanistic studies, we have observed that the cyclopentylmethyl derivative, Cp<sup>\*</sup><sub>2</sub>ScCH<sub>2</sub>(*cyclo*-C<sub>5</sub>H<sub>8</sub>), slowly and cleanly decomposes in cyclohexane to give methylcyclopentane and a yellow crystalline precipitate. The <sup>1</sup>H NMR spectrum of the yellow product is consistent with a compound containing one Cp<sup>\*</sup> and one (η<sup>5</sup>,η<sup>1</sup>)-C<sub>5</sub>(CH<sub>3</sub>)<sub>4</sub>CH<sub>2</sub>, the latter arising *via* metallation of a Cp<sup>\*</sup> ligand (*i.e.* a "tuck-in" complex). This same tuck in complex has been previously obtained from thermolysis of Cp<sup>\*</sup><sub>2</sub>ScCH<sub>3</sub>;<sup>1</sup> however, the solid product obtained previously was not crystalline and was postulated to be oligomeric based on its solubility properties. We report herein the structure of the complex which crystallizes as the dimer, [Cp<sup>\*</sup>Sc{μ-(η<sup>5</sup>,η<sup>1</sup>)-C<sub>5</sub>(CH<sub>3</sub>)<sub>4</sub>CH<sub>2</sub>}]<sub>2</sub>, when allowed to form slowly at room temperature.

## Results and Discussion

The dimer (Figure 1) is joined across an inversion center by an (η<sup>5</sup>,η<sup>1</sup>)-Cp<sup>\*</sup> group which bridges the two symmetry-related Sc atoms. The η<sup>1</sup>-methylene (C6) has been formed as the result of C-H activation of a Cp<sup>\*</sup> methyl group. A somewhat surprising result is that, in all other regards, the bonding is very similar to that determined for Cp<sup>\*</sup><sub>2</sub>ScCH<sub>3</sub>.<sup>1</sup> The (η<sup>5</sup>,η<sup>1</sup>)-ring remains planar with a maximum deviation of only 0.22 Å from the least squares plane calculated for C1 through C10.



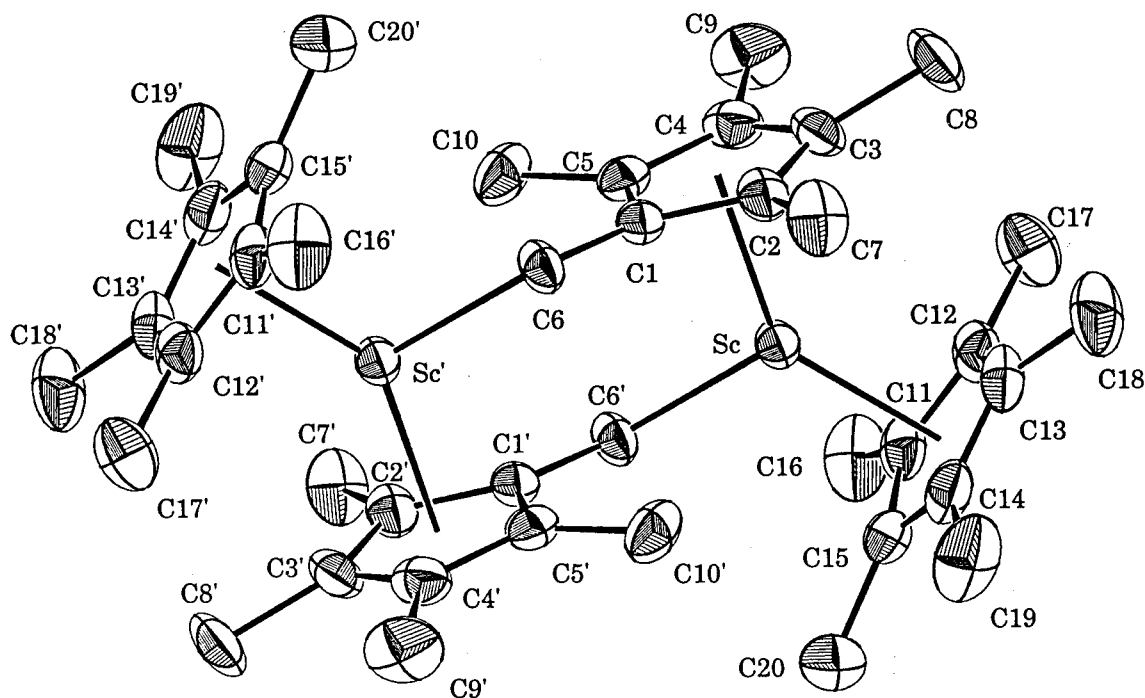


**Figure 1.** ORTEP drawing of the dimer with 50% probability ellipsoids showing the numbering system. H atoms omitted for clarity.

The geometry about C6 is essentially tetrahedral; the angles C1-C6-Sc', C1-C6-H6A, C1-C6-H6B, H6A-C6-H6B, are 118.9, 107.3, 104.8, and 98.1° respectively, giving an average value of 107.3 (8.6)°. The H6A-C6-H6B angle is slightly compressed (98.1°) while the C1-C6-Sc angle is somewhat opened (118.9°). The Sc'...H6A and Sc'...H6B distances are 2.76(3) and 2.79(3) Å indicating that there is no agostic interaction for the  $\alpha$ -H atoms with the Sc center. The Cp\*-Sc-Cp\* angle (141.8°) is approximately the same as for Cp\*<sub>2</sub>ScCH<sub>3</sub> (144.7°) suggesting that formal replacement of a methyl ligand with a bulkier ( $\eta^5, \eta^1$ )-Cp\* group as the alkyl does not significantly perturb the Sc-Cp\* bonding.

## Experimental

**Preparation of  $[\text{Cp}^*\text{Sc}((\eta^5\text{-C}_5(\text{CH}_3)_4(\mu\text{-}\eta\text{-CH}_2)))]_2$ .** A small swivel frit equipped with two 25 ml flasks and a 90° needle valve was taken into the glovebox and charged with  $\text{Cp}^*_2\text{ScCH}_2(\text{cyclo-C}_5\text{H}_8)$  (264.7 mg). On the vacuum line, cyclohexane (*ca.* 15 ml) was condensed onto the solid. The assembly was filled with an atmosphere of argon, taken off the line, and was stored in the dark. After 2-3 weeks, beautiful, yellow, x-ray quality crystals were observed to have precipitated. The frit assembly was returned to the vacuum line and the product was filtered, dried *in vacuo* and collected. Yield 152 mg.  $^1\text{H}$  NMR ( $\text{C}_6\text{D}_{12}$ ):  $\delta$  2.07 (singlet, broad, 6H),  $\delta$  1.91 (singlet, broad, 15H),  $\delta$  1.29 (singlet, broad, 3H),  $\delta$  1.14 (singlet, broad, 3H),  $\delta$  0.88 (multiplet, broad, 2H). Elemental analysis calculated for  $\text{C}_{40}\text{H}_{58}\text{Sc}_2$ : C 76.39%, H 9.31%; found: C 76.25%, H 9.10%.

**Crystal Structure Determination for  $[\text{Cp}^*\text{Sc}((\eta^5\text{-C}_5(\text{CH}_3)_4(\mu\text{-}\eta\text{-CH}_2)))]_2$ .** A suitable yellow crystal of approximate dimensions  $0.4 \times 0.2 \times 0.05$  mm was grown as above and mounted in a glass capillary in the glove box to prevent decomposition. The crystal was optically centered on an Enraf Nonius CAD 4 diffractometer equipped with a Mo  $\text{K}\alpha$  source. 25 well dispersed reflections in the range of  $\theta$  between 12.47 and 13.68 degrees were used for determining the unit cell parameters. No absorption correction was applied to the data. Data were collected for  $h$ ,  $k$ , and  $l$  within the limits -10 to 10, -11 to 11, and -14 to 14 respectively. The maximum value of  $\sin \theta / \lambda$  was 0.5761. Three intensity check reflections were used to monitor crystal decay. No significant decay was measured and therefore no decay correction was applied. The total number of reflections measured was 6239. The total number of independent measurements was 3068. There were no unobserved reflections and all reflections were used for solution and refinement. Patterson methods were used to determine the

scandium atom position and subsequent structure factors-least squares analysis revealed all the carbon atoms as the top twenty peaks. All non-hydrogen atoms were refined anisotropically using full matrix least squares on  $F_{\text{obs}}^2$ . The positions of the methyl-hydrogens were determined using difference maps calculated in the idealized least squares planes from their respective carbon atoms and were included in the structure factor but not refined. The hydrogen atoms on C6 were located in the penultimate difference map and were allowed to refine freely with isotropic thermal parameters. The final R was 0.062 and the esd of an observation of unit weight was 2.19. The maximum and minimum heights in the final difference Fourier were 0.40 and -0.35 electrons/ $\text{\AA}^3$  respectively. Atomic scattering factors were taken from Cromer, D.T. and Waber, J.T., *International Tables For X-ray Crystallography, Vol. IV*, pp. 99-101, 1974. Programs used were the CRYM crystallographic computing system<sup>3</sup> and ORTEP.<sup>4</sup>

#### References and Notes

1. Thompson, M.E.; Baxter, S.M.; Bulls, A.R.; Burger, B.J.; Nolan, M.C.; Santarsiero, B.D.; Schaefer, W.P.; Bercaw, J.E. *J. Am. Chem. Soc.* **1987**, *109*, 203.
2. Burger, B.J.; Thompson, M.E.; Cotter, W.D.; Bercaw, J.E. *J. Am. Chem. Soc.* **1990**, *112*, 1566.
3. Duchamp, D. J. (1964). Am. Crystallogr. Assoc. Meet., Bozeman, Montana, Paper B14, p. 29.
4. Johnson, C. K. (1976). ORTEPII. Report ORNL-3794. Oak Ridge National Laboratory, Oak Ridge, Tennessee, USA.

## Appendix 2

X-ray Crystal Structure Data for  
 $[\text{Cp}^*\text{Sc}\{\mu\text{-(}\eta^5\text{,}\eta^1\text{)-C}_5\text{(CH}_3\text{)}_4\text{CH}_2\}\}_2$ .

**Table 1. Crystal Data for [Cp\*Sc{ $\mu$ -( $\eta^5$ , $\eta^1$ )-C<sub>5</sub>(CH<sub>3</sub>)<sub>4</sub>CH<sub>2</sub>}]<sub>2</sub>**Formula: C<sub>40</sub>H<sub>58</sub>Sc<sub>2</sub>

Formula Wt.: 628.90

Space Group: P<sub>1</sub> (#2)

Temperature: 298 K

 $a = 8.641(5) \text{ \AA}$  $\alpha = 75.58(3) \text{ deg}$  $b = 9.478(2) \text{ \AA}$  $\beta = 80.39(4) \text{ deg}$  $c = 12.338(5) \text{ \AA}$  $\gamma = 63.75(3) \text{ deg}$  $V = 875.8(7) \text{ \AA}^3$  $\lambda_{\text{MoK}\alpha} = 0.71073 \text{ \AA}$  $\rho_{\text{calc}} = 1.19 \text{ g cm}^{-3}$  $Z = 1$  $\mu = 4.11 \text{ cm}^{-1}$

Table 2. Final Refined Parameters for  $[\text{Cp}^*\text{Sc}(\mu\text{-}(\eta^5\eta^1)\text{-C}_5(\text{CH}_3)_4\text{CH}_2)]_2$ 

$x, y, z$ and $U_{eq}^a \times 10^4$				
Atom	$x$	$y$	$z$	$U_{eq}$ or $B$
Sc	3717(.8)	1165(.7)	3300(.5)	300(1)
C1	3923(4)	2104(3)	4991(2)	301(7)
C2	3513(4)	3428(3)	4061(2)	344(7)
C3	1831(4)	3845(3)	3769(3)	377(8)
C4	1223(4)	2744(4)	4459(3)	394(8)
C5	2516(4)	1685(3)	5216(2)	331(7)
C6	5429(4)	1412(4)	5718(3)	340(7)
C7	4619(5)	4333(4)	3583(3)	495(9)
C8	706(5)	5401(4)	3035(3)	611(11)
C9	-558(4)	2824(5)	4496(3)	611(11)
C10	2290(4)	480(4)	6200(3)	466(8)
C11	3154(4)	217(4)	1759(2)	397(8)
C12	2251(4)	1905(4)	1524(2)	410(8)
C13	3485(4)	2559(4)	1263(2)	414(8)
C14	5129(4)	1276(4)	1334(2)	435(9)
C15	4929(4)	-173(4)	1624(2)	408(9)
C16	2318(5)	-943(5)	2048(3)	625(10)
C17	332(5)	2804(4)	1391(3)	616(10)
C18	3157(5)	4283(4)	740(3)	647(11)
C19	6805(5)	1458(5)	1009(3)	713(12)
C20	6366(5)	-1823(4)	1620(3)	653(11)
H6 A	6294(36)	1604(32)	5299(23)	2.7(7) *
H6 B	5132(33)	2166(32)	6200(22)	2.8(6) *

$$^a U_{eq} = \frac{1}{3} \sum_i \sum_j [U_{ij}(a_i^* a_j^*)(\vec{a}_i \cdot \vec{a}_j)]$$

\* Isotropic displacement parameter,  $B$

Table 3. Anisotropic Thermal Parameters for [Cp\*Sc( $\mu$ -( $\eta^5$ , $\eta^1$ )-C<sub>5</sub>(CH<sub>3</sub>)<sub>4</sub>CH<sub>2</sub>)]<sub>2</sub>

Atom	$U_{11}$	$U_{22}$	$U_{33}$	$U_{12}$	$U_{13}$	$U_{23}$
Sc	332(3)	264(3)	285(3)	-99(2)	-64(2)	-43(2)
C1	314(18)	236(15)	333(16)	-70(13)	-50(13)	-91(12)
C2	418(19)	261(15)	363(17)	-125(14)	-73(14)	-79(13)
C3	387(19)	256(16)	409(18)	-24(14)	-125(15)	-81(14)
C4	287(18)	438(19)	437(19)	-75(15)	-47(15)	-183(15)
C5	358(18)	310(16)	296(16)	-96(14)	2(13)	-109(13)
C6	382(20)	328(17)	326(18)	-137(15)	-72(15)	-82(14)
C7	640(24)	368(18)	519(21)	-257(17)	-139(18)	-4(16)
C8	660(26)	393(20)	623(24)	6(18)	-283(20)	-110(17)
C9	387(21)	802(27)	636(25)	-187(19)	-29(18)	-249(21)
C10	531(22)	521(21)	396(19)	-261(18)	49(16)	-153(16)
C11	523(22)	438(19)	289(17)	-241(17)	-123(15)	-34(14)
C12	411(19)	496(20)	311(17)	-171(16)	-132(14)	-25(15)
C13	521(22)	436(19)	307(17)	-236(17)	-141(15)	33(14)
C14	468(21)	620(23)	259(17)	-286(18)	-35(15)	-40(15)
C15	481(22)	417(19)	253(16)	-99(16)	-74(15)	-81(14)
C16	853(29)	683(25)	522(23)	-454(23)	-175(21)	-92(19)
C17	522(24)	695(26)	594(24)	-191(20)	-248(19)	-50(20)
C18	942(31)	564(24)	456(22)	-400(22)	-178(21)	111(18)
C19	633(27)	1083(34)	445(22)	-466(25)	6(19)	-15(22)
C20	706(27)	625(24)	497(23)	-96(21)	-37(20)	-241(19)

$U_{i,j}$  values have been multiplied by  $10^4$

The form of the displacement factor is:

$$p - 2\pi^2(U_{11}h^2a^{*2} + U_{22}k^2b^{*2} + U_{33}\ell^2c^{*2} + 2U_{12}hka^*b^* + 2U_{13}h\ell a^*c^* + 2U_{23}k\ell b^*c^*)$$

Table 4. Complete Distances and Angles for  $[\text{Cp}^*\text{Sc}\{\mu-(\eta^5, \eta^1)\text{-C}_5(\text{CH}_3)_4\text{CH}_2\}]_2$ 

Distance(Å)			Distance(Å)		
Sc	-Cp*1	2.181	C16	-H16C	0.954
Sc	-Cp*2	2.212	C17	-H17A	0.952
Sc	-C6	3.643(5)	C17	-H17B	0.951
Sc	-C6'	2.282(5)	C17	-H17C	0.952
C1	-C2	1.429(4)	C18	-H18A	0.951
C1	-C5	1.404(4)	C18	-H18B	0.953
C1	-C6	1.507(4)	C18	-H18C	0.950
C2	-C3	1.412(4)	C19	-H19A	0.951
C2	-C7	1.510(5)	C19	-H19B	0.954
C3	-C4	1.408(4)	C19	-H19C	0.949
C3	-C8	1.517(5)	C20	-H20A	0.952
C4	-C5	1.420(4)	C20	-H20B	0.954
C4	-C9	1.501(5)	C20	-H20C	0.949
C5	-C10	1.498(5)			
C6	-H6 A	0.90(3)			
C6	-H6 B	0.96(3)			
C7	-H7 A	0.953			
C7	-H7 B	0.953			
C7	-H7 C	0.952			
C8	-H8 A	0.953			
C8	-H8 B	0.951			
C8	-H8 C	0.951			
C9	-H9 A	0.952			
C9	-H9 B	0.952			
C9	-H9 C	0.953			
C10	-H10A	0.950			
C10	-H10B	0.951			
C10	-H10C	0.953			
C11	-C12	1.412(5)			
C11	-C15	1.400(5)			
C11	-C16	1.510(5)			
C12	-C13	1.412(5)			
C12	-C17	1.508(5)			
C13	-C14	1.401(5)			
C13	-C18	1.514(5)			
C14	-C15	1.410(5)			
C14	-C19	1.510(5)			
C15	-C20	1.508(5)			
C16	-H16A	0.949			
C16	-H16B	0.949			



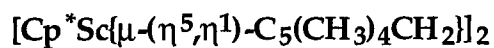
Table 4. Complete Distances and Angles for  $[\text{Cp}^*\text{Sc}\{\mu\text{-(}\eta^5\text{,}\eta^1\text{)-C}_5\text{(CH}_3\text{)}_4\text{CH}_2\}]_2$ 

(cont.)	Angle(°)			Angle(°)	
Cp*2 -Sc -Cp*1	141.6		H10B -C10 -C5	108.9	
C6' -Sc -Cp*1	107.9		H10C -C10 -C5	108.8	
C6' -Sc -Cp*2	108.6		H10B -C10 -H10A	110.2	
C5 -C1 -C2	106.9(3)		H10C -C10 -H10A	110.0	
C6 -C1 -C2	127.9(3)		H10C -C10 -H10B	109.9	
C6 -C1 -C5	124.7(3)		C15 -C11 -C12	108.2(3)	
C3 -C2 -C1	108.2(3)		C16 -C11 -C12	125.0(3)	
C7 -C2 -C1	124.8(3)		C16 -C11 -C15	126.8(3)	
C7 -C2 -C3	126.6(3)		C13 -C12 -C11	107.9(3)	
C4 -C3 -C2	108.3(3)		C17 -C12 -C11	124.6(3)	
C8 -C3 -C2	126.0(3)		C17 -C12 -C13	126.8(3)	
C8 -C3 -C4	124.3(3)		C14 -C13 -C12	107.6(3)	
C5 -C4 -C3	107.3(3)		C18 -C13 -C12	126.8(3)	
C9 -C4 -C3	126.0(3)		C18 -C13 -C14	124.2(3)	
C9 -C4 -C5	126.2(3)		C15 -C14 -C13	108.6(3)	
C4 -C5 -C1	109.2(3)		C19 -C14 -C13	124.3(3)	
C10 -C5 -C1	125.5(3)		C19 -C14 -C15	126.7(3)	
C10 -C5 -C4	124.7(3)		C14 -C15 -C11	107.7(3)	
H6 A -C6 -C1	107.3(19)		C20 -C15 -C11	126.3(3)	
H6 B -C6 -C1	104.8(17)		C20 -C15 -C14	125.5(3)	
H6 B -C6 -H6 A	98.1(26)		H16A -C16 -C11	109.0	
H7 A -C7 -C2	108.9		H16B -C16 -C11	108.9	
H7 B -C7 -C2	109.1		H16C -C16 -C11	108.7	
H7 C -C7 -C2	109.2		H16B -C16 -H16A	110.3	
H7 B -C7 -H7 A	109.8		H16C -C16 -H16A	109.9	
H7 C -C7 -H7 A	109.9		H16C -C16 -H16B	110.0	
H7 C -C7 -H7 B	109.9		H17A -C17 -C12	108.9	
H8 A -C8 -C3	109.0		H17B -C17 -C12	109.0	
H8 B -C8 -C3	109.0		H17C -C17 -C12	108.9	
H8 C -C8 -C3	109.0		H17B -C17 -H17A	110.1	
H8 B -C8 -H8 A	109.9		H17C -C17 -H17A	109.9	
H8 C -C8 -H8 A	109.9		H17C -C17 -H17B	110.1	
H8 C -C8 -H8 B	110.1		H18A -C18 -C13	109.0	
H9 A -C9 -C4	109.1		H18B -C18 -C13	108.8	
H9 B -C9 -C4	109.2		H18C -C18 -C13	109.0	
H9 C -C9 -C4	108.9		H18B -C18 -H18A	109.8	
H9 B -C9 -H9 A	110.0		H18C -C18 -H18A	110.1	
H9 C -C9 -H9 A	109.8		H18C -C18 -H18B	110.0	
H9 C -C9 -H9 B	109.8		H19A -C19 -C14	109.0	
H10A -C10 -C5	109.0		H19B -C19 -C14	108.8	

**Table 4. Complete Distances and Angles for [Cp\*Sc( $\mu$ -( $\eta^5$ , $\eta^1$ )-C<sub>5</sub>(CH<sub>3</sub>)<sub>4</sub>CH<sub>2</sub>)]<sub>2</sub>  
(cont.)**

Angle(°)		
H19C -C19 -C14		109.1
H19B -C19 -H19A		109.7
H19C -C19 -H19A		110.2
H19C -C19 -H19B		110.0
H20A -C20 -C15		109.0
H20B -C20 -C15		108.7
H20C -C20 -C15		109.1
H20B -C20 -H20A		109.8
H20C -C20 -H20A		110.2
H20C -C20 -H20B		110.1

Table 5. Non-refined Hydrogen Atom Parameters for



Atom	$x, y \text{ and } z \times 10^4$			$B$
	$x$	$y$	$z$	
H7 A	4181	5031	2894	4.7
H7 B	5778	3584	3451	4.7
H7 C	4580	4941	4103	4.7
H8 A	-186	6053	3497	5.8
H8 B	212	5162	2509	5.8
H8 C	1401	5944	2651	5.8
H9 A	-1193	3173	5160	5.7
H9 B	-470	1788	4494	5.7
H9 C	-1121	3567	3853	5.7
H10A	2055	901	6861	4.4
H10B	3322	-485	6254	4.4
H10C	1347	278	6088	4.4
H16A	1724	-871	2767	5.9
H16B	3189	-1998	2049	5.9
H16C	1521	-661	1497	5.9
H17A	33	3926	1234	5.8
H17B	-268	2521	2067	5.8
H17C	54	2518	786	5.8
H18A	1944	4912	705	6.1
H18B	3706	4322	2	6.1
H18C	3622	4669	1186	6.1
H19A	6804	1987	245	6.7
H19B	7742	416	1103	6.7
H19C	6904	2067	1477	6.7
H20A	6878	-1878	878	6.1
H20B	5891	-2595	1865	6.1
H20C	7202	-2015	2113	6.1

## Chapter 3

### **A New Class of Highly Electron Deficient Group III Organometallic Complexes Based on 1,4,7-Trimethyl-1,4,7-triazacyclononane**

<b>Abstract</b>	<b>65</b>
<b>Introduction</b>	<b>66</b>
<b>Results and Discussion</b>	<b>68</b>
<b>Conclusions</b>	<b>82</b>
<b>Experimental</b>	<b>83</b>
<b>References and Notes</b>	<b>92</b>
<b>Appendix</b>	<b>95</b>

### Abstract

Reaction of the neutral ligand 1,4,7-trimethyl-1,4,7-triazacyclononane (Cn) with  $MCl_3(THF)_3$  ( $M = Sc, Y$ ) in acetonitrile affords the novel trihalide complexes  $CnMCl_3$ . Subsequent alkylation with  $LiCH_3$  in THF cleanly gives the corresponding trimethyl species  $CnMMe_3$ . Reactivity studies reveal that the metal carbon bonds of these  $12 e^-$ ,  $d^0$  complexes are remarkably unreactive toward insertion chemistry with typical unsaturated substrates such as olefins and acetylene. 2-butyne does, however, react with  $CnYMe_3$  by C-H activation to give a compound that is characterized as an equilibrium mixture of a major allenyl form with a minor propargyl component. In general,  $CnScMe_3$  is significantly more stable, but less reactive, than  $CnYMe_3$ . Activation of  $CnScMe_3$  with  $B(C_6F_5)_3$  or  $[HMe_2NPh][B(C_6F_5)_4]$  results in partially characterized complexes which exhibit olefin polymerization chemistry. The crystal structure of  $CnScCl_3$  has been determined.

## Introduction

There has recently been a renewed interest in the investigation of novel ligand combinations for early transition metal organometallic systems. One aspect of these studies has involved "bent metallocene-like" systems which incorporate dianionic cyclopentadienyl analogs.<sup>1</sup> Metal complexes possessing one cyclopentadienyl ligand  $\text{Cp}^-$  and one dianionic analog afford systems which, relative to the parent metallocene, carry an additional net negative charge. Some recent examples are shown in Figure 1, and the charge differences are made apparent by comparing  $\text{A}^{1a}$  and  $\text{D}^{1c}$  with their parent structures **B** and **E** respectively

Similarly, formal substitution of  $\text{Cp}^-$  with a suitable neutral ligand would, in principle, lead to metallocene analogs such as **C** which possess an "extra" positive charge. Systematic investigation of an appropriate series of complexes with these ligand combinations might help clarify the relationship of net charge to the observed reactivity within an isoelectronic series (Figure 1).

While the inorganic and bioinorganic coordination chemistry of azamacrocycles and other neutral polyamines and polyethers has been extensively developed,<sup>2</sup> and these type of ligands have been shown to coordinate quite strongly to a broad range of transition metals, their use as ancillary ligands in organometallic systems<sup>3</sup> - especially for early transition metals - remains virtually unexplored.<sup>4</sup> Accordingly, we have undertaken a study of the chemistry of scandium and yttrium in the coordination sphere of the neutral ligand, 1,4,7-trimethyl-1,4,7-triazacyclononane (**Cn**). The initial targets of these studies were the metallocene-like compounds of general formula **C** as depicted in Figure 1.

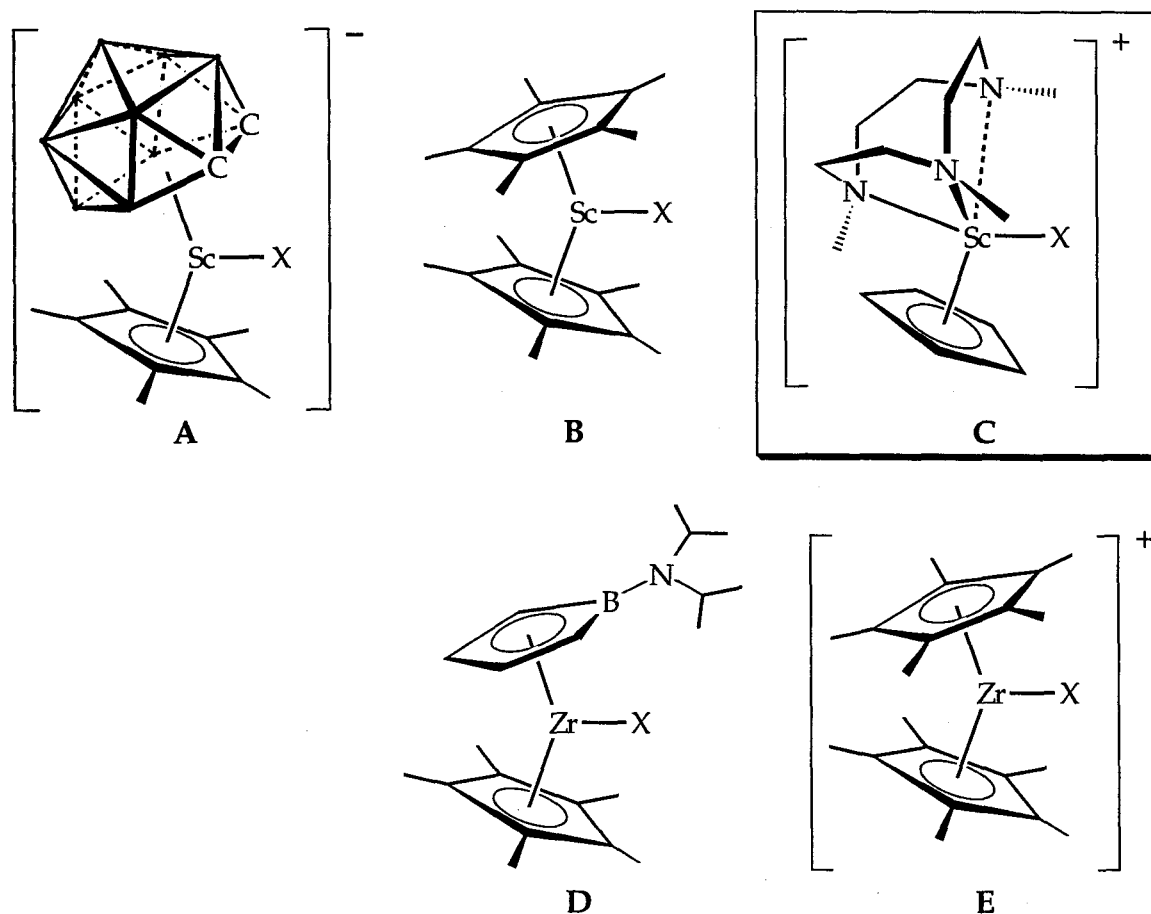


**Figure 1.** Examples of isoelectronic group III and group IV complexes, with the target complex, C, highlighted in the box (see text for details).

Recent results with later metals indicate that employment of properly tailored neutral chelating complexes as ancillary ligands can be a successful strategy towards the development of new classes of organometallic compounds (Figure 2). Flood and coworkers have found that the azamacrocyclic complex  $\text{CnRhCl}_3$  can be cleanly converted to the trimethyl species  $\text{CnRhMe}_3$  (**1**).<sup>5</sup> Rhodium dimethyl and monomethyl cations derived from **1** are quite robust and exhibit interesting and unusual reactivity in comparison with closely related cyclopentadienyl-rhodium systems.<sup>3</sup> Köhn *et al.* have also recently begun to study the organometallic chemistry of iron and chromium derivatives of the related triazacyclohexane-metal complexes.<sup>6</sup>

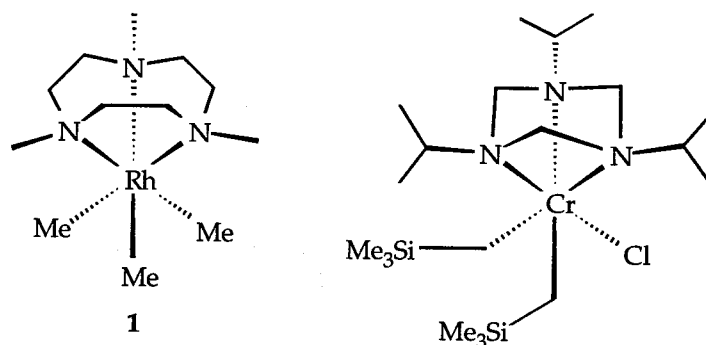
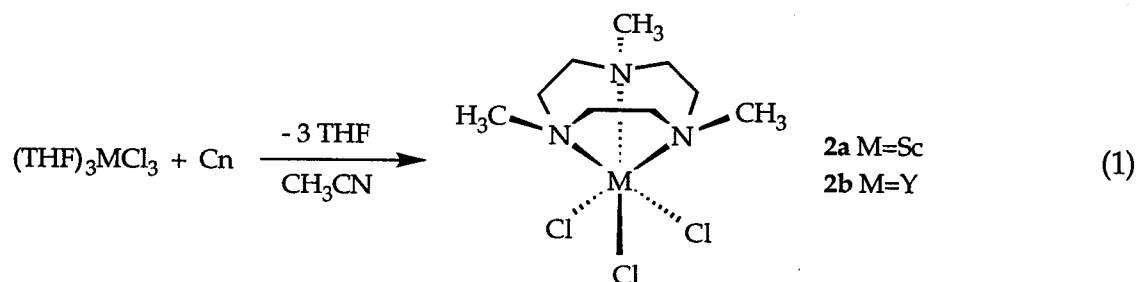


**Figure 2.** Examples of recently reported late transition metal organometallic systems supported by neutral azamacrocycles.

Although we have not yet succeeded in our initial goal of preparing metallocene analogs, **C**, we have been able to examine the properties of the  $C_n$  supported metal fragment,  $[C_nM]$  ( $M=Sc, Y$ ), which retains the full 3+ valency of the group three metal. As in the case of Flood's rhodium system, **1**, use of the  $C_n$  ligand affords a new class of scandium- and yttrium-alkyl compounds whose reactivity patterns differ markedly from those of the previously studied metallocene derived systems.<sup>4,7</sup>

## Results and Discussion

**Synthesis and Characterization of  $C_nMCl_3$  (**2**) and  $C_nMMe_3$  (**3**).** The syntheses of the novel trihalides  $C_nMCl_3$  (**2**) (**2a**,  $M=Sc$ ; **2b**,  $M=Y$ ) are readily accomplished by allowing the corresponding tris-THF adducts,  $(THF)_3MCl_3$ , to react with the  $C_n$  ligand in acetonitrile (eqn 1).





Our initial synthetic strategies for **2** were directed toward noncoordinating solvent systems in order to minimize competition with Cn ligand coordination, however, we have found that the relatively strongly coordinating acetonitrile is critical to obtaining high yields in these reactions; both reactants are highly soluble whereas the product is not. Apparently, the tridentate Cn ligand competes quite effectively with both THF and acetonitrile for metal binding.<sup>8</sup>

Both complexes have been characterized by NMR and elemental analysis. The scandium complex **2a** is moderately air stable and a suitable crystal grown from acetonitrile has been characterized by x-ray diffraction (Figure 3). The ligand is facially coordinated (as expected) and the complex has a slightly distorted octahedral geometry.

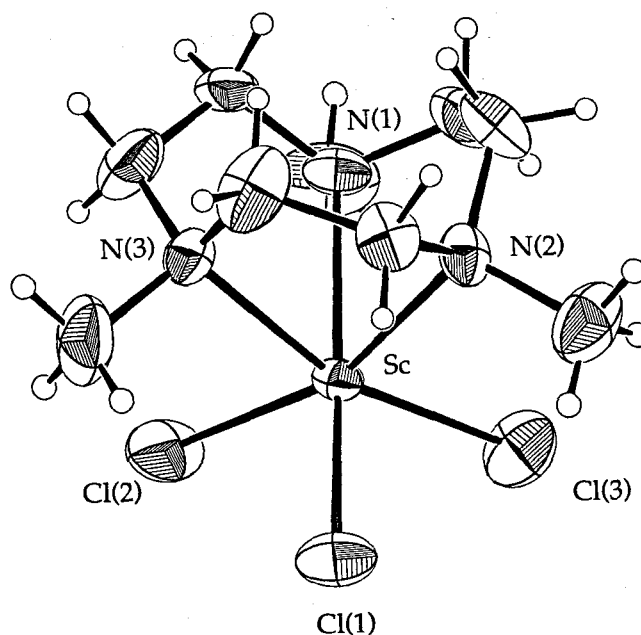


**Figure 3.** ORTEP diagram for  $\text{CnScCl}_3$  (**2a**). Selected bond distances: Sc-Cl (avg) 2.406 Å; Sc-N (avg) 2.337 Å. Selected bond angles: Cl-Sc-Cl (avg) 98.7°; N-Sc-N 75.4°; N-Sc-Cl 91.9°.

We have been unable to prepare Cp derivatives of **2** by reaction with cyclopentadienyl anion under a variety of conditions. We have found, however, that methylation of **2** proceeds quickly and cleanly in THF under ambient conditions to afford the trimethyl complexes  $\text{CnMMe}_3$  (**3**) (**3a**,  $\text{M}=\text{Sc}$ ; **3b**,  $\text{M}=\text{Y}$ ) in good yield (eqn 2).  $^1\text{H}$  NMR spectra for compounds **3b** and **3a** are shown in Figures 4 and 5 respectively. The  $\text{M}-\text{CH}_3$  and the *endo*- and *exo*-methylene resonances of the Cn ligand for **3** exhibit strongly solvent dependant  $^1\text{H}$  NMR chemical shifts (Figure 5). The cause of this effect has not been determined but the more coordinating solvent  $\text{THF}-d_8$ , and less coordinating benzene- $d_6$ , yield markedly different spectra, suggesting that there may be a site or sites on these 6-coordinate complexes for weak ligand binding.

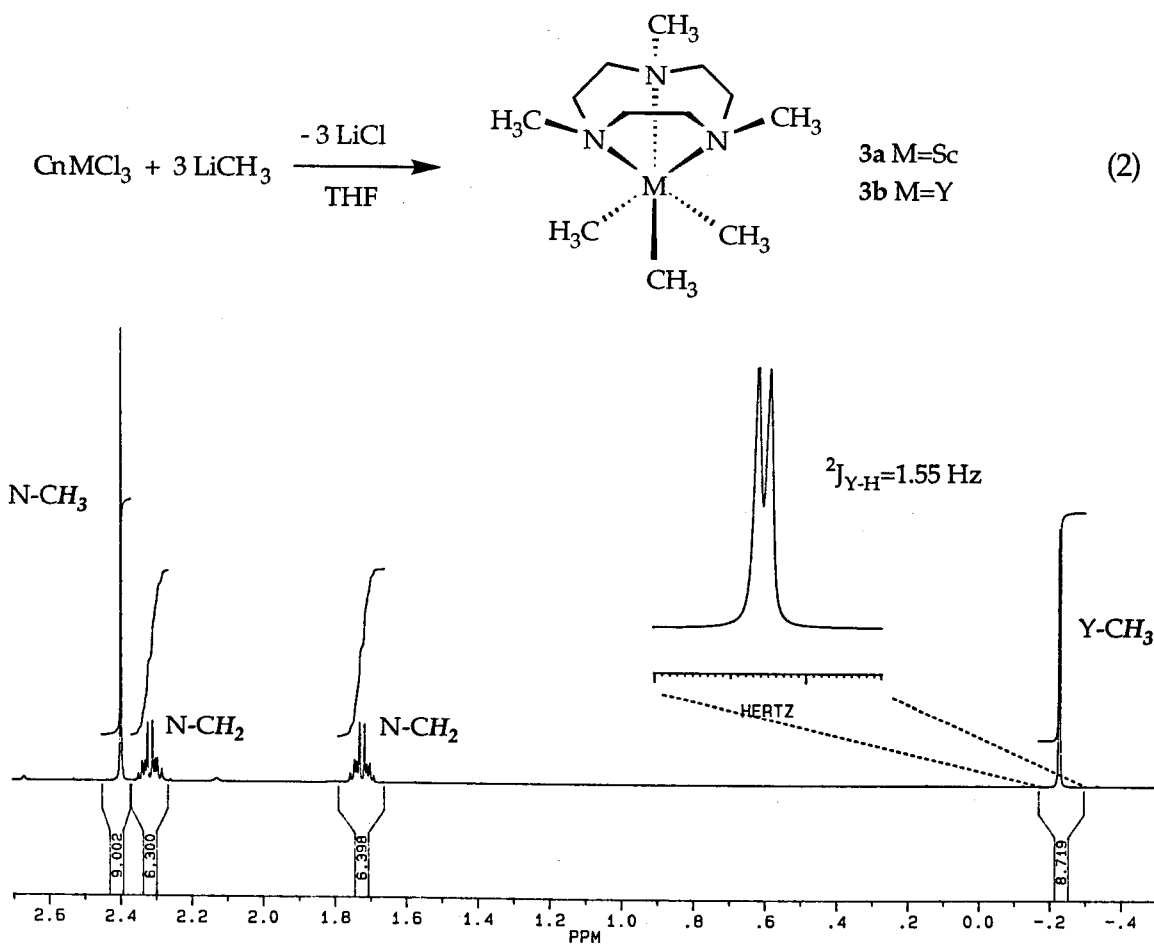


**Figure 4.**  $^1\text{H}$  NMR spectrum of **3b** acquired in benzene- $d_6$ .

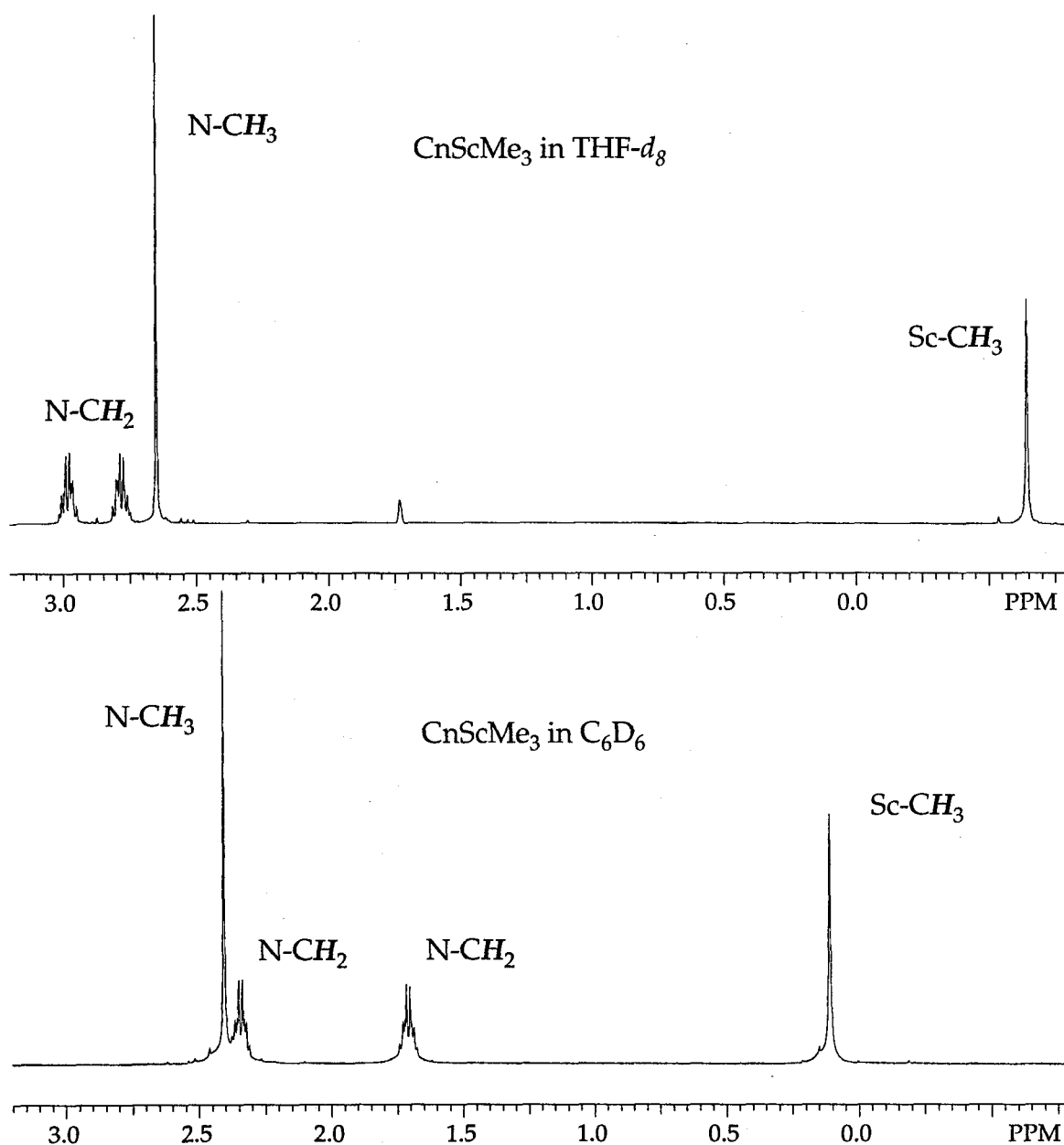


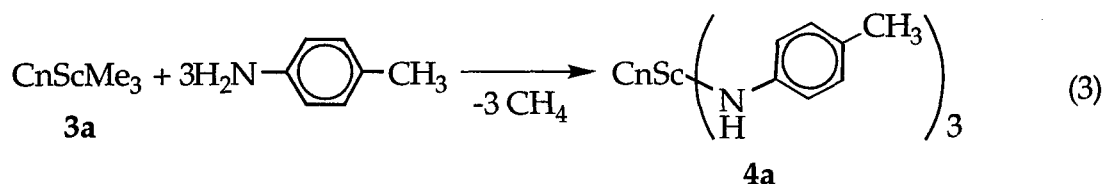
**Figure 5.**  $^1\text{H}$  NMR spectra of **3a** acquired in  $\text{THF-}d_8$  solvent (top) and  $\text{benzene-}d_6$  (bottom) reveal large solvent dependent chemical shifts of the coordinated Cn ligand *endo*- and *exo*-methylene multiplets and  $\text{Sc-CH}_3$  (see also Figure 4 for comparison).

Although we presume on the basis of the crystal structure of **2a** that the complexes **3** are octahedral, it has also been proposed that such  $d^0$  transition metal systems should have trigonal prismatic ground state geometries.<sup>9</sup> In an

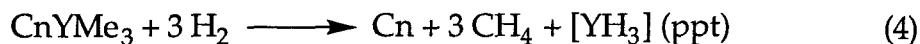
effort to clarify this situation, we have attempted repeatedly to grow crystals of complexes **3**. Indeed, when saturated solutions of **3a** are allowed to slowly cool in aromatic solvents, large, clear colorless crystals are reproducibly formed. Unfortunately, these crystals rapidly lose integrity by an apparent loss of co-crystallized solvent, and we have been unable to find suitable conditions for their isolation thus far.

**Reactivity Studies of 3.** Reactivity studies of **3a** reveal that the scandium-methyl bonds in this 12e<sup>-</sup> complex are surprisingly unreactive toward unsaturated organic substrates such as olefins, acetylenes, and even acetonitrile. In fact, **3a** reacts with H<sub>2</sub> only under forcing conditions (4 atm, 80 °C, several days) to afford a product which appears (by <sup>1</sup>H NMR) to be the trihydride CnScH<sub>3</sub>. Unfortunately this assignment is somewhat tentative because the large quadrupole for <sup>45</sup>Sc (100% abundant, I=7/2) normally precludes the observation of Sc-H resonances. An alternative interpretation is that the product is actually the perdeuteriotriphenyl complex, CnSc(C<sub>6</sub>D<sub>5</sub>)<sub>3</sub>, arising from σ bond metathesis of solvent (benzene-*d*<sub>6</sub>) with transient, highly reactive Sc-H bonds, however, HD (the expected coproduct) is not observed in the sealed NMR tube.

Interestingly, **3a** does react slowly at ambient temperature with *p*-toluidine giving a compound whose <sup>1</sup>H NMR spectrum is consistent with formation of the tris-amido complex CnSc[N(H)(*p*-C<sub>6</sub>H<sub>4</sub>(CH<sub>3</sub>))]<sub>3</sub> (**4a**) (eqn 3). This result suggests that whereas the methyl groups in **3a** do not readily undergo insertion reactions, they are quite basic. While **4a** is formed quite cleanly by precipitation in aromatic solvents, it is rather capricious in others: it decomposes in THF but is stable and moderately soluble in acetonitrile.



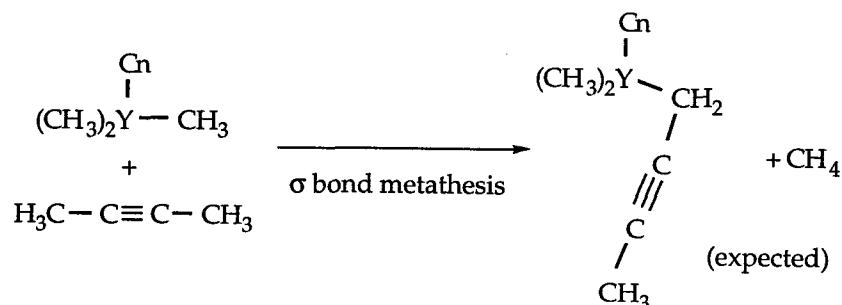
Like **3a**, **3b** reacts with *p*-toluidine to give the tris-amido complex  $\text{CnY}[\text{N}(\text{H})(\textit{p}\text{-C}_6\text{H}_4(\text{CH}_3))]\text{3}$ , but does so significantly more rapidly (minutes vs hours). In contrast to **3a**, which fails to react with the much bulkier secondary amine 2,4,6-tri(*tert*-butyl)aniline, **3b** reacts readily, but decomposes to intractable products. In general, we have found that the yttrium complex, **3b**, is somewhat more reactive than the scandium analog, but is also significantly less stable. Thus whereas **3a** requires forcing conditions to effect reaction with dihydrogen, **3b** reacts quite rapidly at room temperature; unfortunately, the products are not the expected methane and  $\text{CnYH}_3$ , but rather the components of a subsequent decomposition to give free Cn ligand and a gray precipitate which is presumed to be amorphous  $\text{YH}_3$  (eqn 4).



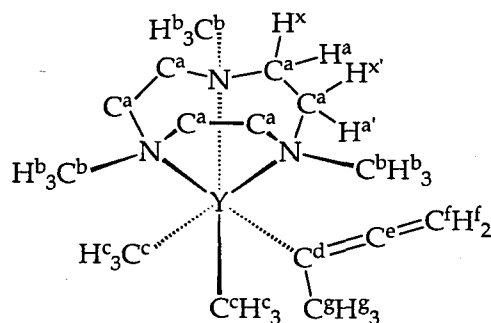
Upon exposure to air, **3b** decomposes rapidly; remarkably, the Cn ligand is not demetallated from scandium when **3a** is treated analogously. When room air is bubbled through a benzene- $d_6$  solution of **3a** in an NMR tube, the solution takes on a slight cloudiness, however, a subsequent  $^1\text{H}$  NMR spectrum does not indicate free Cn ligand and **3a** is still present. Presumably the cloudy precipitate is a Cn-scandium oxide of possible formulation  $\text{CnSc}(\mu\text{-O})_3\text{ScCn}$ .

**Reaction of 3b with 2-butyne.** We have not succeeded in observing any reactivity of **3b** with olefinic substrates, however, 2-butyne does react slowly at room temperature to give a product arising from C-H activation rather than insertion. The normal course of C-H activation for group III metal-alkyls is the

well documented  $\sigma$  bond metathesis reaction;<sup>10</sup> the expected products, in this case, would simply be the propargyl complex,  $\text{CnMe}_2\text{Y}-\text{CH}_2\text{CCCH}_3$  and methane.



Upon inspection of the room temperature NMR data (Figure 6), however, it is apparent that the situation here is rather more complicated.



<sup>13</sup> C NMR (125 MHz)	<sup>1</sup> H NMR (500 MHz)
Ca δ 54.90 (6 C), triplet, <sup>1</sup> J <sub>CH</sub> = 135 Hz	Ha, Ha' δ 2.34 (6 H), broad Hx, Hx' δ 1.71 (6 H), multiplet
Cb δ 47.67 (3 C), quartet, <sup>1</sup> J <sub>CH</sub> = 141 Hz	Hb δ 2.39 (9 H), broad
Cc δ 19.90 (2 C), quartet of doublets, <sup>1</sup> J <sub>CH</sub> = 104 Hz, <sup>1</sup> J <sub>YC</sub> = 46 Hz	Hc δ -0.37 (6 H), doublet, <sup>2</sup> J <sub>YH</sub> = 1.47 Hz
Cd δ 109.91 (1 C), broad	
Ce δ 169.15 (1 C), singlet	
Cf δ 55.47 (1 C), triplet, <sup>1</sup> J <sub>CH</sub> = 159 Hz	Hf δ 3.87 (2 H), quartet, <sup>5</sup> J <sub>HH</sub> = 2.7 Hz
Cg δ 13.44 (1 C), quartet, <sup>1</sup> J <sub>CH</sub> = 127 Hz	Hg δ 2.11 (3 H), triplet, <sup>5</sup> J <sub>HH</sub> = 2.7 Hz

Spectra recorded at room temperature in C<sub>6</sub>D<sub>6</sub>

**Figure 6.** NMR data for the 2-butyne reaction product, **5**, are most consistent with the  $\eta^1$ -allenyl isomer shown (see text for details).

Indeed, detailed NMR studies of this product lead us to assign its solution structure as an equilibrium between a major  $\eta^1$ -allenyl form along with a minor  $\eta^1$ -propargyl isomer. Perhaps most telling is the anomalous low field chemical shift observed for the methylene resonance ( $H^f$   $\delta$  3.87) along with an absence of the two-bond coupling to yttrium that would be expected if the product were predominantly the propargyl isomer. The  $^{13}\text{C}$  NMR data are also in accord with an allenyl moiety, particularly on the basis of the significantly low field chemical shift of the central ( $C^e$ ) carbon ( $\delta$  169.15).<sup>11</sup> The simple  $\eta^1$ -allenyl bonding picture is complicated, however, by the lack of a *ca.* 50 Hz one-bond coupling between yttrium and  $C^d$ . This observation, along with the broadness observed for the resonance ( $C^d$ ), suggested some sort of fluxional averaging. Subsequent VT- $^1\text{H}$  NMR data show a strong correlation between temperature and chemical shift, particularly for the methylene ( $H^f$ ) resonance of the allenyl moiety (Figure 7). This effect is readily accommodated by the proposed  $\eta^1$ -allenyl to  $\eta^1$ -propargyl fluxional behavior since the temperature dependent shift for  $H^f$  is in the correct direction for a minor isomer possessing a large (*ca.* 4 ppm) downfield shift vs the major one. The fluxional  $\eta^1$ - formulation is also consistent with bonding of an unsaturated fragment to a  $d^0$  metal where there is no possibility for back-bonding stabilization of a coordinated  $\pi$ -bond.

Casey has recently characterized rhenium-propargyl complex for which the ground state resonance forms are, in the limit of no  $\pi$ -bond coordination, the two different isomers proposed in our case (Figure 8). Additionally, the ground state of the rhenium complex provides an attractive model of the transition state for the isomerization of the yttrium complex. The stronger Y-C bond presumably provides the driving force towards the allenyl isomer, but sterics and other subtle factors that may also be causal, cannot easily be dismissed.

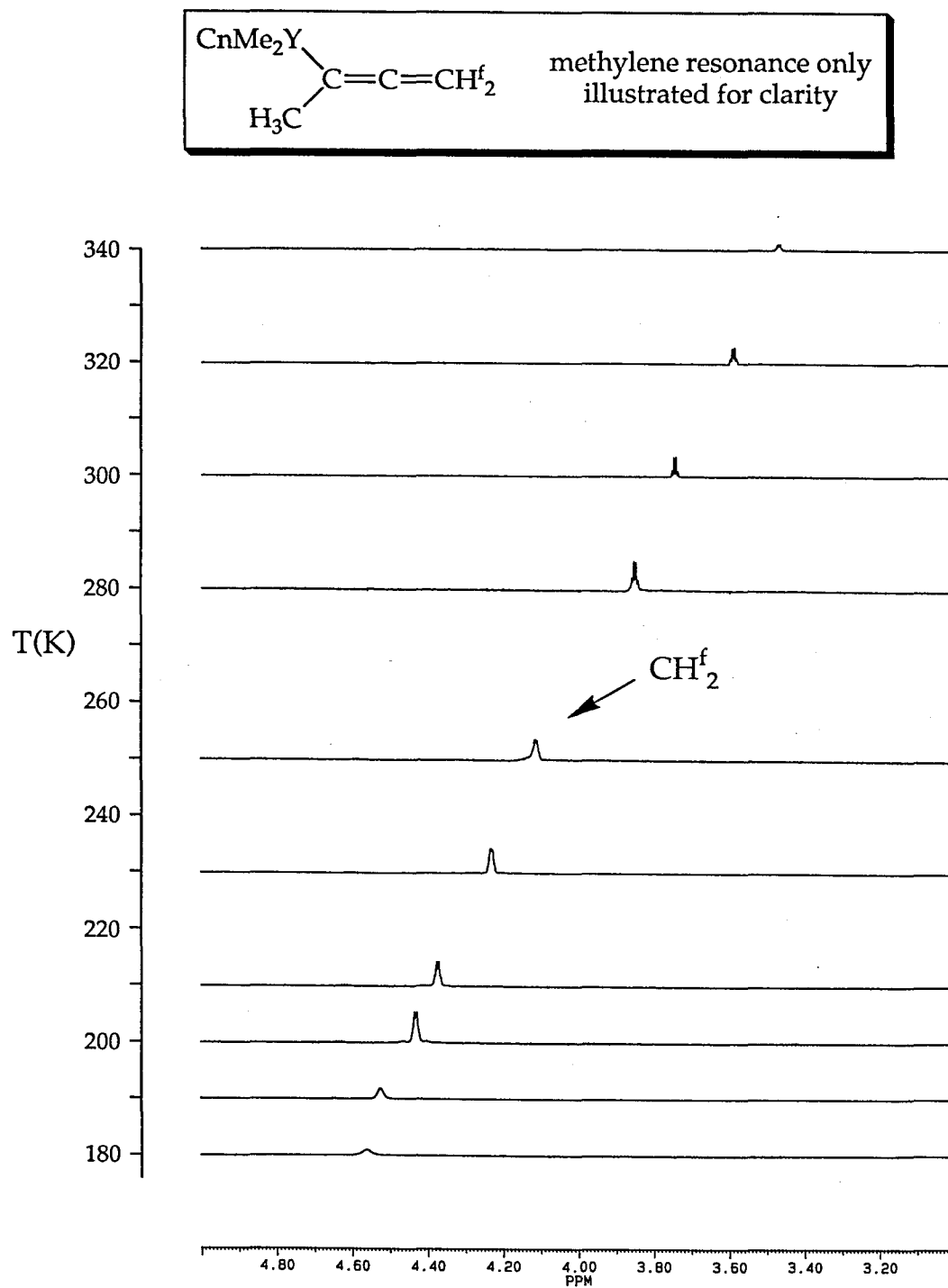


**Figure 7.** VT-<sup>1</sup>H NMR studies of **5** reveal large temperature dependant shifts for the allenyl moiety.



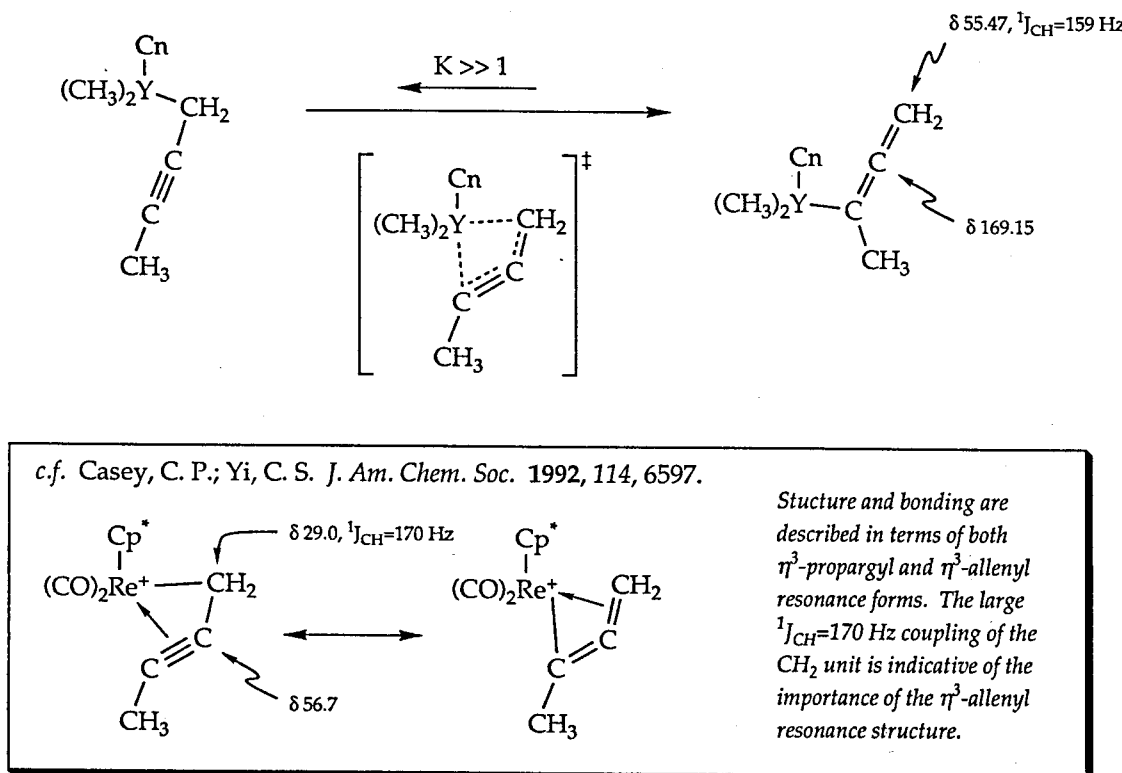
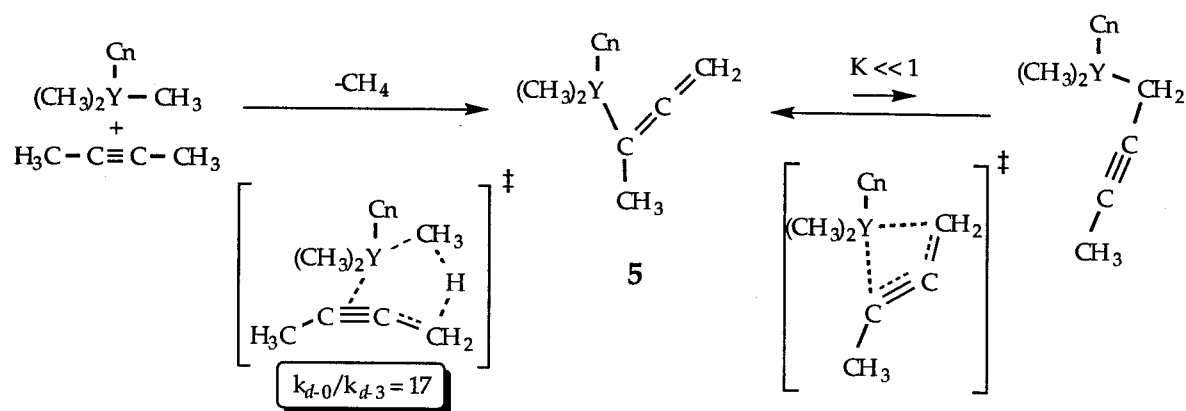


**Figure 8.** Comparison of **5** with Casey's propargyl complex (see text for details).

We have not yet established a firm mechanistic view of the C-H activation step in this reaction although  $\sigma$  bond metathesis followed by equilibration to the observed product is certainly plausible. It occurred to us that an isotope effect study might be a revealing probe for this possibility since the magnitude of the deuterium isotope effect for  $\sigma$  bond metathesis has been shown to be on the order of 3 (*i.e.*,  $k_H/k_D \approx 3$ ).<sup>8,12</sup> On the basis of the contraindicating (very large) isotope effect ( $k_H/k_D = 17$ ) observed upon perdeuteration of one of the methyl groups of 2-butyne, we are forced to conclude that the  $\sigma$  bond metathesis pathway is not operative in this case. An example of methane extrusion from a tantalum-amido complex which also proceeds with a large deuterium isotope effect is suggestive of a mechanism. As shown in Figure 9, the transition states for the two reactions look quite similar if 2-butyne coordination is invoked in the rate determining step for formation of **5**. Unfortunately, this reaction is

apparently not general for other methyl acetylenes; in contrast to 2-butyne, even 2-pentyne fails to react cleanly with **3b**. Presumably the required acetylene coordination is too disfavored for even modestly more bulky substrates.



*c.f.* Mayer, J.M.; Curtis, C.J.; Bercaw, J.E. *J. Am. Chem. Soc.* **1983**, *105*, 2651.

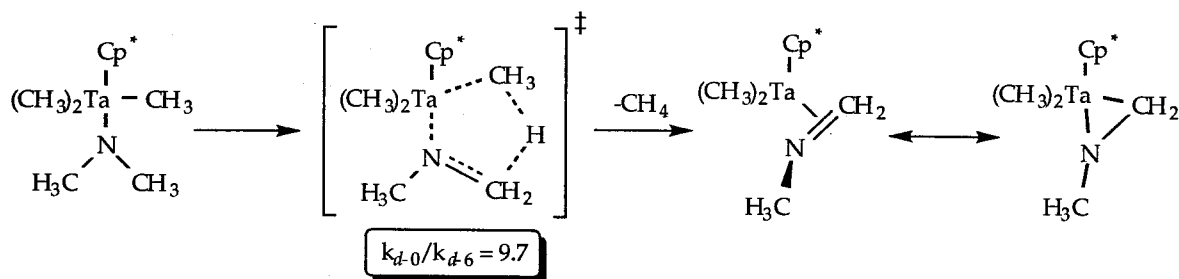


**Figure 9.** The cited precedent suggests that acetylene coordination might be required for this (top) reaction.

**Activation of 3a with [HN(Me)<sub>2</sub>Ph][B(C<sub>6</sub>F<sub>5</sub>)<sub>4</sub>] and B(C<sub>6</sub>F<sub>5</sub>)<sub>3</sub>.** The reactivity patterns observed for the trimethyl complexes **3** suggested that protonolysis of one methyl group to give the corresponding dimethyl cation [CnMMe<sub>2</sub>]<sup>+</sup> might be accomplished.<sup>13</sup> We were initially hesitant to pursue these reactions since we expected that the resultant 10e<sup>-</sup> cations would be quite unstable based on their extremely low formal electron count. Indeed, reaction of the yttrium complex, **3b**, with N,N-dimethylanilinium perfluorotetraphenylborate results in rapid decomposition accompanied by methane loss and demetallation of the Cn ligand.

Surprisingly, however, the analogous reaction with **3a** in THF leads to formation of methane and dimethylaniline *with no concomitant ligand demetallation*. The organometallic product(s) of this reaction have not been unambiguously identified since they exhibit quite complicated NMR signals; nevertheless, we can not rule out formation of a THF solvated species such as  $[\text{CnScMe}_2 \cdot (\text{THF})_n]^+[\text{B}(\text{C}_6\text{F}_5)_4]^-$ . Significantly, addition of ethylene to a THF solution of this putative product results in slow formation of polyethylene precipitate.

The analogous reaction of **3a** with anilinium perfluorotetraphenylborate in benzene-*d*<sub>6</sub> results in gas (CH<sub>4</sub>) evolution, and eventually yields a dense orange-red oil. The <sup>1</sup>H NMR spectrum (Figure 10) of the reaction mixture shows a sharp set of signals which have been assigned to N,N-dimethylaniline and a small amount of residual methane, as well as very broad signals centered around δ 2 ppm and -0.5 ppm which are tentatively assigned to the Cn and Sc-CH<sub>3</sub> moieties of the expected product,  $[\text{CnScMe}_2]^+[\text{B}(\text{C}_6\text{F}_5)_4]^-$ . The two fractions were easily separated by decanting residual liquid (solvent and N,N-dimethylaniline) away from the oily product. Decantation of benzene followed by addition of THF-*d*<sub>8</sub> results in redissolution of the oil giving a colorless solution which has essentially the same spectral features as the THF-*d*<sub>8</sub> reaction described above (with the exception of missing methane and dimethylaniline resonances), thus implicating formation of the same product in both solvents. Addition of neat 1-pentene to a sample of the red oil formed as above results in moderately fast formation of a highly viscous solution of poly(1-pentene) after about 2 hours at room temperature. GPC analysis of the polymer reveals a rather low molecular weight ( $M_w = 3666$ ), but a surprisingly low polydispersity (PDI = 1.32).

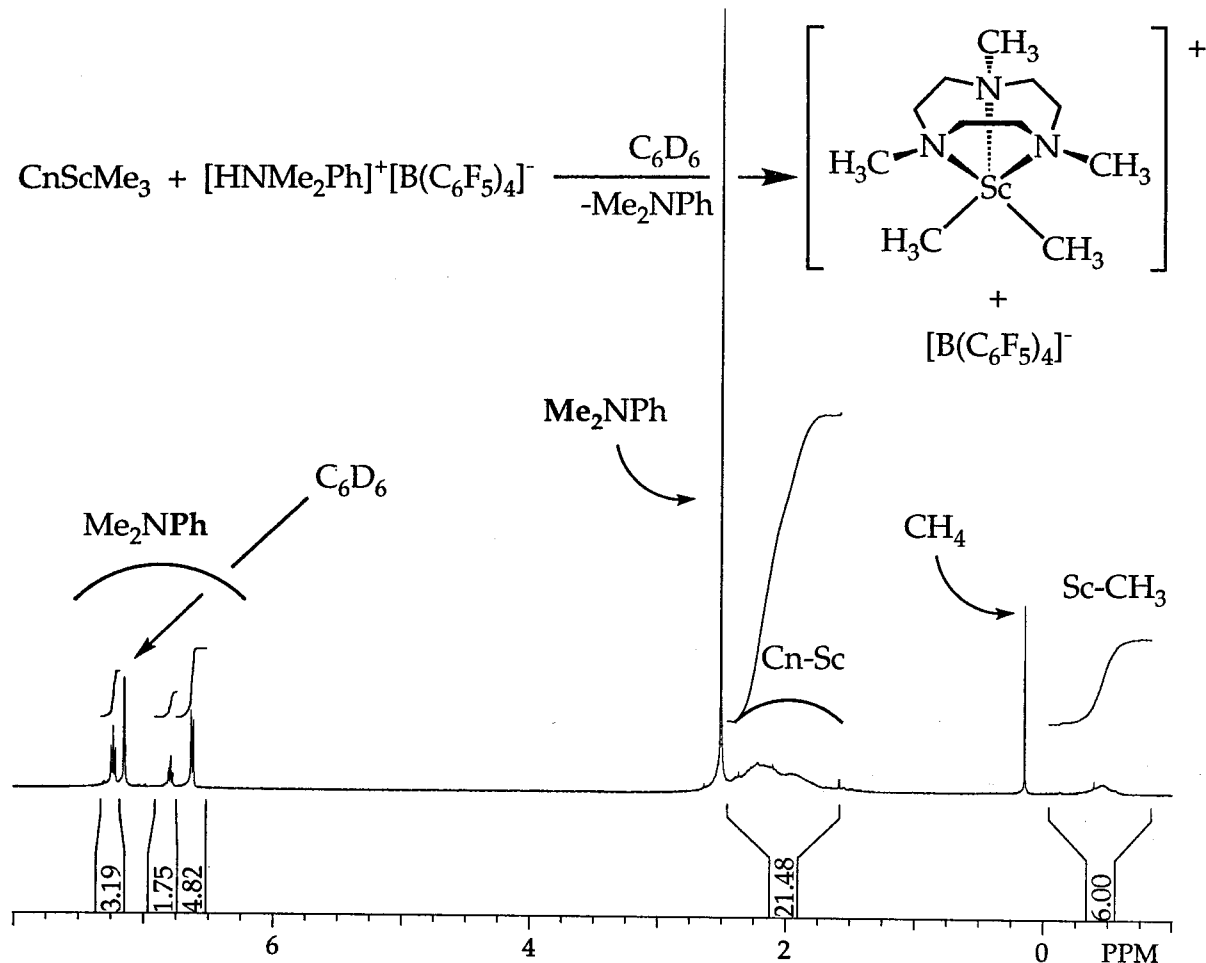


**Figure 10.**  $^1\text{H}$  NMR spectrum of the product from reaction of 3a as indicated (see text for details).

The ability of perfluoro-triphenylborane to activate group IV metal-alkyl systems via a  $\mu$ -methyl complex as has been observed.<sup>14</sup> We hoped that this relatively mild form of activation might generate a more easily characterized species pertinent to the olefin polymerization reactions with the cationic systems.

Indeed, when 3a and  $\text{B}(\text{C}_6\text{F}_5)_3$  are allowed to react in an NMR tube in  $\text{THF-}d_8$ , a subsequent  $^1\text{H}$  NMR spectrum (Figure 11), though broad, is consistent with clean formation of  $\text{CnScMe}_2(\mu\text{-CH}_3)\text{B}(\text{C}_6\text{F}_5)_3$ . As in the case for the cationic species above, the THF solution obtained proves competent for ethylene polymerization

at modest temperatures (80 °C); however, it does not react with propene even after several days at 80 °C.

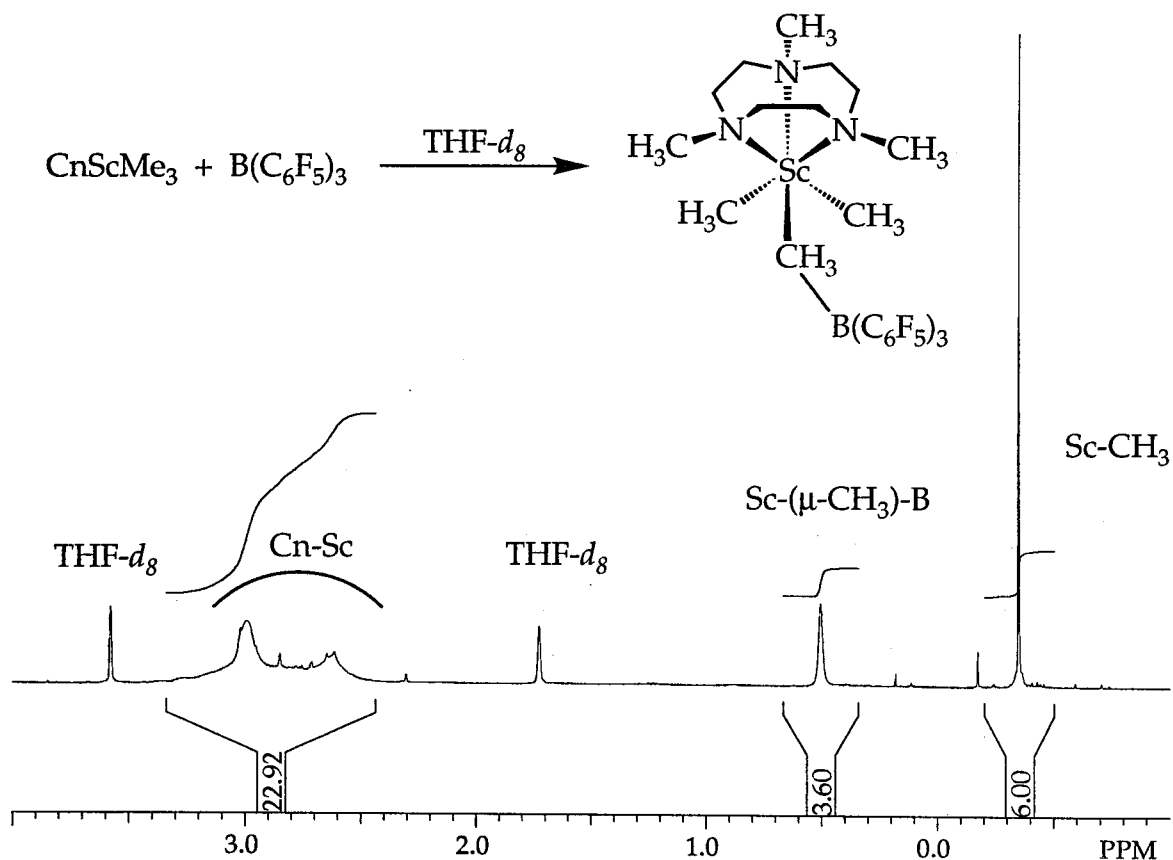


**Figure 11.**  $^1\text{H}$  NMR spectrum of the product from reaction of **3a** as indicated (see text for details).

Similar to the behavior of the cations described above, treatment of **3a** with  $\text{B}(\text{C}_6\text{F}_5)_3$  in benzene results in formation of an insoluble red oil. Room temperature polymerization of 1-pentene with this red oil results in poly(1-pentene) which, quite remarkably, has exactly the same properties as that obtained from the cationic activation route:  $M_n=2782$ ,  $M_w=3665$ ,  $\text{PDI}=1.32$  (*vide supra*).

## Conclusions

The syntheses of Cn complexes of scandium and yttrium  $\text{CnMCl}_3$  (**2**) (**2a**,  $\text{M}=\text{Sc}$ ; **2b**,  $\text{M}=\text{Y}$ ) and the corresponding trimethyl species  $\text{CnMMe}_3$  (**3**) (**3a**,  $\text{M}=\text{Sc}$ ; **3b**,  $\text{M}=\text{Y}$ ) are readily accomplished in high yield. These formally  $12\text{ e}^-$ ,  $\text{d}^0$  compounds comprise a new class of highly electron deficient group III metal complexes.

Although extensive studies have not yet been completed, the initial findings suggest that **3a** is similar in reactivity to the isoelectronic group IV monocyclopentadienyl trimethyl complexes  $\text{CpMMe}_3$  (**4**) ( $\text{M}=\text{Ti}, \text{Zr}, \text{Hf}$ ), which are of current interest as catalyst precursors for  $\alpha$ -olefin polymerization and syndiotactic polystyrene production.<sup>15</sup> The detailed mechanism of the polymerization reactions mediated by **4** remains to be determined, however, the active catalysts are believed to be the cationic dialkyls of general formula  $[\text{CpMR}_2]^+$  rather than the neutral complexes. These findings are in accord with our observation that insertion reactions for **3a** also require cation formation by methyl group protonolysis or abstraction. The absence of insertion reactions for both **3** and **4** apparently derives from steric factors and coordinative saturation, which are alleviated upon cation formation.

In contrast to the scandium complex **3a** and Flood's rhodium complex,  $\text{CnRhMe}_3$  (**1**), preliminary studies indicate that Cn does not provide a sufficiently stable coordination environment for significant organometallic chemistry at yttrium despite the observation that the trihalide **2b** and also the trimethyl complex **3b** are both obtained in high yield. It is likely that the large size of yttrium<sup>3+</sup> (1.04 Å) is less compatible with the bite size of the Cn ligand resulting

in weaker binding relative to the smaller metals scandium<sup>3+</sup> (0.89 Å) and rhodium<sup>3+</sup> (0.81 Å).

The marked differences in the reactivity of **3a** to that of the permethylscandocene derived systems offers the opportunity to study some of the factors which control reactivity at the metal center. For example, the effect of the electronic properties of substituents could be examined by testing a series of compounds of general formula  $C_nM(CH_3)_2Z$  or  $C_nM(CH_3)Z_2$  ( $Z$ =halide, amido, alkoxy). Simple synthetic strategies for the preparation of these compounds involve stoichiometric reaction of **3** with the appropriate halide, amine, or alcohol. The cations derived from these systems could also be studied. It might also be possible to generate less sterically hindered neutral species such as  $C_nM(CH_3)Z'$  ( $Z'$ =oxo, sulfido, or imido) by reaction of **3** with 1 equivalent of  $H_2O$ ,  $H_2S$ , or  $H_2NR$ . The possibilities for interesting reaction chemistry with such coordinatively unsaturated, electron-poor systems are intriguing.

## Experimental Section

**General Considerations.** All air and/or moisture sensitive compounds were manipulated using standard high vacuum line, Schlenk, or cannula techniques, or in a dry box under a nitrogen atmosphere, as described previously.<sup>16</sup> Argon and hydrogen gases were purified and dried by passage over columns of  $MnO$  on vermiculite and activated molecular sieves. Solvents were stored under vacuum over titanocene<sup>17</sup> or sodium benzophenone ketyl. 1,4,7-trimethyl-1,4,7-triazacyclononane was either purchased (Aldrich) and used as received, or synthesized from tacntt by the method of Flood and coworkers.<sup>4</sup>  $B(C_6F_5)_3$  was synthesized and provided by Robert E. Blake, Jr. A generous loan of

N,N-dimethylanilinium perfluorotetraphenylborate by Dr. Howard Turner is gratefully acknowledged.

Unless otherwise specified, all NMR spectra were recorded at ambient temperature on a Bruker AM500 (500.13 MHz for  $^1\text{H}$ ; 125.76 MHz for  $^{13}\text{C}$ ) spectrometer. The crystal structure for  $\text{CnScCl}_3$  was determined at the Caltech Crystallography Facility by Dr. William P. Schaefer and Lawrence M. Henling. GPC and DSC analyses of polymer samples were carried out in the laboratories of Prof. Robert H. Grubbs with the help of Dr. Geoffrey W. Coates and Amy Pangborn.

**NMR Tube Reactions.** Many of the reactions were carried out in sealed NMR tubes. The tubes were fitted with a 180°, concentric, Teflon needle valve which was blown directly on to the tube (the tubes employed were purchased from J. Young<sup>18</sup>), which could be attached to the high vacuum line by a simple adapter tube. These assemblies allow convenient loading of solids in the glove-box as well as a reversible vacuum tight seal which allows facile manipulations of volatiles into and out of the tube assembly. In a typical experiment, the NMR tube was loaded with 10 - 30 mg (*ca.* 0.03 - 0.1 mmol, for 1 eq) of the desired reactants.

**Preparation of  $\text{CnYCl}_3$ .** In the glovebox a 50 ml djeldahl flask was charged with  $\text{YCl}_3(\text{THF})_3$  (5.0g, 12.15 mmol, 1 eq). The solid was dissolved, with stirring, in a minimum amount of acetonitrile (*ca.* 40-50 ml). To this solution was added the Cn ligand (2.5 g, 14.57 mmol, 1.2eq), dropwise with a pipet. During the addition a yellow precipitate began to form and this increased over a period of a few minutes after the addition. The flask was attached to a medium sized swivel frit assembly, taken onto the vacuum line, filtered, and dried *in vacuo*. Yield 3.41 g



(77%) of  $\text{CnYCl}_3$  as a free flowing, yellow, microcrystalline powder. Analysis calculated for  $\text{C}_9\text{H}_{21}\text{Cl}_3\text{N}_3\text{Y}$ : C 29.49%, H 5.79%, N 11.46%; found (two runs with oxidant): C 30.02%, 29.84%; H 5.81%, 5.78; N 11.11%, 11.43%.  $^1\text{H}$  NMR ( $\text{CD}_3\text{CN}$ ):  $\delta$  3.097 (m, 6H,  $\text{CH}_2$ ), 2.890 (m, 6H,  $\text{CH}_2$ ), 2.807 (s, 9H,  $\text{CH}_3$ ).  $\{^1\text{H}\}^{13}\text{C}$  NMR ( $\text{THF}-d_8$ ):  $\delta$  56.99 ( $\text{CH}_2$ ), 49.68 ( $\text{CH}_3$ ).

**Preparation of  $\text{CnScCl}_3$ .** An analogous procedure to that employed above for  $\text{CnYCl}_3$  gave  $\text{CnScCl}_3$  as a white powder in 59% yield. Analysis calculated for  $\text{C}_9\text{H}_{21}\text{Cl}_3\text{N}_3\text{Sc}$ : C 33.50%, H 6.57%, N 13.02%; found (three runs): C 32.85%, 33.19%, 32.96%; H 6.43%, 6.50%, 6.44%; N 12.74%, 12.96%, 12.86%.  $^1\text{H}$  NMR ( $\text{CD}_3\text{CN}$ ):  $\delta$  3.212 (m, 6H,  $\text{CH}_2$ ), 2.911 (m, 6H,  $\text{CH}_2$ ), 2.870 (s, 9H,  $\text{CH}_3$ ).  $\{^1\text{H}\}^{13}\text{C}$  NMR ( $\text{CD}_3\text{CN}$ ):  $\delta$  56.48 ( $\text{CH}_2$ ), 50.87 ( $\text{CH}_3$ ).

**Preparation of  $\text{CnScMe}_3$ .** A medium sized swivel frit assembly was charged with  $\text{CnScCl}_3$  (1.000 g, 3.100 mmol, 1 eq) and halide-free  $\text{LiCH}_3$  (204.4 mg, 9.300 mmol, 3 eq). On the vacuum line, *ca.* 75 ml of THF was condensed onto the solids and the reaction was warmed to room temperature. The milky white suspension was allowed to stir for about 6 hr after which the solvent was removed *in vacuo* leaving an off-white solid residue. Toluene (*ca.* 100 ml) was condensed in and the resulting yellow solution was warmed slightly ( $\sim 40^\circ\text{C}$ ) and filtered to remove  $\text{LiCl}$ . The white filtrate was washed once with fresh solvent and the supernatant solution was concentrated to *ca.* 10 ml giving an orange precipitate. An equal volume of petroleum ether was condensed into the solution to affect a more complete precipitation of the product, which was collected by filtration and dried *in vacuo*. Yield 551.2 mg (68%) of  $\text{CnScMe}_3$  as a light orange powder. Analysis calculated for  $\text{C}_{12}\text{H}_{30}\text{N}_3\text{Sc}$ : C 55.13%, H 11.59%, N 16.08%; found (two runs): C 54.67%, 54.43%; H 10.94%, 11.02%; N 15.59%, 15.89%.  $^1\text{H}$  NMR ( $\text{THF}-d_8$ ):  $\delta$  2.984 (m, 6H,  $\text{CH}_2$ ), 2.780 (m, 6H,  $\text{CH}_2$ ), 2.650 (s,

9H, N-CH<sub>3</sub>), -0.643 (s br, 9H, Sc-CH<sub>3</sub>). <sup>1</sup>H <sup>13</sup>C NMR (THF-*d*<sub>8</sub>): δ 55.97 (CH<sub>2</sub>), 48.97 (N-CH<sub>3</sub>); Sc-CH<sub>3</sub> not detected.

**Preparation of CnYMe<sub>3</sub>.** Starting with CnYCl<sub>3</sub>, an analogous procedure to that employed above for CnScMe<sub>3</sub> gave CnYMe<sub>3</sub> as a light yellow powder in 78% yield. Analysis calculated for C<sub>12</sub>H<sub>30</sub>N<sub>3</sub>Y: C 47.20%, H 9.92%, N 13.76%; found (two runs): C 46.75%, 47.18%; H 9.38%, 9.43%; N 13.76%, 13.81%. <sup>1</sup>H NMR (C<sub>6</sub>D<sub>6</sub>): δ 2.266 (m, 6H, CH<sub>2</sub>), 1.723 (m, 6H, CH<sub>2</sub>), 2.394 (s, 9H, N-CH<sub>3</sub>), -0.220 (d, <sup>2</sup>J<sub>Y-H</sub> = 1.55 Hz, 9H, Y-CH<sub>3</sub>). <sup>1</sup>H <sup>13</sup>C NMR (C<sub>6</sub>D<sub>6</sub>): δ 54.57 (CH<sub>2</sub>), 47.13 (CH<sub>3</sub>), 21.3 (d, <sup>1</sup>J<sub>Y-C</sub> = 44.59 Hz, Y-CH<sub>3</sub>).

**Reaction of CnScMe<sub>3</sub> with p-toluidine.** A small swivel frit assembly equipped with two 100 ml djeldahl was charged with CnScMe<sub>3</sub> (200 mg, 0.76500 mmol, 1 eq) and p-toluidine (246 mg, 2.296 mmol, 3 eq). On the vacuum line, *ca.* 70 ml of toluene was condensed onto the solids and the reaction was warmed to room temperature. The reaction was stirred for 30 min and filtered, leaving a small amount of residue on the frit. The resulting clear solution (presumably saturated in CnScMe<sub>3</sub> with now a slight excess of p-toluidine) was allowed to stand unstirred overnight. The next day, wispy white needles were observed to have precipitated, and the solution was allowed to stand an addition day to ensure complete reaction. The reaction was worked up by degassing the solution (CH<sub>4</sub> evolution), followed by filtering and drying *in vacuo*.. Yield 124 mg of fine white needles which have a fluffy cotton texture.

**Reaction of CnYMe<sub>3</sub> with 2-butyne.** Typical reactions were carried out in NMR tubes as described above using toluene-*d*<sub>8</sub> as solvent. CH<sub>3</sub>CCCD<sub>3</sub> had been previously synthesized in our lab by W. D. Cotter.<sup>19</sup> 2-butyne-*d*<sub>6</sub> was purchased (Fluka) and purified by drying over activated 3A molecular sieves followed by

low temperature vacuum distillation prior to use. The isotope effect was determined by relative integration of the appropriate product resonances in the  $^1\text{H}$  NMR spectra.

**Reaction of  $\text{CnScMe}_3$  with  $[\text{HMe}_2\text{NPh}][\text{B}(\text{C}_6\text{F}_5)_4]$  in  $\text{C}_6\text{D}_6$ .** In a typical reaction,  $\text{CnScMe}_3$  (10 mg, 0.0383 mmol, 1 eq) and  $[\text{HMe}_2\text{NPh}][\text{B}(\text{C}_6\text{F}_5)_4]$  (30.7 mg, 0.0383 mmol, 1 eq) were loaded into an NMR tube in the glove box as described above. Addition (in the glove box, by pipet) of  $\text{C}_6\text{D}_6$  solvent resulted in gas ( $\text{CH}_4$ ) evolution and gave, eventually, a dense orange-red oil. The two fractions were easily separable by simple decantation of residual liquid (solvent and N,N-dimethylaniline) away from the oily product. The  $^1\text{H}$  NMR spectrum of the reaction before decantation shows a sharp set of signals which have been assigned to N,N-dimethylaniline and a small amount of residual methane, as well as very broad signals centered around  $\delta$  2 ppm and -0.5 ppm which are tentatively assigned to the Cn and Sc- $\text{CH}_3$  moieties of the expected product,  $[\text{CnScMe}_2]^+[\text{B}(\text{C}_6\text{F}_5)_4]^-$ .

**Polymerization of 1-pentene using product red oil of previous reaction.** A preparation of "decanted" red oil was carried out as above, but in a moderately sized (*ca* 200 ml) thick walled reaction vessel (bomb) rather than an NMR tube. The bomb was taken onto the vacuum line and 1-pentene (25 ml) was condensed into the reactor at  $-78\text{ }^\circ\text{C}$ . Although the oil did not seem to dissolve to any appreciable extent, after about 2 hr, polymer formation was in evidence as the solution had become quite thick and viscous. The reaction was opened to air, and the crude polymer/pentene mixture was analyzed by GPC in  $\text{CH}_2\text{Cl}_2$  against a polystyrene calibration:  $M_n=2782$ ,  $M_w=3666$ ,  $\text{PDI}=1.32$ .

**Reaction of  $\text{CnScMe}_3$  with  $[\text{HMe}_2\text{NPh}][\text{B}(\text{C}_6\text{F}_5)_4]$  in  $\text{THF-}d_8$  and subsequent polymerization of ethylene.**  $\text{CnScMe}_3$  (10 mg, 0.0383 mmol, 1 eq) and  $[\text{HMe}_2\text{NPh}][\text{B}(\text{C}_6\text{F}_5)_4]$  (30.7 mg, 0.0383 mmol, 1 eq) were loaded into an NMR tube in the glove box. On the vacuum line, condensation of  $\text{THF-}d_8$  into the assembly at  $-78\text{ }^\circ\text{C}$  resulted in vigorous gas (methane) evolution, which persisted for *ca.* 15 min. The tube was allowed to warm to R.T. and a subsequent NMR spectrum revealed, as above, sharp resonances for N,N-dimethylaniline and methane. Broad resonances are also apparent in the region for Cn coordinated to scandium, however, the expected  $\text{Sc-CH}_3$  resonances are either completely coalesced into the baseline, or are non-existent. The tube was taken back onto the vacuum line and ethylene (0.2ml) was condensed into the reaction mixture  $-198\text{ }^\circ\text{C}$ . NMR spectra indicated no significant changes over the next few hours so the tube was placed in a  $80\text{ }^\circ\text{C}$  oil bath overnight. Inspection of the tube the next day revealed a white polymeric precipitate.

**Reaction of  $\text{CnScMe}_3$  with  $\text{B}(\text{C}_6\text{F}_5)_3$  in  $\text{THF-}d_8$  and subsequent polymerization of ethylene.** In the glovebox, a J. Young NMR tube was charged with  $\text{CnScMe}_3$  (10 mg, 0.0383 mmol, 1 eq) and  $\text{B}(\text{C}_6\text{F}_5)_3$  (19.5 mg, 0.0383 mmol, 1 eq). On the vacuum line,  $\text{THF-}d_8$  (1 ml) was condensed onto the solids; a subsequent  $^1\text{H}$  NMR spectrum, though broad, is consistent with clean formation of  $\text{CnScMe}_2(\mu\text{-CH}_3)\text{B}(\text{C}_6\text{F}_5)_3$ . **CAUTION! The following procedure may result in extremely high pressure and should be carried out with great care behind an adequate blast shield.** The tube was taken back onto the vacuum line and ethylene (0.4ml) was condensed into the reaction mixture  $-198\text{ }^\circ\text{C}$ . The tube was allowed to warm to R.T. (*ca.* 1 hr) behind a blast shield in a fume hood and was then carefully moved to an  $80\text{ }^\circ\text{C}$  oil bath overnight. Inspection of the tube the next day revealed a white polymeric precipitate which was isolated by

extraction/precipitation from hot toluene. A melting point of 117 °C was determined for this polymer by DSC.

**Reaction of  $\text{CnScMe}_3$  with  $\text{B}(\text{C}_6\text{F}_5)_3$  in  $\text{C}_6\text{D}_6$ .**  $\text{CnScMe}_3$  (10 mg, 0.0383 mmol, 1 eq) and  $\text{B}(\text{C}_6\text{F}_5)_3$  (19.5 mg, 0.0383 mmol, 1 eq) and  $\text{C}_6\text{D}_6$  (*ca.* 1 ml) were sequentially loaded into an NMR tube in the glove box. Upon stirring, an initially clear oily film was observed clinging to the walls of the tube. The oil slowly darkened to an orange-red color over about 30 min. The NMR spectrum of this mixture was very broad and not easily interpretable. The tube was taken back into the box and the solvent decanted into a fresh NMR tube, and the spectrum obtained from this tube indicated only the presence of residual protons from the  $\text{C}_6\text{D}_6$  solvent. To the tube containing the oil was added chlorobenzene- $d_5$  which took on a light red color indicating partial solubility of the still largely undissolved oil; the broad NMR spectrum obtained from this tube could not be unambiguously assigned, but contained peaks in the spectral regions expected for  $\text{Cn-Sc}$ ,  $\text{Sc-CH}_3$ , and  $\text{Sc}(\mu\text{-CH}_3)\text{B}$  (*vide supra*). The solvent was removed *in vacuo* and the red oil obtained was used in the following reaction.

**Polymerization of 1-pentene using product red oil of previous reaction.**

1-pentene was condensed onto the red oil in the tube obtained from the previous procedure. The assembly was stirred by slow rotation overnight. The next day, polymer formation was in evidence as the solution had become quite thick and viscous.  $^{13}\text{C}$  NMR analysis revealed that the tube contained mostly poly(pentene) and a relatively smaller amount of unreacted monomer. The tube was opened to air, and the crude polymer/pentene mixture was analyzed by GPC in  $\text{CH}_2\text{Cl}_2$  against a polystyrene calibration:  $M_n=2782$ ,  $M_w=3665$ ,  $\text{PDI}=1.32$ .

**Crystal Structure Determination for  $\text{CnScCl}_3$ .** A suitable clear, colorless crystal of approximate dimensions  $0.18 \times 0.24 \times 0.34$  mm was selected from a batch grown by slow evaporation of an acetonitrile solution of  $\text{CnScCl}_3$  in a loosely capped small vial in air. The crystal was optically centered on an Enraf Nonius CAD 4 diffractometer equipped with a  $\text{Mo K}\alpha$  source, operating in omega scan mode. 25 well dispersed reflections in the range of  $\theta$  between 12 and 13 degrees were used for determining the unit cell parameters. No absorption correction was applied to the data. Data were collected for  $h$ ,  $k$ , and  $l$  within the limits 0 to 14, -8 to 8, and -19 to 19 respectively. Four intensity check reflections were used to monitor crystal decay. An approximately linear increase of 3% was observed over 49.56 hr. The total number of reflections measured was 5625. The total number of independent measurements was 2603. There were no unobserved reflections; however, only 2370 of the reflections were used for solution and refinement (*vide infra*). Patterson methods were used to determine the scandium atom position and one of the chlorine atoms. Subsequent structure factors-least squares analysis revealed the remaining heavy atom positions. All non-hydrogen atoms were refined anisotropically using full matrix least squares on  $F_{\text{obs}}^2$ ,  $w=1/\sigma^2(F_{\text{obs}}^2)$ . The hydrogen atoms were positioned by calculation in their idealized staggered geometry at a distance of  $0.95\text{\AA}$  from their respective carbon atoms and were included in the structure factor but not refined. The final  $R$  was 0.077 on  $F$  for 2249 reflections with  $F_{\text{obs}}^2 > 0$  and 0.069 on  $F$  for 1969 reflections with  $F_{\text{obs}}^2 > 3\sigma(F_{\text{obs}}^2)$ .  $wR$  on  $F^2$  for all 2370 reflections used was 0.018. The esd of an observation of unit weight ( $S$ ) was 2.19. The maximum and minimum heights in the final difference Fourier were 1.07 and  $-0.60$  electrons/ $\text{\AA}^3$  respectively. A Secondary Extinction parameter<sup>20</sup> of 1.72(19) was used. Atomic scattering factors were taken from Cromer, D.T. and Waber, J.T., *International Tables For X-ray Crystallography*, Vol. IV, pp. 99-101, 1974. Programs used were

the CRYM crystallographic computing system,<sup>21</sup> MULTAN88,<sup>22</sup> and ORTEP.<sup>23</sup>

**Note:** The crystal used was a twin, with a minor component about 10% that of the major one. The two sets of reflections overlapped, however, as shown by scan profiles on selected reflections. Of the 2603 total independent reflections, 232 that were seriously affected by this overlap, and one with a bad background correction, were eventually deleted. The data, unfortunately, are still contaminated as shown by the high value for the goodness of fit and by the observation that of the 47 reflections with the largest values of  $w(F_{obs}-F_{calc})$ , 34 are positive - well over half. While more peaks could have been removed, a point of diminishing returns had been reached: the largest  $w(\Delta F)$ 's are now negative, and the largest  $\Delta F$ 's are about 6 electrons (one, the 600, is 8.98 electrons). The details of the thermal motions are probably affected by this, as are the noise peaks in the difference map, but the molecular geometry is correct within the reported esd's.

## References and Notes

1. For recent examples with leading references see:
  - (a) Quan, R. W.; Bazan, G. C.; Kielly, A. F.; Schaefer, W. P.; Bercaw, J. E. *J. Am Chem. Soc.* **1994**, *116*, 4489.
  - (b) Bazan, G. C.; Donnelly, S. J.; Rodriguez, G. J. *Am Chem. Soc.* **1995**, *117*, 2671.
  - (c) Bazan, G. C.; Schaefer, W. P.; Bercaw, J. E. *Organometallics* **1993**, *12*, 2126.
  - (d) Tjaden, E. B.; Swenson, D. C.; Jordan, R. F.; Peterson, J. L. *Organometallics* **1995**, *14*, 371 and references therein.
2. (a) Chaudhuri, P.; Wieghart, K. *Prog. Inorg. Chem.* **1987**, *35*, 329 and references therein.
3. For a recent review of nitrogen donors in organometallic chemistry see: Togni, A.; Venanzi, L. M. *Angew. Chem. Int. Ed. Engl.* **1994**, *33*, 497.
4. A Ti(0) tricarbonyl species has been reported: Ellis, J. E.; DiMaio, A. J.; Rheingold, A. L.; Haggerty, B. S. *J. Am Chem. Soc.* **1992**, *114*, 10676.
5. (a) Wang, L.; Flood, T. C. *J. Am Chem. Soc.* **1992**, *114*, 3169.  
(b) Wang, L.; Lu, R. S.; Bau, R.; Flood, T. C. *J. Am Chem. Soc.* **1993**, *115*, 6999.
6. Köhn, R., D.; Kociok-Köhn, G. *Angew. Chem. Int. Ed. Engl.* **1994**, *33*, 1877.
7. (a) Thompson, M.E.; Bercaw, J.E. *Pure Appl. Chem.* **1984**, *56*, 1  
(b) Thompson, M.E.; Baxter, S.M.; Bulls, A.R.; Burger, B.J.; Nolan, M.C.; Santarsiero, B.D.; Schaefer, W.P.; Bercaw, J.E. *J. Am. Chem. Soc.* **1987**, *109*, 203.  
(c) Bercaw, J.E. *Pure Appl. Chem.* **1990**, *62*, 1151 and references therein.  
(d) Piers, W. E.; Shapiro, P. J.; Bunel, E. E.; Bercaw, J. E. *Synlett* **1990**, *2*, 74, and references therein.  
(e) Bunel, E.; Burger, B.J.; Bercaw, J.E. *J. Am. Chem. Soc.* **1988**, *110*, 976.
8. In a related reaction, Wieghart and coworkers have observed that the cyclic triamine 1,4,7-triisopropyl-1,4,7-triazacyclononane (tiptacn) reacts with  $\text{Ti}(\text{CH}_3\text{CN})_3\text{Cl}_3$  in acetonitrile solution to give (tiptacn) $\text{TiCl}_3$ : Jeske, P.; Wieghart, K.; Nuber, B. *Inorg. Chem.* **1994**, *33*, 47.
9. Haaland et. al. *J. Am Chem. Soc.* **1991**, *112*, 4547.
10. Thompson, M.E.; Baxter, S.M.; Bulls, A.R.; Burger, B.J.; Nolan, M.C.; Santarsiero, B.D.; Schaefer, W.P.; Bercaw, J.E. *J. Am. Chem. Soc.* **1987**, *109*, 203.



11. The chemical shifts for the central carbon in free allenes are around 200 ppm whereas those for acetylenic carbons are about 70 ppm.
12. Thompson, M. E. Ph. D. Thesis California Institute of Technology, 1982.
13. (a) Hlatky, G. G.; Turner, H. W.; Eckman, R. R. *J. Am Chem. Soc.* **1989**, *111*, 2728.  
(b) For a recent example with leading references see: Pellicchia, C.; Immirzi, A.; Grassi, A.; Zambelli, A. *Organometallics* **1993**, *12*, 4473.
14. (a) Yang, X.; Stern, C. L.; Marks, T. J. *J. Am Chem. Soc.* **1991**, *113*, 3623.  
(b) For a recent example with leading references see: Bochmann, M.; Lancaster, S. J.; Hursthouse, M. B.; Malik, K. M. A. *Organometallics* **1994**, *13*, 2235.
15. For recent examples see:  
(a) Longo, P.; Proto, A.; Oliva, L. *Macromol. Rapid Commun.* **1994**, *15*, 151, and references therein.  
(b) Quyoum, R.; Wang, Q.; Tudoret, M.-J.; Baird, M. C.; Gillis, D. J. *J. Am Chem. Soc.* **1994**, *116*, 6435.  
(c) Gillis, D. J.; Tudoret, M.-J.; Quyoum, R.; Irving, J. R.; Baird, M. C.; *Abs. Pap. ACS* **1993**, *203*, 37-INORG.  
(d) Pellicchia, C.; Longo, P.; Proto, A.; Zambelli, A. *Makromol. Chem., Rapid Commun.* **1992**, *13*, 265.
16. Burger, B. J.; Bercaw, J. E. *Experimental Organometallic Chemistry*; Wayda, A. L., Darensbourg, M. Y., Eds.; ACS Symposium Series 357; American Chemical Society: Washington, DC, 1987.
17. Marvich, R. H.; Brintzinger, H. H. *J. Am. Chem. Soc.* **1971**, *93*, 2046.
18. Purchased from Brunfelt Co. cat. no. 1300-060-528PP-7
19. Cotter, W.D.; Bercaw, J.E. *J. Organomet. Chem.* **1991**, *417*, C1.
20. Larson, A. C. *Acta. Cryst.* **1964**, *23*, 644.
21. Duchamp, D. J. (1964). Am. Crystallogr. Assoc. Meet., Bozeman, Montana, Paper B14, p. 29.
22. Debaerdemaeker, T.; Germain, G.; Main, P.; Refaat, L. S.; Tate, C.; Woolfson, M. (1988). MULTAN 88. *Computer Programs for the Automatic Solution of Crystal Structures from X-ray Diffraction Data*, Univs. of York, England and Louvain, Belgium.

23. Johnson, C. K. (1976). ORTEPII. Report ORNL-3794. Oak Ridge National Laboratory, Oak Ridge, Tennessee, USA.

## Appendix 3

### X-ray Crystal Structure Data for $\text{CnScMe}_3$ (2a).

**Table 1.** Crystal Data for  $\text{CnScCl}_3$  (**2a**).

Formula: $\text{C}_9\text{H}_{21}\text{Cl}_3\text{Sc}$	Formula Wt.: 322.60
Space Group: $P2_1/c$ (#14)	Temperature: 298 K
$a = 12.477(3) \text{ \AA}$	$\alpha = 90 \text{ deg}$
$b = 7.462(2) \text{ \AA}$	$\beta = 90.45 \text{ deg}$
$c = 15.984(4) \text{ \AA}$	$\gamma = 90 \text{ deg}$
$V = 1488.1(7) \text{ \AA}^3$	$\lambda_{\text{MoK}\alpha} = 0.71073 \text{ \AA}$
$\rho_{\text{calc}} = 1.44 \text{ g cm}^{-3}$	$Z = 4$
$\mu = 10.19 \text{ cm}^{-1}$	

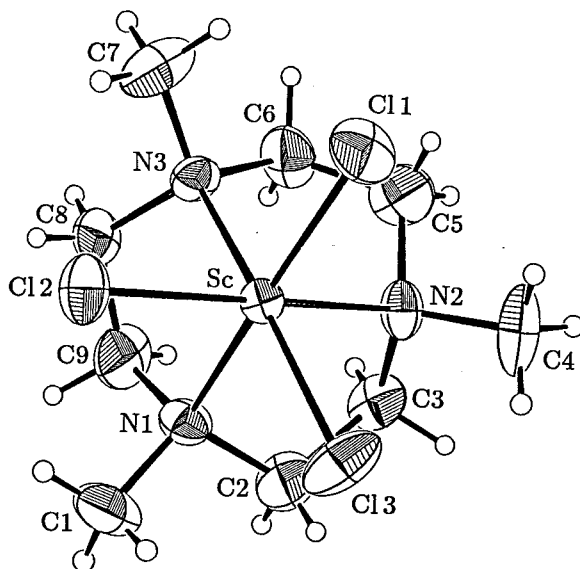
**Figure 1.** ORTEP diagram for  $\text{CnScCl}_3$  (**2a**) with 50% probability ellipsoids showing the atomic numbering scheme.

Table 2. Final Heavy Atom Parameters for CnScCl<sub>3</sub> (2a).

$x, y, z$ and $U_{eq}^a \times 10^4$				
Atom	$x$	$y$	$z$	$U_{eq}$
Sc	2448(1)	200(1)	1318(1)	264(2)
Cl1	2533(1)	-413(2)	2798(1)	596(4)
Cl2	869(1)	-1519(2)	982(1)	490(4)
Cl3	3774(1)	-1896(2)	855(1)	606(5)
N1	2460(3)	1588(6)	3(3)	376(10)
N2	3733(3)	2470(6)	1436(3)	360(10)
N3	1435(3)	2796(6)	1478(3)	343(9)
C1	2179(6)	303(10)	-684(4)	648(18)
C2	3582(4)	2178(8)	-126(4)	503(14)
C3	3992(4)	3266(7)	607(4)	452(14)
C4	4755(5)	1804(9)	1833(5)	668(19)
C5	3242(5)	3792(8)	2007(4)	526(15)
C6	2162(5)	4373(7)	1733(4)	471(14)
C7	589(5)	2579(9)	2111(4)	585(16)
C8	924(4)	3140(8)	660(3)	431(13)
C9	1709(5)	3149(9)	-40(4)	527(15)

$$^a U_{eq} = \frac{1}{3} \sum_i \sum_j [U_{ij}(a_i^* a_j^*)(\vec{a}_i \cdot \vec{a}_j)]$$

Table 3. Anisotropic Displacement Parameters for CnScCl<sub>3</sub> (2a).

Atom	$U_{11}$	$U_{22}$	$U_{33}$	$U_{12}$	$U_{13}$	$U_{23}$
Sc	291(5)	195(5)	305(5)	-2(4)	11(4)	13(4)
Cl1	730(11)	686(11)	370(8)	17(8)	-59(7)	179(7)
Cl2	397(8)	433(8)	639(10)	-139(6)	-65(7)	34(7)
Cl3	470(8)	320(8)	1032(14)	109(6)	253(9)	7(8)
N1	414(24)	435(26)	280(22)	-26(20)	62(19)	-6(19)
N2	307(21)	294(22)	479(27)	-52(18)	-68(20)	35(19)
N3	314(22)	367(23)	348(23)	87(19)	21(19)	3(18)
C1	725(44)	836(49)	383(33)	-137(39)	42(31)	-124(34)
C2	414(31)	587(37)	508(35)	-89(28)	81(27)	114(29)
C3	407(30)	279(27)	673(40)	-83(24)	139(29)	4(26)
C4	408(33)	639(43)	952(54)	-73(31)	-237(36)	-24(39)
C5	503(34)	426(33)	648(40)	-122(28)	-21(31)	-219(29)
C6	509(33)	315(28)	590(37)	66(26)	-1(29)	-166(26)
C7	517(36)	587(39)	656(42)	87(32)	235(33)	15(33)
C8	391(29)	474(33)	425(31)	133(26)	-100(25)	29(25)
C9	514(34)	657(40)	408(33)	69(31)	-41(28)	167(29)

$U_{i,j}$  values have been multiplied by  $10^4$

The form of the displacement factor is:

$$\exp -2\pi^2(U_{11}h^2a^{*2} + U_{22}k^2b^{*2} + U_{33}\ell^2c^{*2} + 2U_{12}hka^*b^* + 2U_{13}h\ell a^*c^* + 2U_{23}k\ell b^*c^*)$$

Table 4. Complete Distances and Angles for CnScCl<sub>3</sub> (2a).

Distance(Å)		Angle(°)	
Sc -Cl1	2.411(2)	Cl1 -Sc -Cl2	98.5(1)
Sc -Cl2	2.409(2)	Cl1 -Sc -Cl3	98.8(1)
Sc -Cl3	2.398(2)	Cl1 -Sc -N1	164.5(1)
Sc -N1	2.344(4)	Cl1 -Sc -N2	91.9(1)
Sc -N2	2.338(4)	Cl1 -Sc -N3	94.0(1)
Sc -N3	2.328(4)	Cl2 -Sc -Cl3	98.6(1)
N1 -C1	1.497(8)	Cl2 -Sc -N1	92.6(1)
N1 -C2	1.484(7)	Cl2 -Sc -N2	164.3(1)
N1 -C9	1.496(7)	Cl2 -Sc -N3	91.3(1)
N2 -C3	1.491(7)	Cl3 -Sc -N1	90.1(1)
N2 -C4	1.505(8)	Cl3 -Sc -N2	91.3(1)
N2 -C5	1.480(7)	Cl3 -Sc -N3	162.4(1)
N3 -C6	1.539(7)	N1 -Sc -N2	75.1(1)
N3 -C7	1.477(7)	N1 -Sc -N3	74.8(1)
N3 -C8	1.472(7)	N2 -Sc -N3	76.2(1)
C1 -H1A	0.946	Sc -N1 -C1	111.8(3)
C1 -H1B	0.952	Sc -N1 -C2	105.5(3)
C1 -H1C	0.947	Sc -N1 -C9	112.1(3)
C2 -C3	1.511(8)	Sc -N2 -C3	111.8(3)
C2 -H2A	0.950	Sc -N2 -C4	111.9(3)
C2 -H2B	0.948	Sc -N2 -C5	104.2(3)
C3 -H3A	0.953	Sc -N3 -C6	110.2(3)
C3 -H3B	0.951	Sc -N3 -C7	112.1(3)
C4 -H4A	0.941	Sc -N3 -C8	106.2(3)
C4 -H4B	0.960	C2 -N1 -C1	107.7(4)
C4 -H4C	0.948	C9 -N1 -C1	108.8(4)
C5 -C6	1.479(8)	C9 -N1 -C2	110.8(4)
C5 -H5A	0.948	C4 -N2 -C3	108.5(4)
C5 -H5B	0.955	C5 -N2 -C3	112.1(4)
C6 -H6A	0.938	C5 -N2 -C4	108.3(4)
C6 -H6B	0.948	C7 -N3 -C6	109.0(4)
C7 -H7A	0.955	C8 -N3 -C6	110.6(4)
C7 -H7B	0.946	C8 -N3 -C7	108.7(4)
C7 -H7C	0.949	H1A -C1 -N1	109.2
C8 -C9	1.493(8)	H1B -C1 -N1	109.1
C8 -H8A	0.948	H1C -C1 -N1	109.2
C8 -H8B	0.954	H1B -C1 -H1A	109.6
C9 -H9A	0.936	H1C -C1 -H1A	110.1
C9 -H9B	0.953	H1C -C1 -H1B	109.6
		C3 -C2 -N1	111.5(5)

Table 4. Complete Distances and Angles for  $\text{CnScCl}_3$  (2a) (cont.).

Angle(°)		Angle(°)	
H2A -C2 -N1	108.9	H8B -C8 -H8A	109.3
H2B -C2 -N1	108.8	C8 -C9 -N1	112.1(5)
H2A -C2 -C3	109.0	H9A -C9 -N1	109.2
H2B -C2 -C3	109.0	H9B -C9 -N1	108.0
H2B -C2 -H2A	109.6	H9A -C9 -C8	109.0
C2 -C3 -N2	113.6(4)	H9B -C9 -C8	108.2
H3A -C3 -N2	108.4	H9B -C9 -H9A	110.4
H3B -C3 -N2	108.4		
H3A -C3 -C2	108.6		
H3B -C3 -C2	108.6		
H3B -C3 -H3A	109.2		
H4A -C4 -N2	109.9		
H4B -C4 -N2	108.8		
H4C -C4 -N2	109.6		
H4B -C4 -H4A	109.4		
H4C -C4 -H4A	110.4		
H4C -C4 -H4B	108.8		
C6 -C5 -N2	113.1(5)		
H5A -C5 -N2	108.6		
H5B -C5 -N2	108.2		
H5A -C5 -C6	108.7		
H5B -C5 -C6	109.0		
H5B -C5 -H5A	109.2		
C5 -C6 -N3	112.8(5)		
H6A -C6 -N3	108.6		
H6B -C6 -N3	108.2		
H6A -C6 -C5	108.5		
H6B -C6 -C5	108.1		
H6B -C6 -H6A	110.7		
H7A -C7 -N3	109.3		
H7B -C7 -N3	109.8		
H7C -C7 -N3	109.5		
H7B -C7 -H7A	109.3		
H7C -C7 -H7A	109.1		
H7C -C7 -H7B	109.8		
C9 -C8 -N3	112.6(5)		
H8A -C8 -N3	109.0		
H8B -C8 -N3	108.6		
H8A -C8 -C9	108.4		
H8B -C8 -C9	108.9		



Table 5. Non-refined Hydrogen Atom Parameters for  $\text{CnScCl}_3$  (2a).

Atom	$x, y \text{ and } z \times 10^4$			$B$
	$x$	$y$	$z$	
H1A	1463	-88	-617	5.9
H1B	2249	893	-1209	5.9
H1C	2652	-688	-661	5.9
H2A	3613	2889	-618	4.5
H2B	4021	1151	-190	4.5
H3A	3683	4432	578	4.5
H3B	4750	3365	566	4.5
H4A	5087	968	1478	5.9
H4B	5227	2803	1922	5.9
H4C	4602	1271	2357	5.9
H5A	3693	4811	2039	4.5
H5B	3192	3259	2549	4.5
H6A	2235	5139	1272	4.5
H6B	1835	4981	2185	4.5
H7A	913	2357	2644	5.9
H7B	172	3637	2139	5.9
H7C	146	1592	1964	5.9
H8A	580	4272	676	4.5
H8B	403	2230	558	4.5
H9A	2105	4212	-18	4.5
H9B	1318	3073	-554	4.5

## Chapter 4

### **Employment of Chiral Linkers for Directed Synthesis of Enantiopure, C<sub>2</sub>-Symmetric, *ansa*-Metallocenes: A Single Component, Isospecific, Ziegler-Natta Catalyst.**

<b>Abstract</b>	<b>103</b>
<b>Introduction</b>	<b>104</b>
<b>Results and Discussion</b>	<b>106</b>
<b>Experimental</b>	<b>122</b>
<b>References and Notes</b>	<b>134</b>
<b>Appendix</b>	<b>136</b>

### Abstract

We have recently described the highly iso-specific Ziegler-Natta polymerization of  $\alpha$ -olefins using the single component,  $C_2$  symmetric metallocene  $[BpYH]_2$ , ( $Bp = [Me_2Si(C_5H_2-2-SiMe_3-4-CMe_3)_2]$ ). The steric bias exerted by the cyclopentadienyl substitution pattern allows for formation of only the desired *racemic* product upon metallation, with no detectable amount of the undesired *meso* isomer. A natural extension is the further development of methods for obtaining enantiomerically pure catalysts based on the  $[Bp]$  ligand system. Such single-component systems, in addition to serving as powerful mechanistic probes of Ziegler-Natta catalysis, would also be promising candidates for use in a variety of other catalytic asymmetric transformations. The most desirable ligand design would produce *only one enantiomer* upon coordination to the metal. Thus, not only would the wasteful and tedious separation of the *meso* isomer be avoided, but the subsequent resolution of the racemate would also be obviated. We have found that employment of chiral silyl-linkers is an effective design strategy for the synthesis of such enantiomerically pure complexes. Described herein are our efforts which have led to the synthesis of the ligand  $[BnBp]^{2-}$ , designed to coordinate to give only one enantiomer, and  $BnBpY-H$ , the first example, as far as we are aware, of an enantiopure  $C_2$ -symmetric, group III metallocene which is competent for coordination polymerization of  $\alpha$ -olefins.

## Introduction

The fascinating discovery that  $C_2$ -symmetric *ansa*-metallocenes (first developed by Brintzinger) are capable of mediating the highly stereospecific sequential insertion of propene to give the isotactic polymer, has fostered a resurgence in this area of homogeneous organometallic chemistry. In particular, much effort has been directed towards understanding the mechanistic basis for this remarkable process. The incredibly high enantioselectivity in the carbon-carbon bond forming step exhibited in polymerizations by these catalyst systems has also motivated studies by many workers which are aimed at employing chiral metallocenes for other enantiospecific catalytic reactions.<sup>1</sup> Unfortunately, these types of studies are encumbered by the tedious syntheses which are required in order to obtain the necessary enantiopure,  $C_2$ -symmetric metallocene catalyst or pre-catalyst.

In the ethylene(bis-indenyl)-group IV systems, metallocene formation typically proceeds to give a kinetic distribution of desired *rac*- and undesired *meso*-isomer which must then be separated. Synthetic approaches to subsequent resolution of the *rac* isomer are well developed<sup>2</sup> but require first a catalytic hydrogenation to the (EBTHI)MCl<sub>2</sub> (EBTHI=ethylene(bis-tetrahydroindenyl), M=Ti, Zr, Hf) derivative. Jordan has recently reported a high yield synthesis of *rac*-ethylene(bis-indenyl)zirconium dichloride, however, isolation of enantiopure product still requires the hydrogenation/resolution steps, and the method is specific for only zirconium thusfar.<sup>3</sup> Although some examples of enantiomerically pure group III<sup>4</sup> and lanthanide<sup>5</sup> metallocene systems have been reported, none possess  $C_2$ -symmetry.

We have recently described the highly iso-specific Ziegler-Natta polymerization of  $\alpha$ -olefins using the single component,  $C_2$  symmetric metallocene  $[\text{BpYH}]_2$  ( $\text{Bp} = [\text{Me}_2\text{Si}(\text{C}_5\text{H}_2-2-\text{SiMe}_3-4-\text{CMe}_3)_2]$ ) (Figure 1).<sup>6</sup> The key design features of this linked ligand system are (1) incorporation of bulky trimethylsilyl substituents in the narrow portion of the metallocene wedge ( $\alpha$  to the dimethylsilylene linker) and (2) use of *tert*-butyl groups in the 4-positions to control the steric interactions in the reactive (open) part of the wedge. As anticipated, the steric bias exerted by this substitution pattern allows for formation of only the desired *racemic* product upon metallation, with no detectable amount of the undesired *meso* isomer. Significantly, the  $[\text{Bp}]$  ligand gives only the racemic bent metallocene for every group III, lanthanide, and group IV metal tested (Sc, Y, La, Ti, Zr).<sup>6,7</sup>

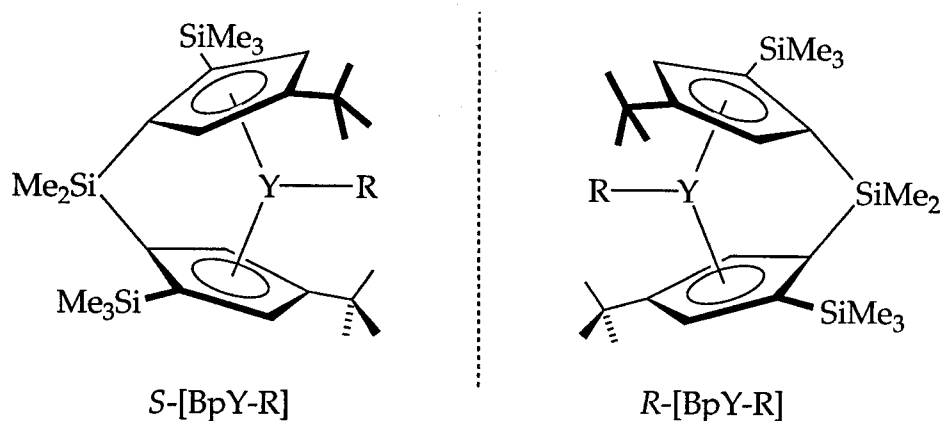


**Figure 1.** Enantiomers of *rac*-BpY-R.

A natural extension is the further development of methods for obtaining enantiomerically pure catalysts based on the  $[\text{Bp}]$  ligand system. Such single-component systems, in addition to serving as powerful mechanistic probes of Ziegler-Natta catalysis, would also be promising candidates for use in a variety of other catalytic asymmetric transformations. The most desirable ligand design would produce *only one enantiomer* upon coordination to the metal. Thus, not only would the wasteful and tedious separation of the *meso* isomer be avoided,

but the subsequent resolution of the racemate would also be obviated. Others, of course, have also recognized the desirability of such a ligand system, and some successes have already been realized.<sup>8</sup>

Described herein are our efforts which have led to the synthesis of the ligand [BnBp]<sup>2-</sup>, designed to coordinate to give only one enantiomer, and BnBpY-H, the first example, as far as we are aware, of an enantiopure C<sub>2</sub>-symmetric, group III metallocene which is competent for coordination polymerization of  $\alpha$ -olefins.

## Results and Discussion

**Ligand Synthesis** The strategy we have developed involves the use of C<sub>2</sub>-symmetric silyl-heterocycles as linking moieties which are able to direct metallocene formation by specific interactions with the TMS groups of the [Bp] ligand framework. In considering a viable approach to the synthesis of such a silicon heterocycle in which the silicon atom also bears two cyclopentadienyl derivatives, we have found the simple retrosynthetic analysis depicted in Figure 2 to be quite useful. Method A, which we also term the "chiral linker" approach was initially favored since we have successfully synthesized the parent Bp ligand, and several other linked ligand systems, by the use of dimethylsilylene as a "linker" (Figure 3).<sup>6,9</sup> Method A is a straightforward extension of this approach since formal substitution of the methyl groups of Me<sub>2</sub>SiCl<sub>2</sub> with the desired chiral moiety would give the chiral linker.

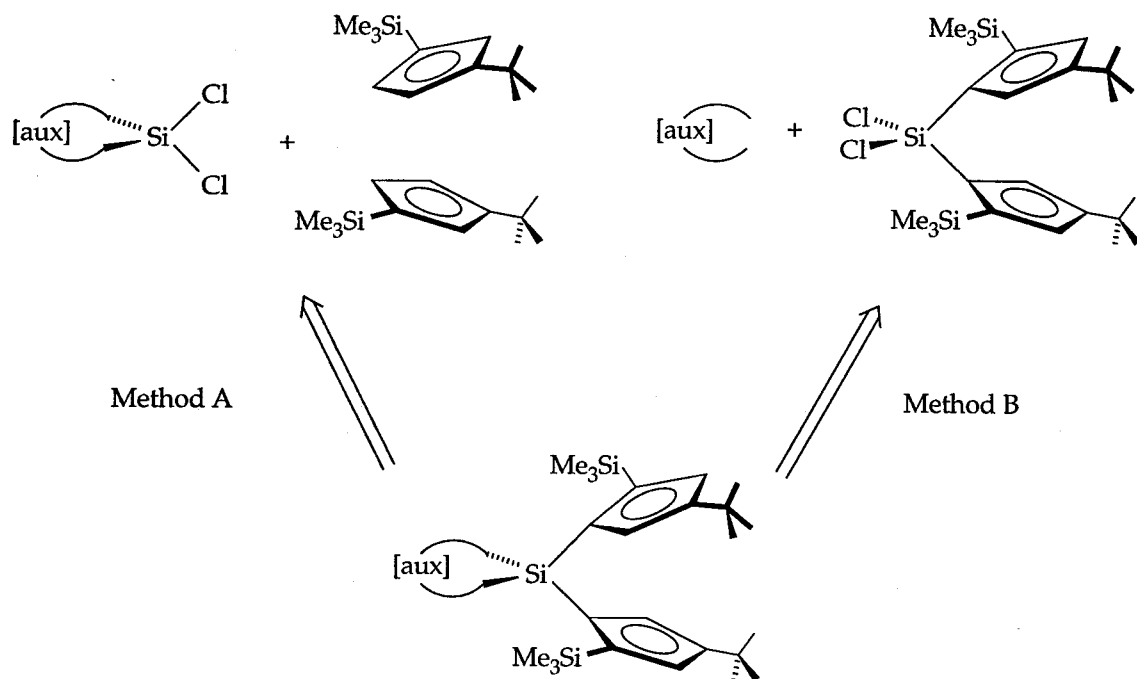


**Figure 2.** Simple retrosynthetic analysis for synthesis of desired ligands. [aux] =  $C_2$ -symmetric with specific interactions with TMS groups of Cp's.

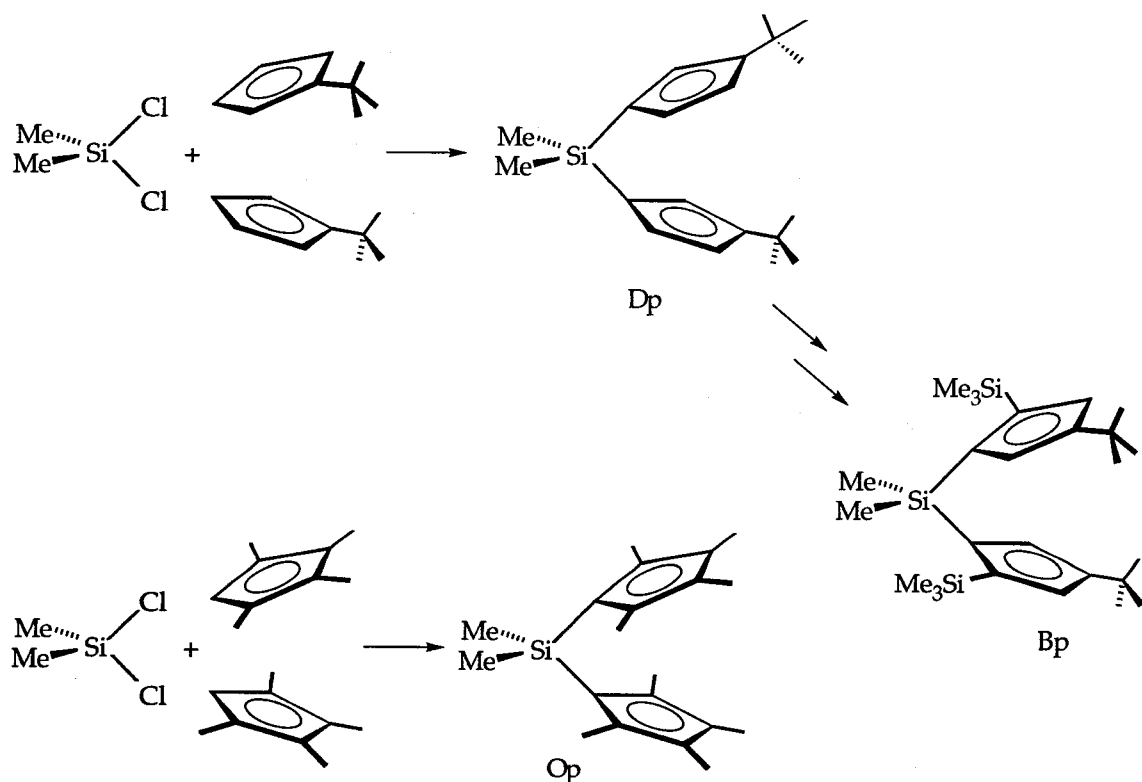


**Figure 3.** Synthesis of some other linked ligands (see text for details).

The two possible metallocene diastereomers of the initial target, **1**, are shown in Figure 4.

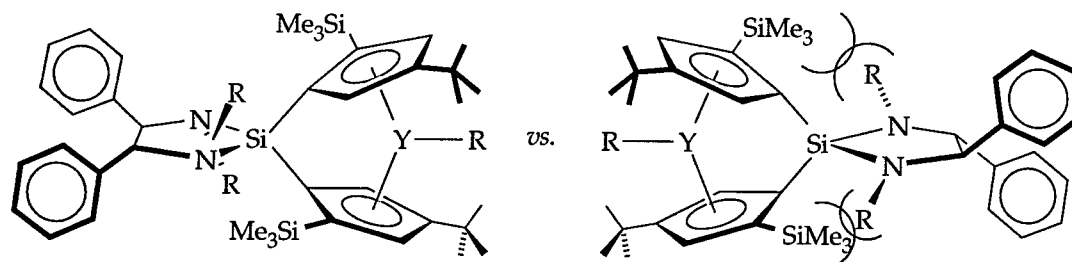
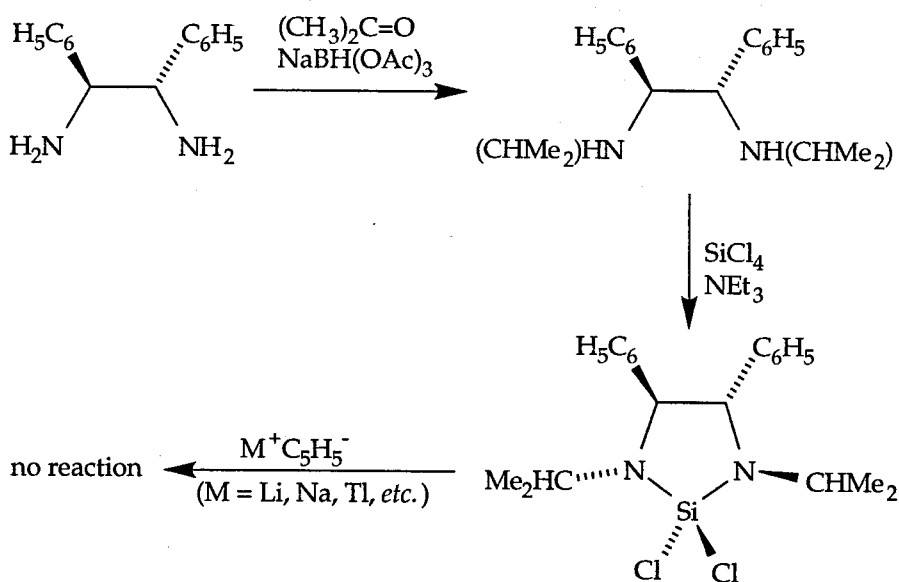


**Figure 4.** One of each of the enantiomeric pairs of diastereomers for *rac*-**1**.

As outlined in Scheme 1, we were able to prepare the necessary chiral linker in a fairly straightforward fashion by reductive amination of the desired enantiomer of (*R,R*)-, or (*S,S*)-1,2-diphenylethylenediamine (trans-stilbenediamine, (*R,R*)-, or (*S,S*)-1,2-diphenyl-1,2-diaminoethane), followed by reaction with  $\text{SiCl}_4$ .

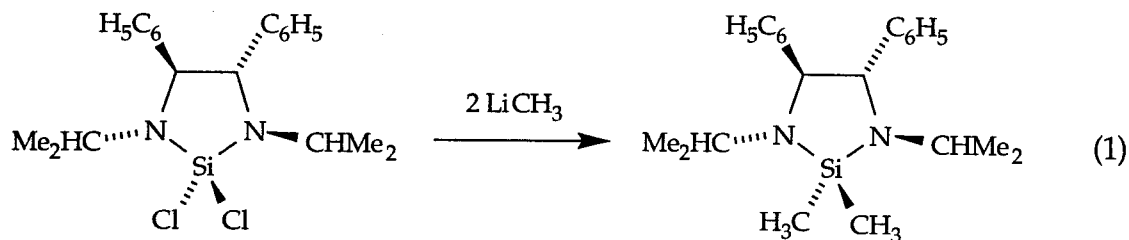
**Scheme 1.**



Unexpectedly, however, solutions of **1** and  $\text{Li}(t\text{-BuCp})$  in THF show no signs of reaction, even after days at room temperature, and only very slowly decompose at 80 °C (weeks)! As indicated in Scheme 1, attempts to effect reaction of **1** with other cyclopentadienide salts (Na, K, Tl), under varying



conditions did not meet with any success. However, **1** does react quickly and cleanly with LiMe·LiBr in THF at room temperature to give the corresponding dimethyl species (eqn 1).



Our initial assumption was that the steric bulk of the chiral linker was responsible for its low reactivity. Some recent studies, however, suggest that the relatively low basicity/nucleophilicity of the cyclopentadienide anion may be the limiting factor in its reaction with **1**, in spite of what appears to be an adequate thermodynamic driving force.<sup>10</sup>

Returning to Figure 2, we note that there is also some precedent for the strategy depicted as Method **B**, which involves bis-cyclopentadienyl substitution prior to further elaboration of the ensuing Cp<sub>2</sub>SiCl<sub>2</sub> fragment. Marks and coworkers have reported the synthesis of the dicyclopentadienylsilicon dichloride, (Me<sub>4</sub>C<sub>5</sub>)SiCl<sub>2</sub>.<sup>11</sup> Corey has also recently demonstrated that dialkylsilylditriflates react cleanly with, and can be used as protecting groups for a variety of diols.<sup>12</sup> The ensuing silicon and oxygen heteroatom containing rings were shown to be moderately stable, particularly for the 5-7 membered rings.

Along these lines, we have recently undertaken the synthesis of a [Bp] derivative, [BnBp], in which the methyl groups on the silyl linker are replaced by the C<sub>2</sub>-symmetric 1,1'-bi-2-naph-diolate group. Simple molecular models and preliminary molecular mechanics calculations suggested that steric interactions between the 3 and 3' methine positions of the naphthalene rings of the chiral

linker with the  $\alpha$ -trimethylsilyl substituents on the cyclopentadienyl rings might be sufficient to force enantioselective metallation of this ligand (Figure 5).

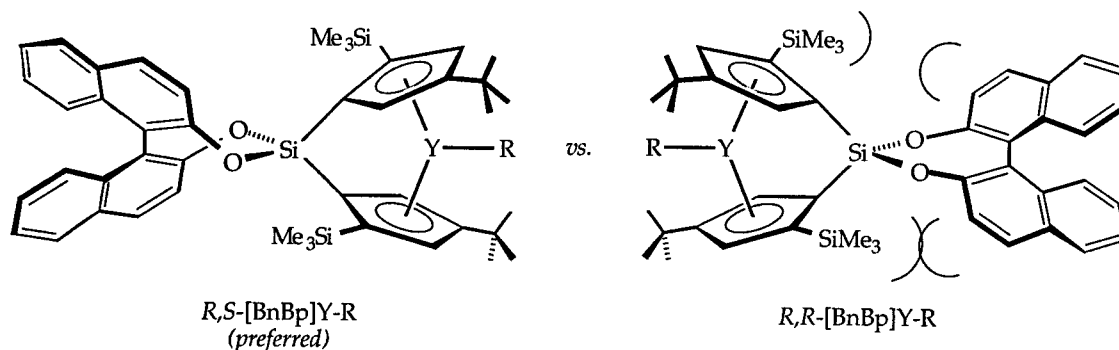
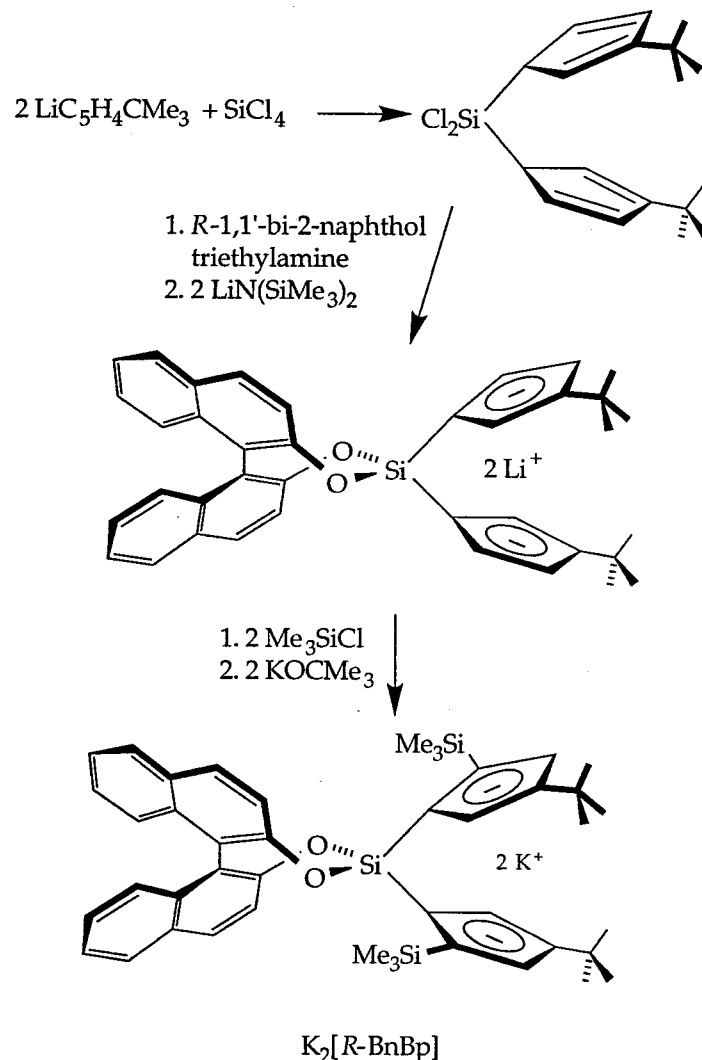


**Figure 5.** One of each of the enantiomeric pairs of diastereomers for [BnBp]Y-R. The bad interactions indicated by modelling studies are shown on the disfavored diastereomer (right).

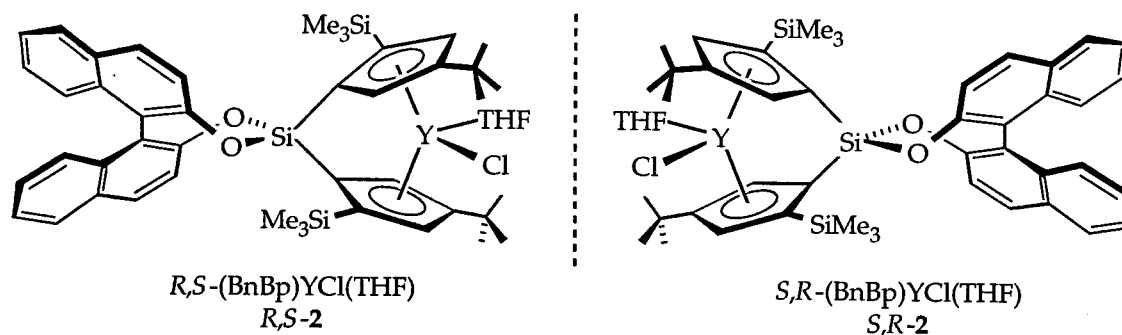
Both *R*- and *S*- enantiomers of 1,1'-bi-2-naphthol are readily available. Thus, in principle, either diastereomer (or the enantiomeric pair of diastereomers from *rac*-1,1'-bi-2-naphthol) could be synthesized.

We have found that the binaphthol-linked ligand,  $K_2\text{[BnBp]}$ , can be conveniently prepared in high overall yield (*ca.* 70% based on binaphthol) (Scheme 2). The binaphthol is conveniently incorporated onto the ligand framework as indicated in the Scheme and the subsequent reactions are analogous to those used for the preparation of  $K_2\text{[Bp]}$ . All reactions can be carried out in multigram quantities and a serendipitous benefit from introduction of the binaphthol moiety is the increased crystallinity of the ligand and its precursors.

Scheme 2.

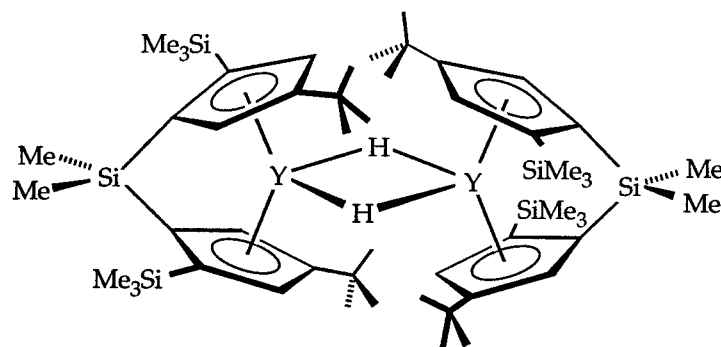


As anticipated,  $YCl_3(THF)_3$  and *rac*- $K_2[BnBp]$  react cleanly in THF to yield  $[BnBp]YCl(THF)$ , (*rac*-2). Significantly,  $^1H$  and  $^{13}C$  NMR spectroscopy indicate formation of a *single isomeric form*. We have subsequently determined (*vide infra*) that it is indeed the preferred pair of enantiomeric diastereomers predicted by molecular modeling. Use of optically pure ligand yields the corresponding enantiomerically pure metallocenes (either *R,S*- $[BnBp]YCl(THF)$ , (*R,S*-2) or *S,R*- $[BnBp]YCl(THF)$ , (*S,R*-2).



The preparation of alkyl and hydride derivatives of **2** are plagued by problems associated with non-stoichiometric amounts of coordinated THF lingering in the desired products. Fortunately we have found that the THF-free species, which is presumably the dimer  $\{[\text{BnBp}]\text{YCl}\}_2$  (**3**), can be obtained from **2** in either of two ways. The first method involves repeated cycles of refluxing **2** in toluene followed by removal of volatiles *in vacuo*. Three such cycles are sufficient for removal of >95% (by NMR) of the THF from **2** to give the THF-free species **3**. Alternatively, a soxhlet thimble is filled with 10X molecular sieves and a toluene solution of **2** in the base of the assembly is extracted through the sieves, which are selective for THF over toluene.<sup>13</sup>

The alkyl derivative  $[\text{BnBp}]\text{YCH}(\text{TMS})_2$  (**4**) is readily prepared from **3** by established methods. In the parent *rac*-BpYCH(TMS)<sub>2</sub> complex, reaction with dihydrogen results in isolation of only the enantiomeric pairs of homochiral hydride dimers shown below. The racemic compound,  $[\text{BpYH}]_2$ , has been characterized by X-ray crystallography and also by the diagnostic triplet observed in the <sup>1</sup>H NMR spectrum for the  $\text{Y}(\mu_2\text{-H})_2\text{Y}$  unit due to coupling with two <sup>89</sup>Y (100% abundant) centers (<sup>2</sup>J<sub>YH</sub> ≈ 30 Hz).



$(R\text{-Bp})\text{Y}(\mu_2\text{-H})_2\text{Y}(R\text{-Bp})$  (and enantiomer)

$D_2$  symmetry

Careful NMR observation of the reaction of  $\text{BpYCH}(\text{TMS})_2$  with  $\text{H}_2$  reveal an unexpected course for this reaction. Immediately upon addition of  $\text{H}_2$  to  $\text{BpYCH}(\text{TMS})_2$ , the  $^1\text{H}$  NMR spectrum reveals that not one, but rather, equal amounts of *two different* yttrium hydride species have been formed (Figure 6). Moreover, both species are highly symmetric dimers as evidenced by the observation of triplets for both hydride resonances and the high overall symmetry of the other spectral features. With time, the set of resonances for one of the dimers grows in at the expense of the other set, and eventually the spectrum is the one found for the isolated homochiral dimer. These observations suggest that both homochiral and heterochiral dimers are initially formed in equal amounts and, significantly, no free monomeric hydride (which should exhibit a characteristic doublet rather than triplet) is observed. Investigation of the *rac*- $(\text{BnBp})\text{YCH}(\text{TMS})_2$  hydrogenolysis under the same conditions as above reveal that it, too, initially forms equimolar amounts of homo- and heterochiral dimers which then yield the thermodynamically more stable form over time.

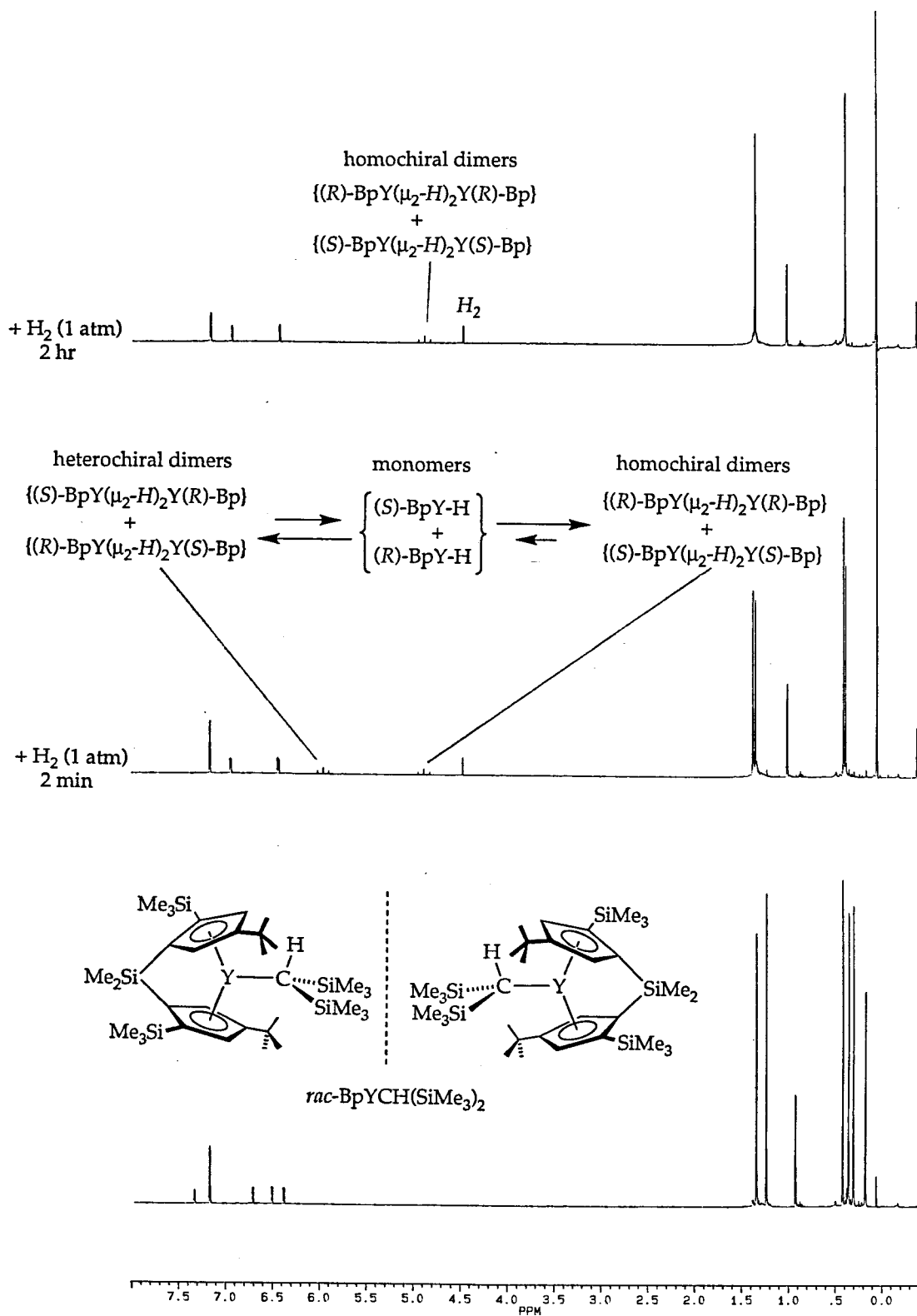


**Figure 6.** Selected spectra from the reaction of  $\text{BpYCH}(\text{TMS})_2$  with  $\text{H}_2$  (see text for details).

The analogous hydrogenolysis reaction using the resolved alkyl (*R,S*)-4 provides a nice example of the utility of these complexes. Now there is only the possibility of forming the homochiral hydride dimer (*R,S*)-5 (Figure 7). And indeed, only one species is observed even immediately upon reaction of (*S*)-4 with dihydrogen.

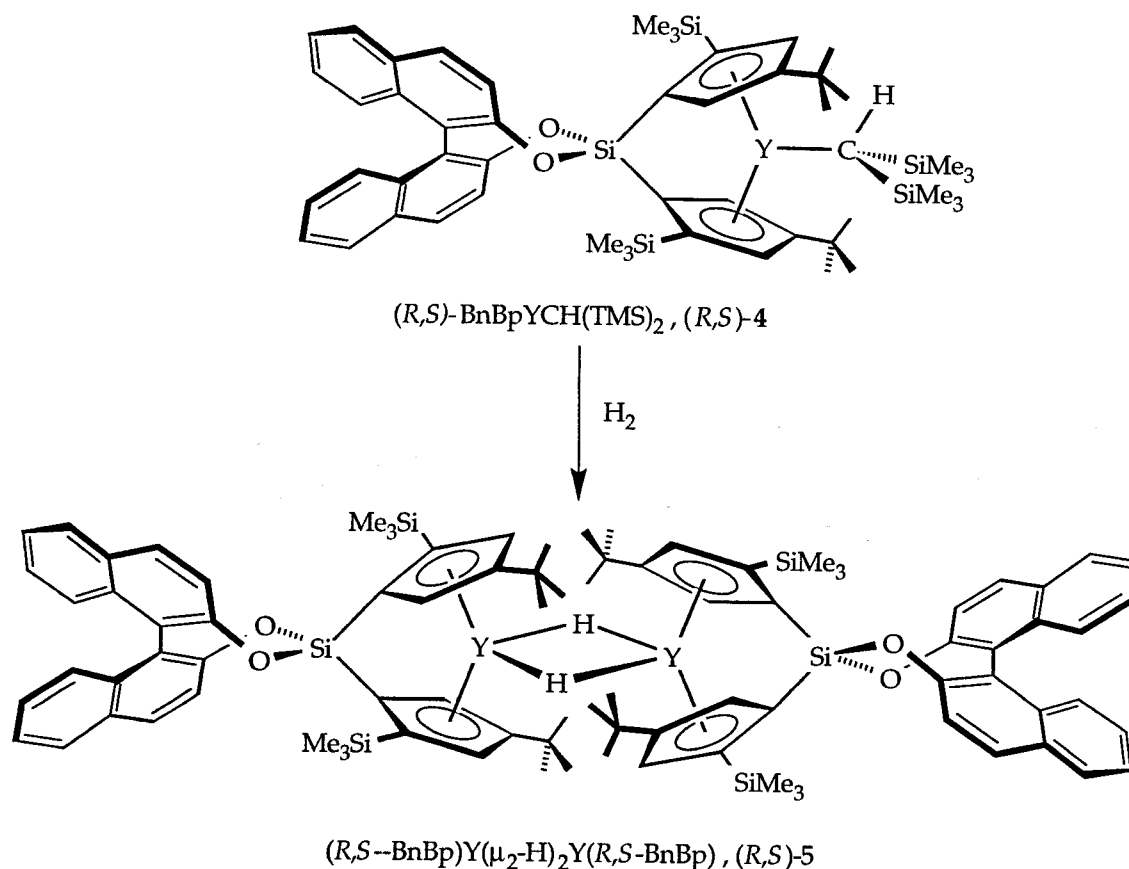


**Figure 7.** Only the homochiral dimer is possible when the starting compound is enantiopure.

The differences between the racemic and resolved complexes are illustrated in Figure 8 which shows the time course of the characteristic hydride triplets for all three reactions.

These studies have also revealed that the racemic dimer,  $[\text{BnBpYH}]_2$  (*rac*-5), is markedly less soluble than the corresponding resolved compounds (apparently, crystal effects favor packing for the racemic material in a centrosymmetric manner). Since centered-symmetry is not allowed for resolved chiral compounds, we presume the the enantiomerically pure materials must crystallize in a relatively higher energy non-centrosymmetric space group and are thus more soluble.

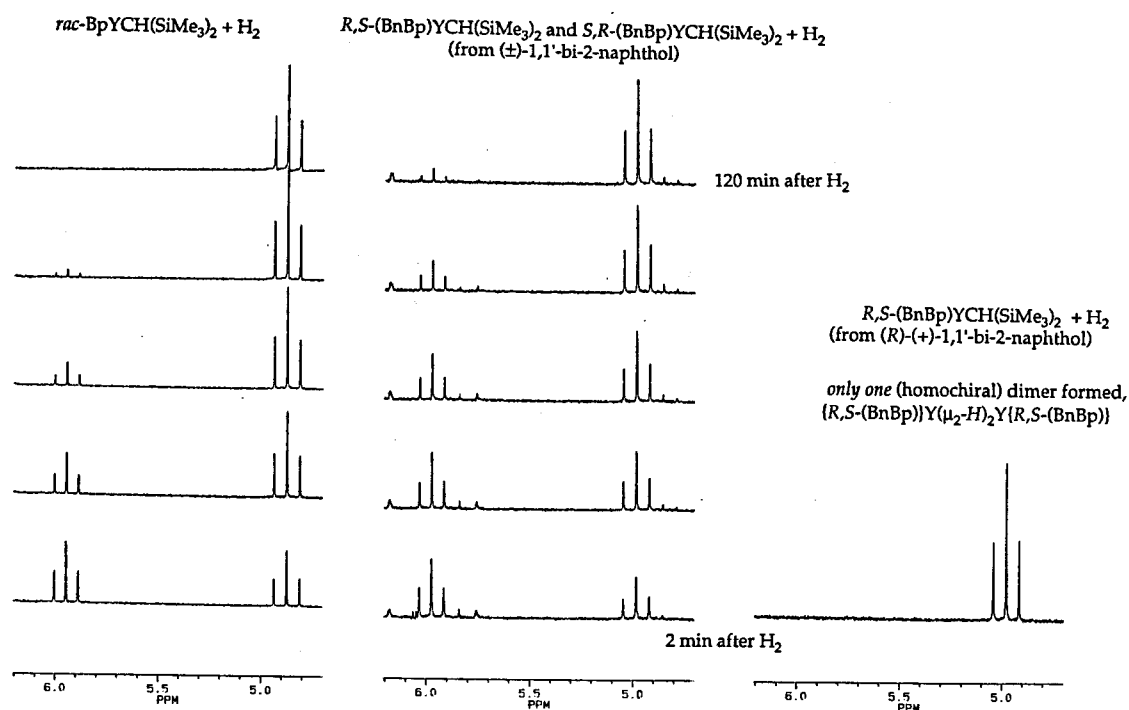
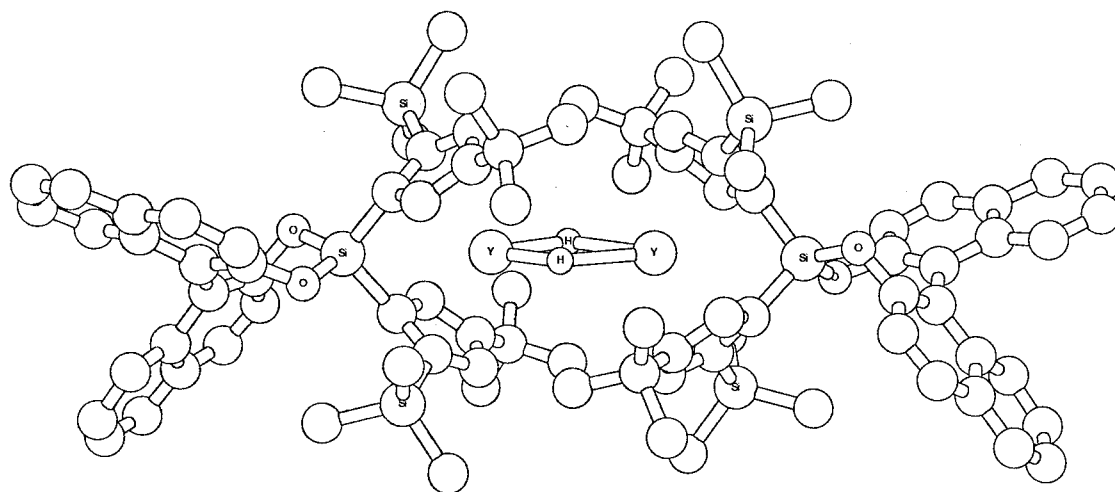


**Figure 8.**  $^1\text{H}$  NMR (hydride region) for reaction of the three complexes with  $\text{H}_2$ .

**Crystal Structure.** We have been able to grow X-ray quality crystals of *rac*-5 by taking advantage of these solubility differences.<sup>14</sup> When a solution of (*R,S*)-5 in petroleum ether is carefully layered over a solution of (*S,R*)-5 in toluene, crystals of the racemic mixture grow slowly at the interface. Crystallographic studies confirm that the ligand is indeed coordinated to the metal as the preferred



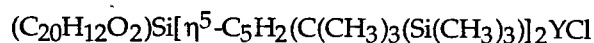
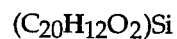
diastereomer (*vide supra*). As shown in Figure 9 the monomeric units of the dimer are symmetrically bridged by the hydride ligands. In contrast to the parent complex  $[\text{BpYH}]_2$  which has nearly ideal  $D_2$ -symmetry (and thus ideal overlap for the orbitals of the  $\text{Y}(\mu_2\text{-H})\text{Y}$  fragment), the structure reveals a twisted rather than "head-on" linkage for the two monomer units. Thus the dimer has overall  $C_2$ -symmetry and the dihedral angle between the two halves is approximately  $40^\circ$ . Similar twisting for a  $C_2$ -symmetric system has been observed for a related Ti(III) hydride dimer.



**Figure 9.** Cache depiction of the crystallographically determined asymmetric unit of *rac*-5 (see also Figure 7). All unlabelled atoms are carbon; for clarity, only the bridging hydrogen atoms are shown.

**Table 1.**  $^1\text{H}$ -NMR Data <sup>a</sup>

Compound	Assignment	$\delta$ (ppm)
$(\text{C}_{20}\text{H}_{12}\text{O}_2)\text{Si}[\text{C}_5\text{H}_3(\text{C}(\text{CH}_3)_3)_2]\text{Li}_2$ $\text{Li}_2[\text{BnDp}]^{\text{b}}$	$(\text{C}_{20}\text{H}_{12}\text{O}_2)\text{Si}$	7.86 (d, 2H);
		7.51 (d, 2H);
		7.46 (d, 2H);
		7.25 (m, 2H);
		7.17 (d, 2H);
		7.08 (m, 2H)
	$[\eta^5\text{-C}_5\text{H}_3(\text{C}(\text{CH}_3)_3)_2]$	5.79 (m, 2H)
		6.00 (br, 2H)
		6.04 (br, 2H)
	$[\eta^5\text{-C}_5\text{H}_3(\text{C}(\text{CH}_3)_3)_2]$	1.21 (s, 18H)
$(\text{C}_{20}\text{H}_{12}\text{O}_2)\text{Si}[\text{C}_5\text{H}_2(\text{C}(\text{CH}_3)_3(\text{Si}(\text{CH}_3)_3))_2]\text{K}_2$ $\text{K}_2[\text{BnBp}]^{\text{b}}$	$(\text{C}_{20}\text{H}_{12}\text{O}_2)\text{Si}$	7.77 (d, over- lapping, 4H);
		7.62 (d, 2H);
		7.19 (m, 2H);
		7.12 (d, 2H);
		7.04 (m, 2H)
	$[\eta^5\text{-C}_5\text{H}_2(\text{C}(\text{CH}_3)_3(\text{Si}(\text{CH}_3)_3))_2]$	6.57 (d, 2H)
		6.00 (d, 2H)
		$^4J_{\text{H-H}}=2.0$ Hz for both peaks
	$[\eta^5\text{-C}_5\text{H}_2(\text{C}(\text{CH}_3)_3(\text{Si}(\text{CH}_3)_3))_2]$	1.23 (s, 18H)
	$[\eta^5\text{-C}_5\text{H}_2(\text{C}(\text{CH}_3)_3(\text{Si}(\text{CH}_3)_3))_2]$	0.14 (s, 18H)

BnBpYCl<sup>b</sup>

7.92 (d, 2H);

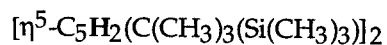
7.85 (d, 2H);

7.65 (d, 2H);

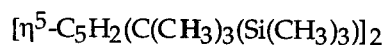
7.28 (t, 2H);

7.17 (d, 2H);

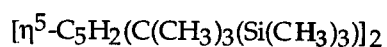
7.12 (t, 2H)



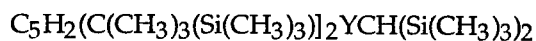
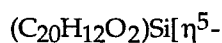
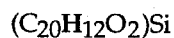
6.54 (m, 4H)



1.31 (s, 18H)



0.22 (s, 18H)

BnBpYCH(TMS)<sub>2</sub><sup>c</sup>

7.77 (d, 1H);

7.74 (d, 1H);

7.63 (m, 2H,

overlapping);

7.58 (d, 1H);

7.57 (d, 1H);

7.45 (d, 1H);

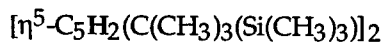
7.44 (d, 1H);

7.09 (m, 2H,

overlapping);

7.91 (m, 2H,

overlapping);



7.30 (d, 1H);

6.96 (d, 1H);

6.85 (d, 1H);

6.70 (d, 1H),

<sup>4</sup>J<sub>H-H</sub>=1.9 Hz

for all peaks

		1.40 (s, 9H);
		1.31 (s, 9H)
		0.36 (s, 9H);
		0.34 (s, 9H)
		0.46 (d, 1H)
		$^2J_{Y-H}=2.3$ Hz
		0.25 (s, 9H);
		0.19 (s, 9H)
$\{(R,S)-[(C_{20}H_{12}O_2)Si[\eta^5-$ $C_5H_2(C(CH_3)_3(Si(CH_3)_3)]_2Y]_2(\mu^2-H)_2$ and enantiomer homochiral hydride dimer <sup>c</sup>		
$(C_{20}H_{12}O_2)Si$		7.78 (d, 4H);
		7.70 (d, 4H);
		7.63 (d, 4H);
		7.50 (d, 4H);
		7.12 (m, 4H);
		6.94 (m, 4H)
		6.97 (d, 4H)
		6.84 (d, 4H)
		$^4J_{H-H}=1.8$ Hz
		for both peaks
		1.44 (s, 36H)
		0.30 (s, 36H)
		4.98 (t, 2H)
		$^1J_{Y-H}=31.4$ Hz

,(*R,S*)-(C<sub>20</sub>H<sub>12</sub>O<sub>2</sub>)Si[η<sup>5</sup>-  
C<sub>5</sub>H<sub>2</sub>(C(CH<sub>3</sub>)<sub>3</sub>(Si(CH<sub>3</sub>)<sub>3</sub>)]<sub>2</sub>Y](μ<sup>2</sup>-H)<sub>2</sub>((*S,R*)-  
(C<sub>20</sub>H<sub>12</sub>O<sub>2</sub>)Si[η<sup>5</sup>-C<sub>5</sub>H<sub>2</sub>(C(CH<sub>3</sub>)<sub>3</sub>(Si(CH<sub>3</sub>)<sub>3</sub>)]<sub>2</sub>Y)  
and enantiomer

hetrochiral hydride dimer<sup>c</sup>

(C<sub>20</sub>H<sub>12</sub>O<sub>2</sub>)Si

7.79 (d, 4H);

7.70 (d, 4H);

7.62 (d, 4H);

7.50 (d, 4H);

7.12 (m, 4H);

6.94 (m, 4H)

[η<sup>5</sup>-C<sub>5</sub>H<sub>2</sub>(C(CH<sub>3</sub>)<sub>3</sub>(Si(CH<sub>3</sub>)<sub>3</sub>)]<sub>2</sub>

7.00 (d, 4H)

6.87 (d, 4H)

<sup>4</sup>J<sub>H-H</sub>=1.8 Hz

for both peaks

[η<sup>5</sup>-C<sub>5</sub>H<sub>2</sub>(C(CH<sub>3</sub>)<sub>3</sub>(Si(CH<sub>3</sub>)<sub>3</sub>)]<sub>2</sub>

1.45 (s, 36H)

[η<sup>5</sup>-C<sub>5</sub>H<sub>2</sub>(C(CH<sub>3</sub>)<sub>3</sub>(Si(CH<sub>3</sub>)<sub>3</sub>)]<sub>2</sub>

0.36 (s, 36H)

Y<sub>2</sub>(μ<sup>2</sup>-H)<sub>2</sub>

5.97 (t, 2H)

<sup>1</sup>J<sub>Y-H</sub>=31.4 Hz

<sup>a</sup> All spectra were recorded at 500 MHz at ambient temperature.

<sup>b</sup> THF-*d*<sub>8</sub> solvent

<sup>c</sup> Benzene-*d*<sub>6</sub> solvent

## Experimental Section

**General Considerations.** All air and/or moisture sensitive compounds were manipulated using standard high vacuum line, Schlenk, or cannula techniques, or in a dry box under a nitrogen atmosphere, as described previously.<sup>15</sup> Argon and hydrogen gases were purified and dried by passage over columns of MnO on vermiculite and activated molecular sieves. Solvents were stored under vacuum over titanocene<sup>16</sup> or sodium benzophenone ketyl. The preparations of 6,6-dimethylfulvene, and *t*-BuCpLi were carried out as previously reported.<sup>17</sup> LiN(TMS)<sub>2</sub> and KO<sup>*t*</sup>-Bu (Aldrich) were purified by sublimation prior to use. (*R*)-, (*S*)-, and *rac*-1,1'-bi-2-naphthol were purchased (Aldrich) and used as received. (*R,R*)-, and (*S,S*)-1,2-diphenyl-1,2-diaminoethane were either synthesized<sup>18</sup> or purchased and used as received. Indenyllithium was synthesized according to the literature method.<sup>19</sup>

NMR spectra were recorded on General Electric QE300 (300 MHz for <sup>1</sup>H) and Bruker AM500 (500.13 MHz for <sup>1</sup>H) spectrometers. Elemental analyses were carried out at the Caltech Elemental Analysis Facility by Fenton Harvey. Mass spectra were acquired, with the assistance of Dr. Peter G. Green, at the Bank of America Environmental Analysis Center at Caltech using an HP 59880B Particle Beam LC/MS Interface to an HP 5989A Mass Spectrometer Engine; air/water exclusion was achieved by using the HP 1090 Liquid Chromatograph's Solvent Delivery System and Variable Volume Injector. The crystal structure determination for *rac*-[BnBpYH]<sub>2</sub> was carried out at the Caltech Crystallography Facility by Prof. Kenneth I. Hardcastle and Lawrence M. Henling.

The following are sample procedures which were performed routinely. The preparations are the same whether the starting materials were racemic or

resolved. All three catalysts were made in the same fashion, with nearly identical NMR spectra and similar yields.

**(*t*-BuCpH)<sub>2</sub>SiCl<sub>2</sub>.** In the glove box, to a stirring solution of 31.5g (1 eq) of SiCl<sub>4</sub> in 700 ml THF was added 47.4g (2 eq) *t*-BuCpLi over 20 minutes, giving a clear yellow solution. After stirring overnight the flask was fitted with a kugekrohr bulb and taken out of the box. All volatiles were removed *in vacuo*, followed directly by a Kugelrohr distillation at 60°C. The product was stored in the glove box freezer. Yield: 31.5g yellow oil, 57%.

**[(±)-Bn]DpH<sub>2</sub>.** In the glove box, 11.78g (1 eq) of (*t*-BuCpH)<sub>2</sub>SiCl<sub>2</sub> was stirred with 350ml THF. A solution of 9.89g (1 eq) of (±)-binaphthol and 10.47g (3 eq) of triethylamine in 200 ml of THF was added dropwise over several hours. The initially clear solution became cloudy and pale green after several minutes. After stirring overnight, the flask was removed from the box and the THF removed *in vacuo*. Approximately 300 ml of petroleum ether was condensed in, the mixture was stirred briefly and then the petroleum ether was removed *in vacuo*. The reaction flask was fitted with a standard fine frit assembly and about 250 ml diethyl ether was condensed onto the mixture and stirred. Filtration and washing with diethyl ether yielded a large amount of a white solid (NEt<sub>3</sub>·HCl) and a clear yellow filtrate. All volatiles were removed *in vacuo*, leaving a shiny yellow solid foam. Yield 17.9g fine yellow powder, 93%.

Analysis for  $C_{38}H_{38}O_2Si$ :

Calculated %	Found %					
	rac		R		S	
	no ox.	with ox.	no ox.	with ox.	no ox.	with ox.
C: 82.25		81.61	81.25	79.19	74.65	82.77
		81.47	81.39	80.85	73.5	
H: 6.92		7.48	7.18	6.4	7.07	6.93
		7.57	7.14	6.57	7.09	

**[(±)-Bn]DpLi<sub>2</sub>**. An extra large fine frit assembly equipped with two 1 L round bottom flasks was loaded in the dry box with 17.7g (1 eq) [(±)-Bn]DpH<sub>2</sub> and 10.7g (2 eq) LiN(TMS)<sub>2</sub>. The entire assembly was evacuated and 600 ml of THF was condensed in at -78°C. The solution was stirred for 15 minutes at -78° and then allowed to warm slowly to room temperature. The solution was stirred for 3 hours at room temperature and then all volatiles were removed *in vacuo*, leaving a pasty beige solid. 150 ml diethyl ether was condensed in at -78°, warmed to room temperature, stirred and then removed *in vacuo*, leaving a foamy yellow paste which was pumped on under dynamic vacuum overnight. 250 ml of petroleum THF. Yield: 18.34g off white solid, 86% [(±)-Bn]DpLi<sub>2</sub>·(THF). Analysis for  $C_{38}H_{36}Li_2O_2Si$ :

Calculated %	Found %					
	rac		R		S	
	no ox.	with ox.	no ox.	with ox.	no ox.	with ox.
C: 80.53			77.56	77.06	74.86	76.87
			77.35	79.01	75.96	
H:6.42			7.5	7.51	7.21	6.91
			7.46	7.3	7.31	

**[(±)-Bn]BpH<sub>2</sub>**. In the glove box, an extra large fine frit assembly fitted with a 500ml kjeldahl flask and a 1 L round bottom was loaded with 18.068g (1eq) (ether was condensed onto the solid at -78°, warmed to room temperature and stirred vigorously for 1 hour, giving a yellow solution and a white precipitate.



The slurry was filtered, the off white solid washed once with petroleum ether and then all volatiles were removed *in vacuo*. NMR shows approximately 1 eq. of  $\pm$ -BnDpLi<sub>2</sub>. The assembly was removed from the box and evacuated.

Approximately 600 ml THF was condensed on at -78°C. The solution was then warmed to room temperature, giving a clear yellow solution. 11 ml (3 eq) of TMSCl was condensed into the solution at -78°. The reaction was allowed to warm to room temperature and stir overnight. All volatiles were removed *in vacuo*, leaving a large light yellow foamy solid. After pumping for 2 hours, 200 ml diethyl ether was condensed in at -78°, allowed to warm to room temperature and stirred for 15 minutes before being pumped off, leaving a light yellow foamy solid. 400 ml of petroleum ether was condensed in at -78°, giving a light yellow solution and a white precipitate (LiCl). After stirring at room temperature for a couple of hours, the LiCl was filtered off and washed, giving a clear yellow solution, which, when pumped down, gave a large yellow foamy solid. Yield: 16.62g micro-crystalline white powder, 87%. Analysis for C<sub>52</sub>H<sub>70</sub>O<sub>4</sub>Si<sub>3</sub>:

Calculated %	Found %					
	rac		R		S	
	no ox.	with ox.	no ox.	with ox.	no ox.	with ox.
C: 75.57			74.42		74.35	69.15
			74.23			
H: 7.80			8.11		8.15	8.15
			8.2			

**[( $\pm$ )-Bn]BpK<sub>2</sub>.** An extra large fine frit assembly fitted with a 1L round bottom and a 500ml kjeldahl flask was taken into the dry box and loaded with 16.22g (1eq) [( $\pm$ )-Bn]BpH<sub>2</sub> and 5.19g (2 eq) K(O<sup>*t*</sup>-Bu). The assembly was removed, evacuated, and 500 ml THF was condensed onto the solids at -78°C. The brownish-yellow solution was warmed to room temperature, all solids dissolved and the solution was allowed to stir overnight. All volatiles were removed *in*

*vacuo*, leaving a light brown foamy paste. 200 ml diethyl ether was condensed in at -78° and warmed to room temperature. All volatiles were removed *in vacuo* leaving a light brown solid. 400 ml of petroleum ether was condensed in at -78°, giving a yellow solution with a white precipitate. 100 ml diethyl ether was condensed in and the solution was warmed to room temperature and stirred for an hour. The yellow supernatant was filtered away from the solid. The solid was washed once with fresh solvent and then all volatiles were removed *in vacuo*. NMR shows 0.5 eq. THF. Yield ( $\pm$ )BnBpK<sub>2</sub>·0.5(THF): 17.62g free flowing yellow powder, 92%. Analysis for C<sub>44</sub>H<sub>52</sub>K<sub>2</sub>O<sub>2</sub>Si<sub>3</sub>:

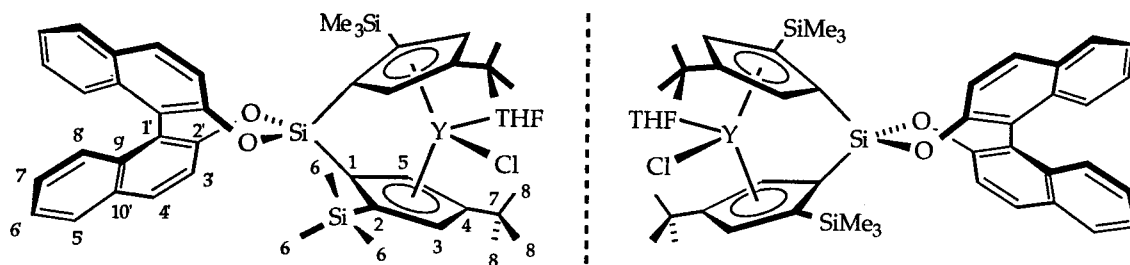
Calculated %	Found %					
	rac		R		S	
	no ox.	with ox.	no ox.	with ox.	no ox.	with ox.
C: 67.90	67.3	66.43		67.49	66.97	67.79
	66.9	66.29		66.75	66.99	68.08
H: 7.47	7.3	7.02		7.19	7.23	7.07
	7.22	7.08		7.16	7.39	7.32

**[(R)-BnBpYCl]<sub>2</sub> (2)** 3.00 g (1 eq.) [(R)-BnBp]]K<sub>2</sub> and 1.59g (1 eq.) YCl<sub>3</sub>(THF)<sub>3</sub> were refluxed overnight in 150 ml THF under an argon atmosphere. After cooling to room temperature, all volatiles were removed *in vacuo* and 100 ml diethyl ether condensed in at -78°C. The mixture was warmed to room temperature, stirred briefly and then all volatiles removed *in vacuo*. The remaining solid was pumped on at high vacuum for another eight hours, at which point 100 ml toluene was condensed into the reaction flask at -78°C. This mixture was refluxed under an argon atmosphere for several hours. All volatiles were again pumped away at high vacuum. Diethyl ether was again condensed on at -78° and pumped away at room temperature under high vacuum. The reaction apparatus was then transferred to the dry box where the flask containing the products was fitted with a large fine frit apparatus and another

flask. After transferring the apparatus back to the vacuum line, it was evacuated and 100 ml Et<sub>2</sub>O was condensed on at -78°. After warming to room temperature, the orange supernatant was filtered away from the white solid (KCl). The filter cake was extracted once with fresh solvent and the volatiles removed *in vacuo*, leaving an orange foam. 100 ml petroleum ether was condensed in and the mixture stirred vigorously for two hours. Once again the orange supernatant was filtered away from the white solid. The filter cake was washed twice with fresh solvent. Petroleum ether and other volatiles removed *in vacuo*. 1.74g white solid obtained. Yield: 55%. Analysis for C<sub>44</sub>H<sub>52</sub>O<sub>2</sub>Si<sub>3</sub>YCl:

Calculated %	Found %					
	rac		R		S	
	no ox.	with ox.	no ox.	with ox.	no ox.	with ox.
C: 64.33	55.57				56.54	
					56.49	
H: 6.38	5.77				6.1	
					5.91	

**<sup>1</sup>H and <sup>13</sup>C NMR Characterization of *rac*-BnBpYCl·THF.** Multidimensional NMR studies have allowed thorough <sup>1</sup>H- and <sup>13</sup>C-spectral assignments for **2** in THF-*d*<sub>8</sub>. The C2' carbon was assigned on the basis of its upfield chemical shift. H<sub>i</sub>C-COSY established the carbon-hydrogen connectivities, and H<sub>i</sub>H-COSY spectra were used to distinguish H3' and H4' from H5'-H8'. Cross peaks found from long range HETCOR studies then allowed unambiguous connectivities to be established for the binaphthyl fragment as follows: C2' with H3'; C10' with H4' and H5'; C9' with H8'; and thus C1' by elimination. The cyclopentadienyl fragment was similarly assigned, however, due to the coincident chemical shifts of H3 and H5, their respective carbon atoms could not be distinguished.



$^{13}\text{C}$ NMR (125 MHz)	$^1\text{H}$ NMR (500 MHz)
C1 $\delta$ 114.93	
C2 $\delta$ 125.47	
C3 $\delta$ 127.69 or 116.81	H3 $\delta$ 6.54 m; 1H
C4 $\delta$ 147.07	
C5 $\delta$ 116.81 or 127.69	H5 $\delta$ 6.54 m; 1H
C6 $\delta$ 1.96	H6 $\delta$ 0.22 s; 9H
C7 $\delta$ 33.29	
C8 $\delta$ 31.91	H8 $\delta$ 1.31 s; 9H
C1' $\delta$ 122.34	
C2' $\delta$ 152.04	
C3' $\delta$ 130.61	H3' $\delta$ 7.92 d, $J=8.65$ ; (1H)
C4' $\delta$ 123.26	H3' $\delta$ 7.65 d, $J=8.40$ ; (1H)
C5' $\delta$ 127.77	H3' $\delta$ 7.17 "d", $J=8.40$ ; (1H)
C6' $\delta$ 126.35	H3' $\delta$ 7.12 "t", $J=7.10$ ; (1H)
C7' $\delta$ 124.53	H3' $\delta$ 7.28 "d", $J=7.13$ ; (1H)
C8' $\delta$ 128.85	H3' $\delta$ 7.85 "d", $J=8.10$ ; (1H)
C9' $\delta$ 134.69	
C10' $\delta$ 131.42	

**(R)-BnBpYCH(TMS)<sub>2</sub> (3).** 1.60g [(R)-BnBpYCl]<sub>2</sub> (1 eq.) and .324g LiCH(TMS)<sub>2</sub> (1 eq.) loaded into flask and fitted with large filter frit. Assembly was evacuated and 150 ml toluene condensed in at -78°C. The mixture was warmed to room temperature and stirred for two days. All volatiles were removed *in vacuo* and 75 ml petroleum ether was condensed in, solution was warmed up and petroleum

ether was removed *in vacuo*, and remaining solid was pumped on under dynamic vacuum for two hours. 150 ml petroleum ether was then condensed in, warmed to room temperature, and stirred vigorously. Orange superatant was filtered away from the white solid (LiCl). Filter cake was washed twice with fresh solvent. All volatiles were removed *in vacuo* and remaining orange foam was pumped on for three hours at high vacuum. 1.147g light brownish-orange free flowing solid obtained. Yield: 62%.  $\{^1\text{H}\}^{13}\text{C}$  NMR ( $\text{C}_6\text{D}_6$ ):  $\delta$  151.7, 151.1, 134.7, 131.5, 131.3, 129.0, 127.9, 127.8, 127.1, 127.0, 126.9, 126.8, 125.0, 122.6, 125.0, 122.6, 122.5, 121.5, 121.3, 120.0, 199.8 (C-aromatic); 32.8, 32.5 (methyl of *t*-Bu); 33.8, 32.5 (quat. of *t*-Bu); 2.2, 1.9 (methyl of  $\text{YCH}(\text{TMS})_2$ ); 1.8 (methine of  $\text{YCH}(\text{TMS})_2$ ).

Analysis for  $\text{C}_{51}\text{H}_{71}\text{O}_2\text{Si}_5\text{Y}$ :

Calculated %	Found %					
	rac		R		S	
	no ox.	with ox.	no ox.	with ox.	no ox.	with ox.
C: 64.78	57.92			64.18		
	57.32			64.13		
H:7.58	6.61			7.49		
	6.64			7.49		

**[(R)-BnBpYH]<sub>2</sub>.** 700 mg (R)-BnBpYCH(TMS)<sub>2</sub> loaded into bomb. After evacuating, approximately 50 ml toluene was condensed in at -78°C. 4 atm dry H<sub>2</sub> was then condensed in. The reaction was stirred at room temperature for two hours. The solution was transferred into a 100 ml kjeldahl flask fitted with a large frit assembly. 30 ml petroleum ether was condensed into the evacuated assembly at -78°C. The mixture was stirred vigorously at room temperature. The orange filtrate was filtered away from the white solid, which was washed twice with fresh solvent. All volatiles were removed in vacuo and the solid was pumped on at high vacuum overnight. 269 mg white solid obtained in two crops. Yield: 46% overall.  $\{^1\text{H}\}^{13}\text{C}$  NMR ( $\text{C}_6\text{D}_6$ ):  $\delta$  147.9, 143.9, 134.8, 131.5,

131.2, 129.3, 127.0, 125.0, 123.2, 122.8, 122.7, 120.1, 120.0 (C-aromatic); 34.5 (methyl of *t*-Bu); 33.4 (quat. of *t*-Bu); 2.4 (methyl of TMS). Analysis:

Calculated %	Found %					
	rac		R		S	
	no ox.	with ox.	no ox.	with ox.	no ox.	with ox.
C:67.15		68.58				
		65.54				
H:6.79		7.35				
		7.07				

**NMR Studies of [BnBpYH]<sub>2</sub>.** Approximately 10 mg of the appropriate alkyl [(R, S)-BnBpYCH(TMS)<sub>2</sub>, (±)-BnBpYCH(TMS)<sub>2</sub>, or BpYCH(TMS)<sub>2</sub>] was loaded into a J.Young NMR tube. The tube was filled with C<sub>6</sub>D<sub>6</sub>, frozen with LN<sub>2</sub>, and evacuated at that temperature. H<sub>2</sub> was condensed into the tube. The tube was kept cold in a dry ice/acetone bath until just before putting it into the spectrometer, at which point it was quickly thawed. Spectra were taken immediately, and then at regular time intervals over several hours.

**Binol chiral linker.** In the glovebox a 500 ml three-neck flask was charged with SiCl<sub>4</sub> (7.400 g, 0.0437 mmol) and THF (300 ml) and taken on to the vacuum line. The clear solution was cooled to 0 °C and, against an argon counterflow, *rac*-1,1'-bi-2-naphthol (12.500 g, 0.0437 mmol) was added as a solid in aliquots over approximately 10 min. There was no apparent heat evolution and the solid quickly dissolved giving a slightly yellow solution which was stirred for 4 hr. Removal of solvent *in vacuo* gave a white foam which upon standing overnight under static vacuum had converted to a light yellow oil. Et<sub>2</sub>O was condensed onto the oil which dissolved upon warming to RT with stirring. Volatiles were again removed *in vacuo* leaving a white foam which was dried for 2 hr under dynamic vacuum. Yield 15.6 g of off white powder which contained some

residual solvent (NMR) but was used without further purification.  $^1\text{H}$  NMR ( $\text{C}_6\text{D}_6$ ):  $\delta$  (overlapping) 7.535 (d, 2H) and 7.521 (d, 2H), (overlapping) 7.258 (d, 2H) and 7.243 (d, 2H), 7.072 (t, 2H), 6.832 (t, 2H).

**(*R,R*)-1,2-diphenyl-1,2-di(isopropylamino)ethane.** The literature procedure<sup>20</sup> for reductive amination using  $\text{NaBH}(\text{OAc})_3$  was employed as follows. A dry 200 ml Schlenk flask was charged with (*R,R*)-1,2-diphenyl-1,2-diaminoethane (2.335 g, 11.00 mmol),  $\text{NaBH}(\text{OAc})_3$  (6.358 g, 30.00 mmol), and approximately 5-7 g of activated 3A molecular sieves. Freshly distilled THF (80 ml) was added by cannula transfer. By syringe, acetone (1.162 g, 1.469 ml, 20.00 mmol) followed by acetic acid (1.201 g, 20 mmol) were both added to the stirred solution. The septum was exchanged for a glass stopper and the solution was allowed to stir. The color gradually changed from cloudy white to cloudy tan as the sieves were slowly ground by the stir bar. After 36 hr, the reaction mixture was filtered (in air) through a 600 ml medium porosity frit to give a clear, colorless solution. The reaction vessel and filter cake were washed with 2x75 ml of  $\text{Et}_2\text{O}$  and the combined organics were reduced to 5-10 ml. 250 ml of 1 M HCl was added to this residue and the aqueous solution was washed with 3x100 ml of  $\text{Et}_2\text{O}$ . The solution was carefully taken to pH 13 by addition of saturated  $\text{NaOH}_{(\text{aq})}$  (approx. 4 ml). The free amine was extracted from the aqueous fraction with 3x100 ml of  $\text{Et}_2\text{O}$  and dried over  $\text{K}_2\text{CO}_3$ . The dried solution was decanted and the solvent removed *in vacuo* to give a waxy white solid. The crude product was purified by taking it up in *ca.* 100 ml of hot (80 °C) heptane, cooling slowly overnight, separating the precipitate by filtration, and removing solvent *in-vacuo*. Yields range from 60-80% of white waxy solid. Analysis calculated for  $\text{C}_{20}\text{H}_{28}\text{N}_2$ : %C 81.02, %H 9.54, %N 9.44; found (2 runs): %C 79.96, 80.33; %H 9.14, 9.96; %N 9.65, 9.98.

**Amine chiral linker.** A swivel frit assembly was charged with (*R,R*)-1,2-diphenyl-1,2-di(isopropylamino)ethane (657.2 mg). On the vacuum line, Et<sub>2</sub>O (80 ml), NEt<sub>3</sub> (3.2 ml), and SiCl<sub>4</sub> (0.254 ml) were sequentially condensed onto the solid at -78 °C. The reaction was allowed to warm to R.T. and was stirred overnight. The reaction was filtered and volatiles removed *in vacuo* to give an amber oil whose NMR spectrum is consistent with formation of a salt with a trichlorosilane group having been delivered to only one nitrogen of the starting material and the other nitrogen being protonated. Et<sub>2</sub>O (50 ml) and 2 ml Et<sub>3</sub>N were added to the solid and the solution was stirred overnight and filtered giving a viscous amber oil upon removal of volatiles. Kugelrohr distillation gave a clear, colorless oil but the NMR still indicated a mixture of products. The oil was loaded into a swivel frit assembly and Et<sub>2</sub>O (50 ml), NEt<sub>3</sub> (1.5 ml), and SiCl<sub>4</sub> were sequentially condensed in at -78 °C. The reaction was allowed to warm to R.T. and was stirred overnight. The reaction was filtered and volatiles removed *in vacuo* to give an amber oil. Kugelrohr distillation of this oil gave a white solid which was consistent with pure product in relatively low overall yield. Analysis calculated for C<sub>20</sub>H<sub>26</sub>N<sub>2</sub>Si: %C 61.05, %H 6.67, %N 7.12; found: %C 60.06; %H 6.78; %N 7.08.

**Amine chiral linker dimethyl derivative.** The identity of the product from the previous reaction was confirmed by its conversion to the corresponding dimethylsilyl derivative and subsequent characterization by NMR and mass spectral analysis as follows. In the glove box a J. Young NMR tube was loaded with "amine chiral linker" (5 mg) and an excess of MeLi·LiBr (5 mg). THF-*d*<sub>8</sub> was condensed into the NMR tube assembly and the NMR spectrum taken 1 hr later indicated clean conversion to the dimethyl species. The NMR tube was opened in air and N<sub>2</sub> was bubbled through the solution to drive off solvent. C<sub>6</sub>D<sub>6</sub> (2 ml)



was subsequently added and the tube was sonicated for a few minutes to help loosen the solids from the walls of the tube. Filtration gave a clear, colorless solution whose NMR spectrum was consistent with clean conversion to the desired dimethylsilyl derivative. The mass spectrum of this solution gave a clean parent ion peak at the expected mass of the product.

## References and Notes

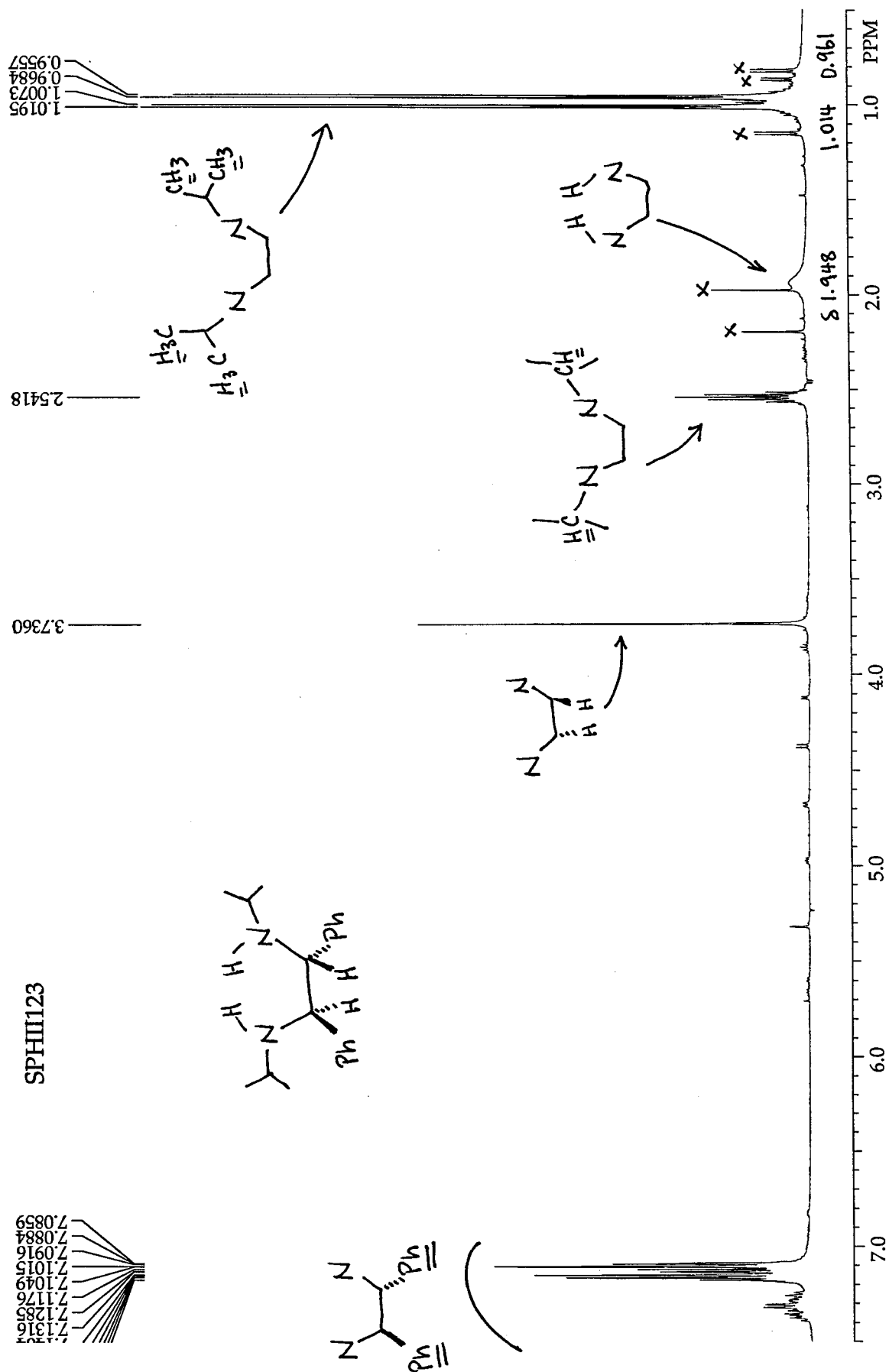
1. For recent examples with leading references see:
  - (a) Carter, M. B.; Scihott, B.; Gutierrez, A.; Buchwald, S. J. *Am. Chem. Soc.* **1994**, *116*, 11667-11670.
  - (b) Willoughby, C. A.; Buchwald, S. L. *J. Org. Chem.* **1993**, *58*, 7627-7629.
  - (c) Willoughby, C.; Buchwald, S. L. *J. Am. Chem. Soc.* **1994**, *116*, 11703-11714.
  - (d) Jaquith, J. B.; Guan, J.; Wang, S.; Collins, S. *Organometallics* **1995**, *14*, 1079.
2. Schäfer, A.; Karl, E.; Zsolnai, L.; Huttner, G.; Brintzinger, H. H. *J. Organomet. Chem.* **1987**, *328*, 87-99.
3. Diamond, G. M.; Rodewald, S.; Jordan, R. F. *Organometallics* **1995**, *14*, 5.
4. Barner, C. J., Ph. D. Thesis, California Institute of Technology, **1984**.
5. Conticello, V. P.; Brard, L.; Giardello, M. A.; Tsuji, Y.; Sabat, M.; Stern, C. L.; Marks, T. J. *J. Am. Chem. Soc.* **1992**, *114*, 2761-2.
6. Coughlin, E. B.; Bercaw, J. E. *J. Amer. Chem. Soc.* **1992**, *113*, 7606.
7. (a) Chacon, S. T.; Coughlin, E. B.; Henling, L. M.; Bercaw, J. E. **submitted**.  
(b) Mitchell, J. P., unpublished results.
8. (a) Bandy, J. A.; Green, M. L. H.; Gardiner, I. M.; Prout, K. *J. Chem. Soc., Dalton Trans.* **1991**, *11*, 2207.  
(b) Burk, M.J.; Colletti, S.L.; Halterman, R.L. *Organometallics*. **1991**, *10*, 2998.  
(c) Chen, Z.; Halterman, R.L. *J. Amer. Chem. Soc.* **1992**, *114*, 2276.  
(d) Halterman, R.L.; Ramsey, T.M. *Organometallics*. **1993**, *12*, 964.  
(e) Rheingold, A.L.; Robinson, N.P.; Whelan, J.; Bosnich, B. *Organometallics*. **1992**, *11*, 1869.  
(f) Ellis, W. W.; Hollis, T. K.; Odenkirk, W.; Whelan, J.; Ostrander, R.; Rheingold, A.L.; Bosnich, B. *Organometallics*. **1993**, *12*, 4391.  
(g) Hollis, T.K.; Rheingold, A.L.; Robinson, N.P.; Whelan, J.; Bosnich, B. *Organometallics*. **1992**, *11*, 2812.

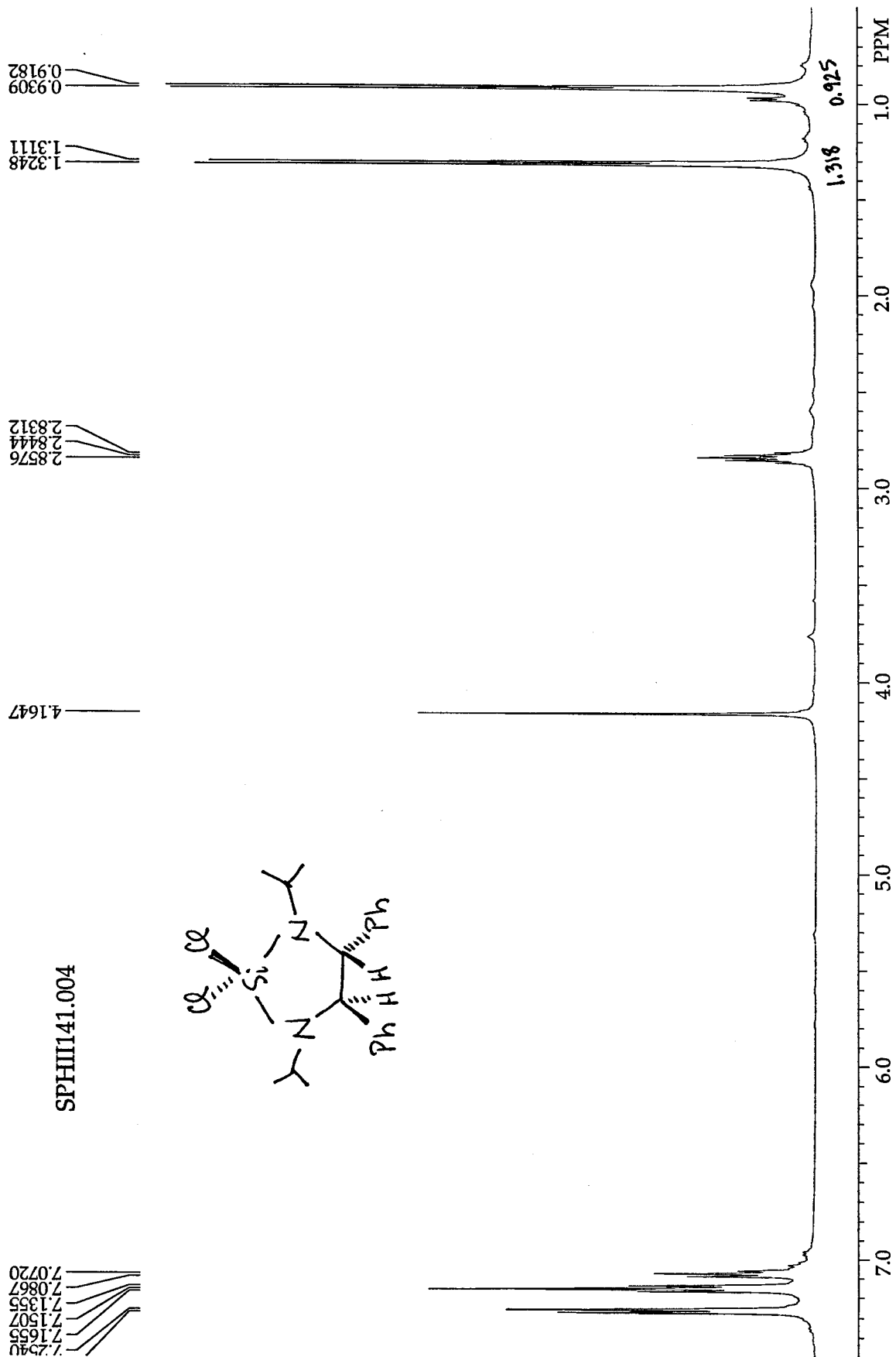
- 
- (h) Grossman, R. B.; Tsai, J.-C.; Davis, W. M.; Gutiérrez, A.; Buchwald, S. L. *Organometallics* **1994**, *13*, 3892-3896, and references therein.
- (i) Sutton, S. C.; Nantz, M. H.; Parkin, S. R. *Organometallics*. **1993**, *12*, 2248.
9. Piers, W. E.; Shapiro, P. J.; Bunel, E. E.; Bercaw, J. E. *Synlett* **1990**, *2*, 74.
10. Indenyl anions do react with these chiral linkers presumably as a consequence of their relatively higher basicity.
11. Fendrick, C. M.; Mintz, E. A.; Schertz, L. D.; Marks, T. J. *Organometallics* **1984**, *3*, 819.
12. Corey, E. J.; Hopkins, P. B. *Tetrahedron Lett.* **1982**, *23*, 4871.
13. Herzog, T. A., unpublished results.
14. Brookhart, S. K., Candidacy Report, California Institute of Technology **1995**.
15. Burger, B.J.; Bercaw, J.E. *Experimental Organometallic Chemistry*; Wayda, A.L., Darensbourg, M.Y., Eds.; ACS Symposium Series 357; American Chemical Society: Washington, DC, 1987.
16. Marvich, R.H.; Brintzinger, H.H. *J. Am. Chem. Soc.* **1971**, *93*, 2046.
17. Caughlin, E. B., Ph. D. Thesis, California Institute of Technology **1994**.
18. Corey, E. J.; Imwinkelried, R.; Pikul, S.; Xiang, Y. B. *J. Am. Chem. Soc.* **1989**, *111*, 5493.
19. Siedle, A. R.; Newmark, R. A.; Lamanna, W. M.; Schroepfer, J. N. *Polyhedron* **1990**, *9*, 301.
20. Abdel-Magid, A. F.; Maryanoff, C. A.; Carson, K. G. *Tetrahedron Lett.* **1990**, *31*, 5595.

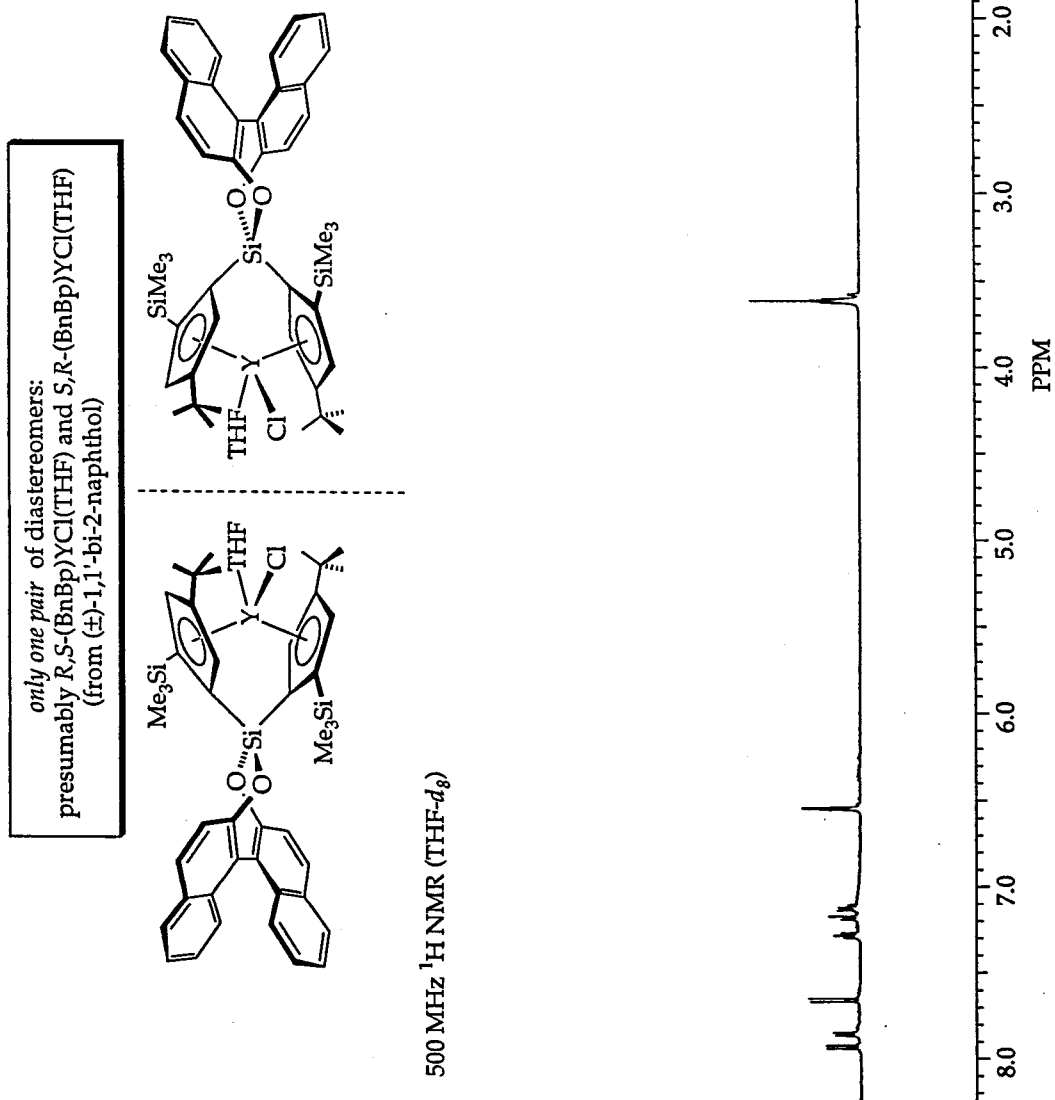
## **Appendix 4**

### **Selected Spectra of Products and Reactions**

#### **For Chapter 4.**

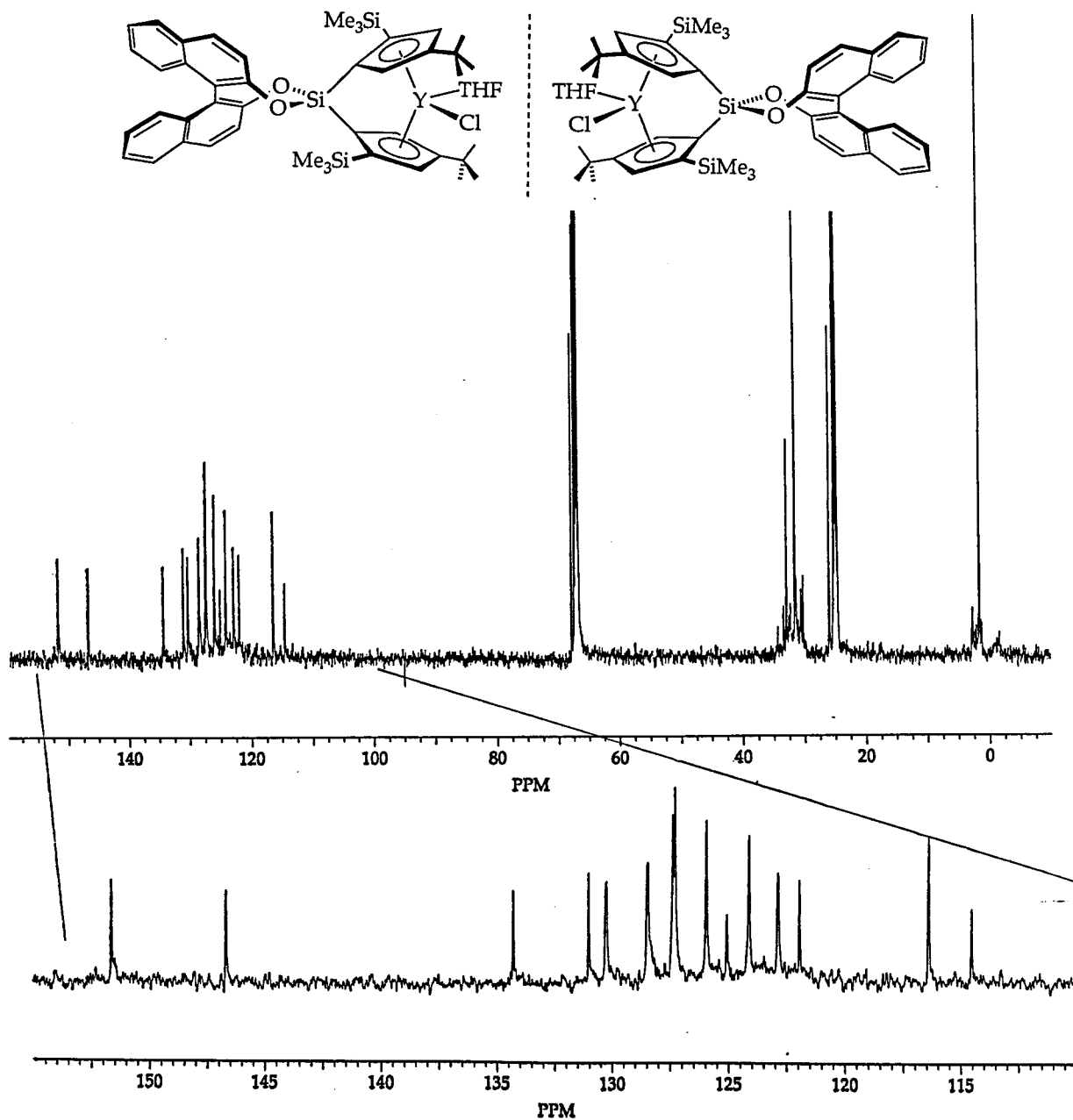




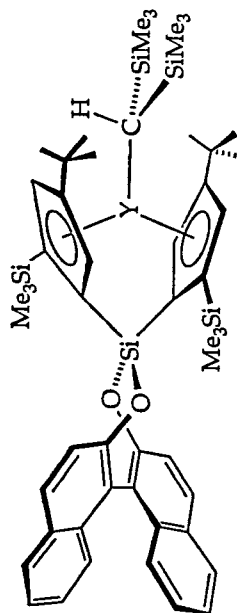
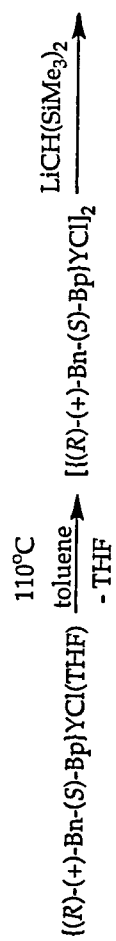


$\{^1\text{H}\} \text{ } ^{13}\text{C}$  NMR (THF- $d_8$ )

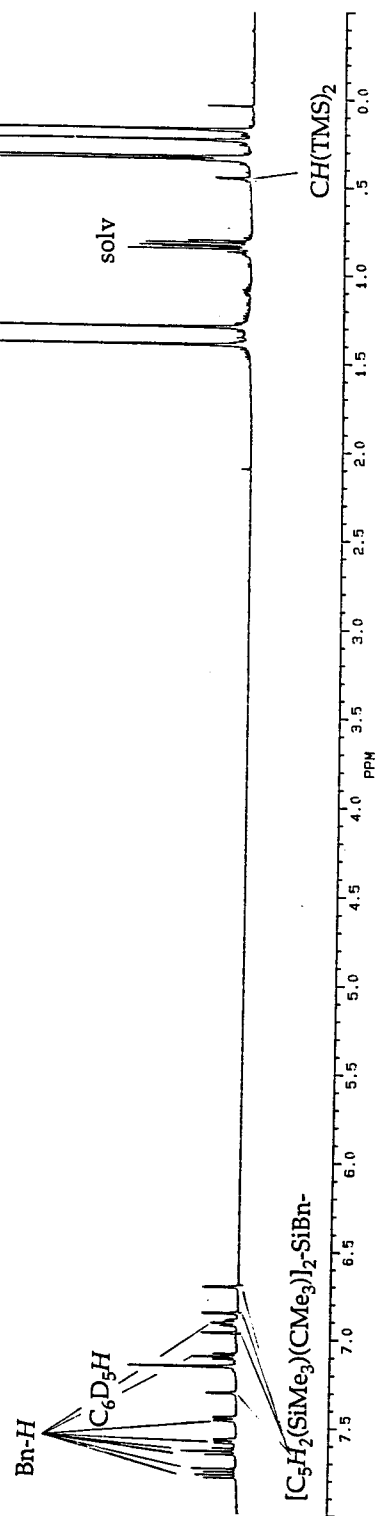
only one pair of diastereomers:  
presumably *R,S*-(BnBp)YCl(THF) and *S,R*-(BnBp)YCl(THF)  
(from  $(\pm)$ -1,1'-bi-2-naphthol)







500 MHz  $^1\text{H}$  NMR (benzene- $d_6$ )



500 MHz  $^1\text{H}$  NMR (benzene- $d_6$ )

